JNRS

JOURNAL OF NEW RESULTS IN SCIENCE

http://dergipark.gov.tr/jnrs

ISSN: 1304 - 7981

VOLUME : 10
NUMBER : 3
YEAR : 2021

jnrs@gop.edu.tr

Journal of New Results in Science -an official journal of the Institute of Graduate Studies of Tokat Gaziosmanpasa University - started its publication in 2012.

J. New Results Sci. is an international, peer-reviewed, and fully open access journal which publishes original English research articles and reviews in **Mathematics and Statistics, Natural Science, Engineering Science, and Agricultural Science**.

JNRS has no processing charges.

Language: English only

Editor-in-Chief: Ali YAKAR

Email: togu.jnrs@gmail.com

Review Process: Blind Peer Review

The policy of Screening for Plagiarism: To begin a manuscript's pre-review, its reference-excluded similarity rate obtained via iThenticate, Turnitin, etc. should be a **maximum of 40%**.

Aim & Scope

Journal of New Results in Science (JNRS) is an Online, Peer-Reviewed, Open-Access journal that aims to contribute to the progress and application of scientific discoveries by publishing Original Research Papers, Review articles that are not published or not being considered for publication elsewhere.

Journal of New Results in Science (JNRS) is a multidisciplinary journal that accepts original research articles written in English in

- Mathematics and Statistics,
- Natural Science,
- Engineering Science,
- Agricultural Science.

Ethical Principles and Publication Policy

Journal Publishing Policy

Journal of New Results in Science is published on the ULAKBIM Journal platform with the "Refereed Journal" status. The journal is published three issues (April, August, and December) per year in electronic form.

The journal publishes original English studies in Mathematics and Statistics, Natural Science, Engineering Science, and Agricultural Science.

Manuscripts sent to the journal are directed to the relevant field editor after the editor and assistant editor review. According to the approval of the field editor, the manuscript will go through a double-blind peer-review process.

No fee is charged for the articles, book reviews, etc., published in the Journal of New Results in Science, and also, the journal does not pay any fees to authors.

Researches should be prepared by ethical rules, and citations in the manuscript should be indicated.

The arguments expressed in the published manuscripts do not represent the journal's views; it is the author's responsibility (s).

Copyright

Authors are obliged to fill and send a "Copyright Form" for the journal's manuscripts.

Publication Ethics

The Journal of New Results in Science's publication process is based on the unbiased production, improvement, and sharing of information using scientific methods.

The publication ethics and open access policy of the Journal of New Results in Science require that all stakeholders of the publication process comply with ethical principles in line with the guidelines and policies (For example, "Publication Ethics Committee (COPE) Code of Conduct and Best Practice Guidelines for Journal Editors;" Code of Conduct and Best Practice Guidelines for Journal Editors "and" COPE Best Practice Guidelines for Journal Editors") published by the Publication Ethics Committee (Committee on Publication Ethics, COPE) on open access.

In situations such as manipulating and distorting the data used in the articles and using make-up data are detected, this situation will be officially reported to the institutions of the author(s), and the manuscript will be rejected. The journal has the right to request the output files of the authors' analysis results according to the feedback given by the editors and/or referees.

Publisher's Ethical Responsibilities

Journal of New Results in Science is in the public interest and non-profit. The editorial board of the journal consists of a chief editor, an assistant editor and field editors. A new member is appointed to replace the leaving member. According to the manuscript's subject, when necessary, the editor may send manuscripts to faculty members who are not members of the editorial board and have at least a PhD degree to be reviewed as field editors. In a year, the number of articles in which Editors are its Authors/Co-Authors cannot be more than 1/5 of the total number of articles published in the year.

The Responsibilities of the Journal Editorial Board

The editorial board is responsible for every manuscript submitted to the journal, and the editorial board is aware of this responsibility.

The editorial board strives to improve the journal and increase its publication quality continuously.

The editorial board ensures that journal policies such as publication, blind review, review process, ethical principles are determined and implemented.

The editorial board is responsible for taking measures regarding intellectual property rights, unscientific, unethical behaviours, and plagiarism during manuscripts and journals.

The editorial board carries out the responsibility of appointing an expert referee for the manuscripts sent to the journal.

Ethical Responsibilities of Editorial Board

While deciding on the publication of manuscripts, editors take care that the manuscripts are original and contribute to the scientific literature.

When editors make decisions about the manuscripts, they consider the original value of the manuscripts, their contribution to the field, the validity and reliability of the research method, the clarity of the language, and the journal's purpose and scope.

Editors implement the policies of blind review and review process, which are among the journal's publishing policies, keep the identity information of the referees confidential, and ensure that each manuscript is reviewed objectively and in time.

Editors send the manuscripts by taking into account the editors and referees' field of expertise, and they support the impartial and independent review.

Editors pay attention to an unbiased review of the manuscript. Editors strive to ensure the diversity of the referee committee and the constant change of the committee.

Editors ensure the protection of personal data in reviewed manuscripts. Editors pay attention to protecting human rights in the manuscripts and care about documenting the participants' explicit consent. They reject the manuscripts when the authors do not have the ethics committee's approval related to the manuscripts' participants.

Editors take precautions against misconduct. When there are complaints about misconduct, they make an objective investigation and share the complaints' findings.

Editors consider the consistent criticism of the manuscripts published in the journal and give the right to reply to the author(s) for the criticism.

Editors examine the complaints submitted to the journal and make the necessary explanations.

Ethical Responsibilities of Referees

In the process of reviewing the manuscripts, the single-blind refereeing principle is applied. Referees cannot communicate directly with the authors. The manuscript review forms and the notes specified on the manuscript and requests for correction are conveyed to the author(s) by the editors through the journal management system. Referees who will review the manuscripts submitted to the Journal of New Results in Science should bear the following ethical responsibilities:

Referees should only accept manuscripts related to their field of expertise.

Referees should notice the neutrality and confidentiality of the review process. In case of a conflict of interest, referees should refuse to review the manuscripts and inform them.

Referees should review the manuscripts in constructive language by academic ethic principles and avoid personal comments containing insults and hostility.

The referees should review the manuscripts, which they accepted, within the time limit. The referees should give detailed reasons for acceptance or refusal.

Ethical Responsibilities of Authors

Author(s) should not send the manuscript they have published elsewhere or sent to be published elsewhere.

The manuscript sent by the author(s) should be distinctive.

Author(s) should refer (cite) to the manuscript sources in line with ethical principles. The names of people who do not contribute to the manuscript should not be mentioned as authors. It should not be suggested to change the order of the authors and to remove or add authors for the manuscript submitted for publication,

If information or data about the manuscript is requested from the author(s) during the review process, the author(s) should provide the editors' expected information.

The author(s) should provide the ethics committee's approval for the research that requires quantitative or qualitative data collection methods such as experiments, questionnaires, scales, interviews, observations, and focus group studies. The document indicating the ethics committee decision should be uploaded to the system with the manuscript's application.

Notification of the Editor for the Unethical Cases

In case of encountering an unethical case regarding editors, referees, and authors or the manuscript in an early view or in the review process that does not comply with ethical principles, it should be reported to jnrs@gop.edu.tr e-mail address.

Obtaining Legal / Private Ethical Committee Approval

The articles related to the Principles of Ethics in the previous years in the EXPLANATION and DISCLOSURE Criteria for the TR Index Principles of Ethics were detailed with explanations in 2020. The issue of "including information about permission in the manuscript" was added to the criteria by assuming permission was obtained for studies requiring ethics committee approval in the field of research.

The researches that require ethical committee approval are as follows, and the forementioned permission must be obtained for the publication of such studies;

All kinds of research conducted with qualitative or quantitative approaches require data collection from participants using a questionnaire, interview, focus group study, observation, experiment, interview techniques.

Use of humans and animals (including material/data) for experimental or other scientific purposes,

Clinical researches on humans,

Research on animals,

Retrospective studies by the law on the protection of personal data

Contact

Prof. Dr. Ali Yakar ali.yakar@gop.edu.tr +903562521616
Departments of Mathematics, Faculty of Arts and Sciences, Tokat Gaziosmanpaşa University, Tokat, Turkey

Assoc. Prof. Serdar Enginoğlu serdarenginoglu@gmail.com +902862180018 / 22154 +905052241254
Departments of Mathematics, Faculty of Arts and Sciences, Çanakkale Onsekiz Mart University, Çanakkale, Turkey

Asst. Prof. Dr. Orhan Özdemir orhan.ozdemir@gop.edu.tr +903562521616
Departments of Mathematics, Faculty of Arts and Sciences, Tokat Gaziosmanpaşa University, Tokat, Turkey

CONTENT

Journal of New Results in Science 10(3) (2021) 1-10

Journal of New Results in Science
https://dergipark.org.tr/en/pub/jnrs
Research Article
Open Access

E-ISSN:1304-7981 https://doi.org/10.54187/jnrs.947322

Some results on generalized Euler-type integrals related to the four parameters Mittag-Leffler function

Umar Muhammad Abubakar[1]

Keywords:
Factorial function, Pochhammer symbol, Mittag-Leffler function, Beta function, Euler-type integral

Abstract —Special functions such as hypergeometric, zeta, Bessel, Whittaker, Struve, Airy, Weber-Hermite and Mittag-Leffler functions are obtained as a solution to complex differential equations in engineering, science and technology. In this work, generalized Euler-type integrals involving four parameters Mittag-Leffler function are proposed. Some special cases of this type of generalized integrals that are corresponding to well-known results in the literature are also inferred.

Subject Classification (2020): 33B15, 33B90.

1. Introduction

Throughout this article, ℕ and ℂ represent the sets of natural and complex numbers, respectively. In 1729, Leonard Euler studied the classical gamma function by extending the factorial function from the domain of natural numbers, to the region in the right half of the complex plane given as follows [1-2]:

$$\Gamma(\sigma) = \int_0^1 t^{\sigma-1} exp(-t)dt, \qquad (\mathrm{Re}\ (\sigma) > 0) \tag{1.1}$$

A year later, He established classical beta function, $B(\sigma, \mathcal{E})$ for a pair of complex numbers σ and $\mathcal{E}$ with positive real parts through the integrand which is given by [3-4].

$$B(\sigma, \mathcal{E}) = \int_0^1 t^{\sigma-1}(1-t)^{\mathcal{E}-1}\, dt, \qquad (\mathrm{Re}\ (\sigma) > 0, \mathrm{Re}\ (\mathcal{E}) > 0) \tag{1.2}$$

Carl Friedrich Gauss [5] generalized the geometric series in the following classical Gauss hypergeometric function:

[1]umabubakar347@gmail.com
[1]Department of Mathematics, Faculty of Computing and Mathematical Sciences, Kano University of Science and Technology, Wudil, P.M.B: 3244 Kano, Kano State-Nigeria
Article History: Received: 03 June 2021 — Accepted: 25 Dec 2021 — Published: 31 Dec 2021

$$F(\sigma,\mathcal{E};\eth;z)=\sum_{n_2}^{\infty}\frac{(\sigma)_{n_2}(\mathcal{E})_{n_2}}{(\eth)_{n_2}}\frac{z^{n_2}}{n_2!}=\sum_{n_2}^{\infty}(\sigma)_{n_2}\frac{B(\mathcal{E}+n_2,\eth-\mathcal{E})}{B(\mathcal{E},\ \eth-\mathcal{E})}\frac{z^{n_2}}{n_2!},\qquad (|z|<1,\mathrm{Re}\,(\eth)>\mathrm{Re}\,(\mathcal{E})>0)\qquad (1.3)$$

and it can reduced to the Kumar confluent hyper geometric function defined by Ernst Eduard Kumar in [6].

$$\Phi(\mathcal{E};\eth;z)=\sum_{n_2}^{\infty}\frac{(\mathcal{E})_{n_2}}{(\eth)_{n_2}}\frac{z^{n_2}}{n_2!}\frac{z^{n_2}}{n_2!}=\sum_{n_2}^{\infty}\frac{B(\mathcal{E}+n_2,\eth-\mathcal{E})}{B(\mathcal{E},\ \eth-\mathcal{E})}\frac{z^{n_2}}{n_2!},\qquad (\mathrm{Re}\,(\eth)>\mathrm{Re}\,(\mathcal{E})>0)\qquad (1.4)$$

Here $(\sigma)_{n_2}$represent classical pochhammer symbol defined as [7-8].

$$(\sigma)_{n_2}=\begin{cases}\sigma(\sigma+1)(\sigma+2)(\sigma+3)\cdots(\sigma+n_2-1), & (n_2\geq 0,\sigma\neq 0)\\ 1\qquad\qquad , & (n_2=0)\end{cases}$$

Other properties of Gauss hypergeometric and confluent hypergeometric such integral representation, transformation formulas, summation formulas and contiguity relations can be found in [9].

Chaudhry and Zubair [10-11] extended classical gamma function in (1.1) by using exponential kernel as follows [12-14]:

$$\Gamma_{\mathfrak{I}}(\sigma)=\int_0^1 t^{\sigma-1}exp\left(-t-\frac{\mathfrak{I}}{t}\right)dt,\qquad (\mathrm{Re}\,(\sigma)>0,\mathrm{Re}\,(\mathfrak{I})>0)$$

Chaudhry et al., [15-17] introduced the following extension of beta function as an extension of classical beta function in (1.2):

$$B_{\mathfrak{I}}(\sigma,\mathcal{E})=\int_0^1 t^{\sigma-1}(1-t)^{\mathcal{E}-1}\,exp\left(-\frac{\mathfrak{I}}{t(1-t)}\right)dt,\qquad (\mathrm{Re}\,(\mathfrak{I})>0,\mathrm{Re}\,(\sigma)>0,\mathrm{Re}\,(\mathcal{E})>0)\qquad (1.5)$$

Chaudhry et al., [18] proposed the following extended of Gauss hypergeometic and confluent hyper geometric functions by using extended beta function in (1.3) and (1.4) as

$$F_{\mathfrak{I}}(\sigma,\mathcal{E};\eth;z)=\sum_{n_2}^{\infty}(\sigma)_{n_2}\frac{B_{\mathfrak{I}}(\mathcal{E}+n_2,\eth-\mathcal{E})}{B(\mathcal{E},\ \eth-\mathcal{E})}\frac{z^{n_2}}{n_2!},\qquad (\mathfrak{I}\geq 0;\ |z|<1,\mathrm{Re}\,(\eth)>\mathrm{Re}\,(\mathcal{E})>0)\qquad (1.6)$$

and

$$\Phi_{\mathfrak{I}}(\mathcal{E};\eth;z)=\sum_{n_2}^{\infty}\frac{B_{\mathfrak{I}}(\mathcal{E}+n_2,\eth-\mathcal{E})}{B(\mathcal{E},\ \eth-\mathcal{E})}\frac{z^{n_2}}{n_2!},\qquad (\mathfrak{I}\geq 0;\ \mathrm{Re}\,(\eth)>\mathrm{Re}\,(\mathcal{E})>0)\qquad (1.7)$$

Lee et al., [19-20] presented and investigated the following extension of beta function as an extension of (1.5):

$$B_{\mathfrak{I}}^{\eth}(\sigma,\mathcal{E})=\int_0^1 t^{\sigma-1}(1-t)^{\mathcal{E}-1}\,exp\left(-\frac{\mathfrak{I}}{t^{\eth}(1-t)^{\eth}}\right)dt,(\mathrm{Re}\,(\mathfrak{I})>0,\mathrm{Re}\,(\sigma)>0,\mathrm{Re}\,(\mathcal{E})>0,\mathrm{Re}\,(\eth)>0)\qquad (1.8)$$

They also [19] extended Gauss and confluent hyper geometric functions in (1.6) and (1.7) as follows:

$$F_{\mathfrak{I}}^{\eth}(\sigma,\mathcal{E};\eth;z)=\sum_{n_2}^{\infty}(\sigma)_{n_2}\frac{B_{\mathfrak{I}}^{\eth}(\mathcal{E}+n_2,\eth-\mathcal{E})}{B(\mathcal{E},\ \eth-\mathcal{E})}\frac{z^{n_2}}{n_2!},\qquad (\mathfrak{I}\geq 0;\ |z|<1,\mathrm{Re}\,(\eth)>\mathrm{Re}\,(\mathcal{E})>0) \tag{1.9}$$

and

$$\Phi_{\mathfrak{I}}^{\eth}(\mathcal{E};\eth;z)=\sum_{n_2}^{\infty}\frac{B_{\mathfrak{I}}^{\eth}(\mathcal{E}+n_2,\eth-\mathcal{E})}{B(\mathcal{E},\ \eth-\mathcal{E})}\frac{z^{n_2}}{n_2!},\qquad (\mathfrak{I}\geq 0;\ \mathrm{Re}\,(\eth)>\mathrm{Re}\,(\mathcal{E})>0) \tag{1.10}$$

Luo et al., [21] presented the following extension of beta function as a generalization of beta function in (1.10):

$$B_{\mathfrak{I}}^{\eth,\lambda}(\sigma,\mathcal{E})=\int_0^1 t^{\sigma-1}(1-t)^{\mathcal{E}-1}\,exp\left(-\frac{\mathfrak{I}}{t^{\eth}(1-t)^{\lambda}}\right)dt \tag{1.11}$$

$$(\mathrm{Re}\,(\mathfrak{I})>0,\mathrm{Re}\,(\sigma)>0,\mathrm{Re}\,(\mathcal{E})>0,\mathrm{Re}\,(\eth)>0,\mathrm{Re}\,(\lambda)>0)$$

The classical Mittag-Leffler function was first studied by G.M. Mittag-Leffler [22-24] as an extension of exponential function as shown below:

$$E_{\omega}(z)=\sum_{n_2=0}^{\infty}\frac{z^{n_2}}{\Gamma(\omega n_2+1)},\qquad (\omega,z\in\mathbb{C},\mathrm{Re}\,(\omega)>0) \tag{1.12}$$

Wiman [25-26] extended classical Mittag-Leffler function in (1.12) by introducing two parameters Mittag-Leffler function as follows:

$$E_{\omega,\varpi}(z)=\sum_{n_2=0}^{\infty}\frac{z^{n_2}}{\Gamma(\omega n_2+\varpi)}\ ,\qquad (\omega,\varpi,z\in\mathbb{C}\ Re\,(\omega)>0,Re(\varpi)>0) \tag{1.13}$$

Prabhakar [27] investigated three parameters Mittag-Leffler function as a generalization of (1.13) as follows:

$$E_{\omega,\varpi}^{\eta}(z)=\sum_{n_2=0}^{\infty}\frac{(\eta)_{n_2}}{\Gamma(\omega n_2+\varpi)}\frac{z^{n_2}}{n_2}\ ,\qquad (\omega,\varpi,\eta,z\in\mathbb{C},\mathrm{Re}\,(\omega)>0,\mathrm{Re}\,(\varpi)>0,\mathrm{Re}\,(\eta)>0) \tag{1.14}$$

Shukla and Prajapati [28] investigated four parameters Mittag-Leffler function as an extension of (1.14) as follows:

$$E_{\omega,\varpi}^{\eta,q}(z)=\sum_{n_2=0}^{\infty}\frac{(\eta)_{qn_2}}{\Gamma(\omega n_2+\varpi)}\frac{z^{n_2}}{n_2}\ ,\qquad (\omega,\varpi,\eta,z\in\mathbb{C},\mathrm{Re}\,(\omega)>0,\mathrm{Re}\,(\varpi)>0,\mathrm{Re}\,(\eta)>0,q\in(0,1)\cup\mathbb{N}) \tag{1.15}$$

where $(\eta)_{qn_2}$ represents generalized pochhammer symbol defined by [29]

$$(\eta)_{qn_2}=\frac{\Gamma(\eta+qn_2)}{\Gamma(\eta)}$$

Related literature is also available in [30-34].

2. Main Result

The generalized Euler-type integrals involving the four parameters Mittag-Leffler function are presented in the following theorems and corollaries:

Theorem 2.1. If $\omega, \varpi, \eta, \sigma, \mathcal{E}, \mathfrak{I} \in \mathbb{C}$, $Re(\omega) > 0, Re(\varpi) > 0$, $Re(\eta) > 0$, $Re(\sigma) > 0$, $Re(\mathcal{E}) > 0$, $Re(\mathfrak{I}) > 0$ and $q \in \mathbb{N}$, then

$$\int_0^1 t^{\sigma-1}(1-t)^{\mathcal{E}-1} exp\left(-\frac{\mathfrak{I}}{t^{\eth}(1-t)^{\lambda}}\right) \mathrm{E}_{\omega,\varpi}^{\eta,q}(zt^{\omega})dt = \sum_{n_2=0}^{\infty} \frac{(\eta)_{n_2 q}}{\Gamma(\omega n_2 + \varpi)} \frac{z^{n_2}}{n_2!} B_{\mathfrak{I}}^{\eth,\lambda}(\sigma + \omega n_2, \mathcal{E}) \tag{2.1}$$

Proof.

Let represent left-hand side of (2.1) by A_1, we have

$$A_1 = \int_0^1 t^{\sigma-1}(1-t)^{\mathcal{E}-1} exp\left(-\frac{\mathfrak{I}}{t^{\eth}(1-t)^{\lambda}}\right) \mathrm{E}_{\omega,\varpi}^{\eta,q}(zt^{\omega})dt$$

Applying (1.15), we obtain

$$A_1 = \int_0^1 t^{\sigma-1}(1-t)^{\mathcal{E}-1} exp\left(-\frac{\mathfrak{I}}{t^{\eth}(1-t)^{\lambda}}\right) \left\{\sum_{n=0}^{\infty} \frac{(\eta)_{n_2 q}}{\Gamma(\omega n_2 + \varpi)} \frac{z^{n_2}}{n_2!} t^{\omega n_2}\right\} dt$$

Interchanging the order of summation and integration, gives

$$A_1 = \sum_{n_2=0}^{\infty} \frac{(\eta)_{n_2 q}}{\Gamma(\omega n_2 + \varpi)} \frac{z^{n_2}}{n_2!} \int_0^1 t^{\sigma+\omega n_2-1}(1-t)^{\mathcal{E}-1}\, exp\left(-\frac{\mathfrak{I}}{t^{\eth}(1-t)^{\lambda}}\right) dt$$

Considering (1.11), we have

$$A_1 = \sum_{n_2=0}^{\infty} \frac{(\eta)_{n_2 q}}{\Gamma(\omega n_2 + \varpi)} \frac{z^{n_2}}{n_2!} B_{\mathfrak{I}}^{\eth,\lambda}(\sigma + \omega n_2, \mathcal{E})$$

Lemma 2.2. The following result holds [35]:

$$\int_a^b (t-a)^{\sigma-1}(b-t)^{\mathcal{E}-1}(tv+h)^{g} dt = B(\sigma, \mathcal{E})(b-a)^{\sigma+\mathcal{E}-1}(av+h)^{g}\, {}_2F_1\left(\sigma, -g; \sigma+\mathcal{E}; -\frac{v(b-a)}{(av+h)}\right) \tag{2.2}$$

$$(Re(\sigma) > 0, Re(\mathcal{E}) > 0;\ |arg((bv+h)(av+h)^{-1})| < \pi)$$

Theorem 2.3. If $\omega, \varpi, \eta, \sigma, \mathcal{E}, \mathfrak{I} \in \mathbb{C}$, $Re(\omega) > 0$, $Re(\varpi) > 0$, $Re(\eta) > 0$, $Re(\sigma) > 0$, $Re(\mathcal{E}) > 0$, $Re(\mathfrak{I}) > 0$, $|arg((bv+h)(av+h)^{-1})| < \pi$ and $q \in \mathbb{N}$, then

$$\int_a^b (t-a)^{\sigma-1}(b-t)^{\mathcal{E}-1}(tv+h)^{g} exp\left(-\frac{\mathfrak{I}}{(t-a)^{\eth}(b-t)^{\lambda}}\right) \mathrm{E}_{\omega,\varpi}^{\eta,q}\left(z(b-t)^{\ell}\right)dt$$

$$= (av+h)^{g}\sum_{n_1}^{\infty}\sum_{n_2}^{\infty}\frac{(-\mathfrak{I})^{n_1}}{n_1}\frac{(\eta)_{n_2q}}{\Gamma(\omega n_2+\varpi)}\frac{z^{n_2}}{n_2!}B(\sigma-\eth n_1, \mathcal{E}-\lambda n_1+\kappa n_2) \tag{2.3}$$

$$\times (b-a)^{\sigma+\mathcal{E}-\eth n_1-\lambda n_1+\kappa n_2-1}{}_2F_1\left(\sigma-\eth n_1, -g; \sigma+\mathcal{E}-\eth n-\lambda n_1+\kappa n_{2_1}; -\frac{v(b-a)}{(av+h)}\right)$$

Proof.

Let donate left-hand side of (2.3) by A_2, we obtain

$$A_2 = \int_a^b (t-a)^{\sigma-1}(b-t)^{\mathcal{E}-1}(tv+h)^{g} exp\left(-\frac{\mathfrak{I}}{(t-a)^{\eth}(b-t)^{\lambda}}\right) \mathrm{E}_{\omega,\varpi}^{\eta,q}\left(z(b-t)^{\ell}\right)dt$$

Using (1.11), we obtain

$$A_2 = \int_a^b (t-a)^{\sigma-1}(b-t)^{\mathcal{E}-1}(tv+h)^{g} exp\left(-\frac{\mathfrak{I}}{t^{\eth}(1-t)^{\lambda}}\right)\left\{\sum_{n_2=0}^{\infty}\frac{(\eta)_{n_2q}}{\Gamma(\omega n_2+\varpi)}\frac{\left(z(b-t)^{\ell}\right)^{n_2}}{n_2!}\right\}dt$$

Considering the definition of exponential function

$$A_2 = \int_a^b (t-a)^{\sigma-1}(b-t)^{\mathcal{E}-1}(tv+h)^{g}\left\{\sum_{n_1=0}^{\infty}\frac{(-\mathfrak{I})^{n_1}}{(t-a)^{n_1\eth}(b-t)^{n_1\lambda}\, n_1!}\right\}$$

$$\times\left\{\sum_{n_2=0}^{\infty}\frac{(\eta)_{n_2q}}{\Gamma(\omega n_2+\varpi)}\frac{\left(z(b-t)^{\ell}\right)^{n_2}}{n_2!}\right\}dt$$

Interchanging the order of integration and summations, yields

$$A_2 = \sum_{n_1=0}^{\infty}\sum_{n_2=0}^{\infty}\frac{(-\mathfrak{I})^{n_1}}{n_1!}\frac{(\eta)_{n_2q}}{\Gamma(\omega n_2+\varpi)}\frac{z^{n_2}}{n_2!}\int_a^b (t-a)^{\sigma-n_1\eth-1}(b-t)^{\mathcal{E}-n_1\lambda+n_2\ell-1}(tv+h)^{g}dt$$

Applying (2.2) and simplifying, we get

$$A_2 = (av+h)^{g}\sum_{n_1}^{\infty}\sum_{n_2}^{\infty}\frac{(-\mathfrak{I})^{n_1}}{n_1}\frac{(\eta)_{n_2q}}{\Gamma(\omega n_2+\varpi)}\frac{z^{n_2}}{n_2!}B(\sigma-\eth n_1, \mathcal{E}-\lambda n_1+\kappa n_2)$$

$$\times (b-a)^{\sigma+\mathcal{E}-\eth n_1-\lambda n_1+\kappa n_2-1}{}_2F_1\left(\sigma-\eth n_1, -g; \sigma+\mathcal{E}-\eth n-\lambda n_1+\kappa n_{2_1}; -\frac{v(b-a)}{(av+h)}\right)$$

Corollary 2.4. Substituting $\mathfrak{I} = 0$, the following result can be obtained

$$\int_a^b (t-a)^{\sigma-1}(b-t)^{\mathcal{E}-1}(tv+h)^{g} exp\left(-\frac{\mathfrak{I}}{(t-a)^{\eth}(b-t)^{\lambda}}\right) \mathrm{E}_{\omega,\varpi}^{\eta,q}\left(z(b-t)^{\ell}\right)dt$$

$$= (av+h)^{g} \sum_{n_2=0}^{\infty} \frac{(\eta)_{n_2 q}}{\Gamma(\omega n_2+\varpi)} \frac{z^{n_2}}{n_2!} B(\sigma, \mathcal{E}+\kappa n_2)\,(b-a)^{\sigma+\mathcal{E}+\kappa n_2-1}$$

$$\times\, {}_2F_1\left(\sigma, -g; \sigma+\mathcal{E}+\kappa n_2; -\frac{v(b-a)}{(av+h)}\right)$$

Corollary 2.5. Putting $a = 0$ and $b = 1$, the following formula can be obtained

$$\int_0^1 (t-a)^{\sigma-1}(b-t)^{\mathcal{E}-1}(tv+h)^{g} exp\left(-\frac{\mathfrak{I}}{t^{\eth}(1-t)^{\lambda}}\right) \mathrm{E}_{\omega,\varpi}^{\eta,q}\left(z(1-t)^{\ell}\right)dt$$

$$= h^{g} \sum_{n_2=0}^{\infty} \frac{(\eta)_{n_2 q}}{\Gamma(\omega n_2+\varpi)} \frac{z^{n_2}}{n_2!}\, B(\sigma-\eth n_1, \mathcal{E}-\lambda n_1+\kappa n_2)\, {}_2F_1\left(\sigma, -g; \sigma+\mathcal{E}+\kappa n_2; -\frac{v}{h}\right)$$

Theorem 2.6. If $\omega,\ \varpi,\ \eta,\ \sigma,\ \mathcal{E},\ \mathfrak{I} \in \mathbb{C},\ Re(\omega) > 0,\ Re(\varpi) > 0,\ Re(\eta) > 0, Re(\sigma) > 0,\ Re(\mathcal{E}) > 0,$ $Re(\mathfrak{I}) > 0;\ \alpha,\ \beta \geq 0$ and $q \in \mathbb{N}$, then

$$\int_0^1 t^{\sigma-1}(1-t)^{\mathcal{E}-\sigma-1}\left\{1-vt^{\alpha}(1-t)^{\beta}\right\}^{-\gamma} exp\left(-\frac{\mathfrak{I}}{t^{\eth}(1-t)^{\lambda}}\right) \mathrm{E}_{\omega,\varpi}^{\eta,q}(zt^{\omega})dt$$
$$= \sum_{n_1}^{\infty}\sum_{n_2}^{\infty} \frac{v^{n_1}(\gamma)_{n_1}}{n_1} \frac{(\eta)_{n_2 q}}{\Gamma(\omega n_2+\varpi)} \frac{z^{n_2}}{n_2!} B_{\mathfrak{I}}^{\eth,\lambda}(\sigma+\alpha n_1+\omega n_2, \mathcal{E}-\sigma+\beta n_1) \tag{2.4}$$

Proof.

Let represent left-hand side of (2.4) by A_3, we have

$$A_3 = \int_0^1 t^{\sigma-1}(1-t)^{\mathcal{E}-\sigma-1}\left\{1-vt^{\alpha}(1-t)^{\beta}\right\}^{-\gamma} exp\left(-\frac{\mathfrak{I}}{t^{\eth}(1-t)^{\lambda}}\right) \mathrm{E}_{\omega,\varpi}^{\eta,q}(zt^{\omega})dt$$

Applying (1.15), we have

$$A_3 = \int_0^1 t^{\sigma-1}(1-t)^{\mathcal{E}-\sigma-1}\left\{1-vt^{\alpha}(1-t)^{\beta}\right\}^{-\gamma} exp\left(-\frac{\mathfrak{I}}{t^{\eth}(1-t)^{\lambda}}\right) \left\{\sum_{n_2=0}^{\infty} \frac{(\eta)_{n_2 q}}{\Gamma(\omega n_2+\varpi)} \frac{z^{n_2}}{n_2!} t^{\omega n_2}\right\} dt$$

Using binomial theorem, we get

$$A_3 = \int_0^1 t^{\sigma-1}(1-t)^{\mathcal{E}-\sigma-1}\left\{\sum_{n_1=0}^{\infty}\frac{v^{n_1}t^{\alpha n_1}(1-t)^{\beta n_1}}{n_1!}(\gamma)_{n_1}\right\} exp\left(-\frac{\mathfrak{I}}{t^{\eth}(1-t)^{\lambda}}\right)$$

$$\times\left\{\sum_{n_2=0}^{\infty}\frac{(\eta)_{n_2 q}}{\Gamma(\omega n_2+\varpi)}\frac{z^{n_2}}{n_2!}t^{\omega n_2}\right\}dt$$

Interchanging the order of integration and summation, we have

$$A_3 = \sum_{n_1}^{\infty}\sum_{n_2}^{\infty}\frac{v^{n_1}(\gamma)_{n_1}}{n_1}\frac{(\eta)_{n_2 q}}{\Gamma(\omega n_2+\varpi)}\frac{z^{n_2}}{n_2!}\int_0^1 t^{\sigma+\alpha n_1+\omega n_2-1}(1-t)^{\mathcal{E}-\sigma+\beta n_1-1} exp\left(-\frac{\mathfrak{I}}{t^{\eth}(1-t)^{\lambda}}\right)dt$$

Re-written this equation using (1.11), gives

$$A_3 = \sum_{n_1}^{\infty}\sum_{n_2}^{\infty}\frac{v^{n_1}(\gamma)_{n_1}}{n_1}\frac{(\eta)_{n_2 q}}{\Gamma(\omega n_2+\varpi)}\frac{z^{n_2}}{n_2!}B_{\mathfrak{I}}^{\eth,\lambda}(\sigma+\alpha n_1+\omega n_2, \mathcal{E}-\sigma+\beta n_1)$$

Corollary 2.7. Setting $\gamma = 0$ in (2.4), we have

$$\int_0^1 t^{\sigma-1}(1-t)^{\mathcal{E}-\sigma-1} exp\left(-\frac{\mathfrak{I}}{t^{\eth}(1-t)^{\lambda}}\right)\mathrm{E}_{\omega,\varpi}^{\eta,q}(zt^{\omega})dt = \sum_{n_2}^{\infty}\frac{(\eta)_{n_2 q}}{\Gamma(\omega n_2+\varpi)}B_{\mathfrak{I}}^{\eth,\lambda}(\sigma+\omega n_2, \mathcal{E}-\sigma)$$

Corollary 2.8. Setting $\mathfrak{I} = \gamma = 0$ in (2.4), we get

$$\int_0^1 t^{\sigma-1}(1-t)^{\mathcal{E}-\sigma-1}\,\mathrm{E}_{\omega,\varpi}^{\eta,q}(zt^{\omega})dt = \sum_{n_2}^{\infty}\frac{(\eta)_{n_2 q}}{\Gamma(\omega n_2+\varpi)}B(\sigma+\omega n_2, \mathcal{E}-\sigma)$$

3. Conclusion

In this work, we have proposed some generalized Euler type integrals involving four parameters Mittag-Leffler function of the form $\mathrm{E}_{\omega,\varpi}^{\eta,q}(z)$ (refer to, [28]). In some special cases of this new generalized Euler type integrals includes:

Setting $\eth = \lambda$ in (2.1), (2.3) and (2.4), we obtained the following Euler-type integrals that are in [36]:

$$\int_0^1 t^{\sigma-1}(1-t)^{\mathcal{E}-1} exp\left(-\frac{\mathfrak{I}}{t^{\eth}(1-t)^{\eth}}\right)\mathrm{E}_{\omega,\varpi}^{\eta,q}(zt^{\omega})dt = \sum_{n=0}^{\infty}\frac{(\eta)_{nq}}{\Gamma(\omega n+\varpi)}\frac{z^n}{n!}B_{\mathfrak{I}}^{\eth}(\sigma+\omega n, \mathcal{E})$$

$$\int_a^b (t-a)^{\sigma-1}(b-t)^{\mathcal{E}-1}(tv+h)^{g} exp\left(-\frac{\mathfrak{I}}{(t-a)^{\eth}(b-t)^{\eth}}\right)\mathrm{E}_{\omega,\varpi}^{\eta,q}\left(z(b-t)^{\ell}\right)dt$$

$$= (av+h)^{g}\sum_{n_1}^{\infty}\sum_{n_2}^{\infty}\frac{(-\mathfrak{I})^{n_1}}{n_1}\frac{(\eta)_{n_2 q}}{\Gamma(\omega n_2+\varpi)}\frac{z^{n_2}}{n_2!}B(\sigma-\eth n_1, \mathcal{E}-\eth n_1+\kappa n_2)$$

$$\times (b-a)^{\sigma+\mathcal{E}-2\eth n_1+\kappa n_2-1} F\left(\sigma-\eth n_1, -\mathscr{g}; \sigma+\mathcal{E}-2\eth n+\kappa n_{2_1}; -\frac{v(b-a)}{(av+h)}\right)$$

and

$$\int_0^1 t^{\sigma-1}(1-t)^{\mathcal{E}-\sigma-1}\left\{1-vt^{\alpha}(1-t)^{\beta}\right\}^{-\gamma} exp\left(-\frac{\mathfrak{J}}{t^{\eth}(1-t)^{\eth}}\right) \mathrm{E}_{\omega,\varpi}^{\eta,q}(zt^{\omega})dt$$

$$=\sum_{n_1}^{\infty}\sum_{n_2}^{\infty}\frac{v^{n_1}(\gamma)_{n_1}}{n_1}\frac{(\eta)_{n_2 q}}{\Gamma(\omega n_2+\varpi)}\frac{z^{n_2}}{n_2!}B_{\mathfrak{J}}^{\eth}(\sigma+\alpha n_1+\omega n_2, \mathcal{E}-\sigma+\beta n_1)$$

Finally, putting $\eth = ƛ = 1$ in (2.1), (2.3) and (2.4), we obtained the following Euler-type integrals that are in [37]:

$$\int_0^1 t^{\sigma-1}(1-t)^{\mathcal{E}-1} exp\left(-\frac{\mathfrak{J}}{t(1-t)}\right) \mathrm{E}_{\omega,\varpi}^{\eta,q}(zt^{\omega})dt = \sum_{n=0}^{\infty}\frac{(\eta)_{nq}}{\Gamma(\omega n+\varpi)}\frac{z^n}{n!}B_{\mathfrak{J}}(\sigma+\omega n, \mathcal{E})$$

$$\int_a^b (t-a)^{\sigma-1}(b-t)^{\mathcal{E}-1}(tv+h)^{\mathscr{g}} exp\left(-\frac{\mathfrak{J}}{(t-a)(b-t)}\right) \mathrm{E}_{\omega,\varpi}^{\eta,q}\left(z(b-t)^{\ell}\right)dt$$

$$=(av+h)^{\mathscr{g}}\sum_{n_1}^{\infty}\sum_{n_2}^{\infty}\frac{(-\mathfrak{J})^{n_1}}{n_1}\frac{(\eta)_{n_2 q}}{\Gamma(\omega n_2+\varpi)}\frac{z^{n_2}}{n_2!}B(\sigma-n_1, \mathcal{E}-n_1+\kappa n_2)$$

$$\times (b-a)^{\sigma+\mathcal{E}-2n_1+\kappa n_2-1} F\left(\sigma-n_1, -\mathscr{g}; \sigma+\mathcal{E}-2n+\kappa n_{2_1}; -\frac{v(b-a)}{(av+h)}\right)$$

and

$$\int_0^1 t^{\sigma-1}(1-t)^{\mathcal{E}-\sigma-1}\left\{1-vt^{\alpha}(1-t)^{\beta}\right\}^{-\gamma} exp\left(-\frac{\mathfrak{J}}{t(1-t)}\right) \mathrm{E}_{\omega,\varpi}^{\eta,q}(zt^{\omega})dt$$

$$=\sum_{n_1}^{\infty}\sum_{n_2}^{\infty}\frac{v^{n_1}(\gamma)_{n_1}}{n_1}\frac{(\eta)_{n_2 q}}{\Gamma(\omega n_2+\varpi)}\frac{z^{n_2}}{n_2!}B_{\mathfrak{J}}(\sigma+\alpha n_1+\omega n_2, \mathcal{E}-\sigma+\beta n_1)$$

Other form of special cases of this generalized Euler-type integral that are in the form of exponential, Classical Mittag-Leffler, Wiman and Prabhakar functions that are in [36-37] also follows.

Conflicts of Interest

The authors declare no conflict of interest.

References

[1] L.C. Andrews, Special functions of mathematics for engineers, SPIE Press, Bellingham, 1998.

[2] E.D. Rainville, Special functions, Macmillan, New York, 1960.

[3] Y.L. Luke, The special functions and their approximations, Academic Press, New York, 1969.

[4] H.M. Srivastava, J. Choi, Zeta and q-zeta functions and associated series and integrals, Elsevier Amsterdam, 2012.

[5] I.N. Sneddon, Special functions of mathematical physics and chemistry, Edinburgh, London, New York,Interscience Publishers, New York, 1956.

[6] K.B. Oldham, J.C. Myland, J. Spaanier, An atlas of functions: with equator, the atlas function calculator, Springer, New York, 2009.

[7] U.M. Abubakar, S.R. Kabara, M.A. Lawan, F.A. Idris, *A new extension of modified gamma and beta functions*, Cankaya University Journal of Science and Engineering, 18 (1), (2021) 9-23.

[8] U.M. Abubakar, *New generalized beta function associated with the Fox-Wright function*, Journal of Fractional Calculus and Application, 12 (2), (2021) 204-227.

[9] R.K. Saxena, D.C. Gokhroo, Special functions, Jaipur Publishing House, Jaipur, 1987.

[10] M.A. Chaudhry, S.M. Zubair, *Generalized incomplete gamma functions with applications*, Journal of Computational and Applied Mathematics, 55, (1994)199-124.

[11] M.A. Chaudhry, S.M. Zubair, *On decomposition of generalized incomplete gamma functions with applications to Fourier transform*, Journal of Computational and Applied Mathematics, 59, (1995) 253-284.

[12] M.A. Chaudhry, S.M. Zubair, *On extension of generalized incomplete gamma functions with applications*, Journal of Australian Mathematical Society Series B, 37, (1996) 392-404.

[13] M.A. Chaudhry, *Transformation of extended gamma function* $\Gamma_{0,\ 2}^{2,\ 0}[(B,X)]$ *with applications to astrophysical thermonuclear functions*, Astrophysics and Space Science, 262, (1999) 263-270.

[14] U.M. Abubakar, S.R. Kabara, *A note on a new extended gamma and beta functions and their properties*, IOSR Journal of Mathematics, 15 (5), (2019) 1-6.

[15] M.A. Chaudhry, A. Qadir, M. Rafique, S.M. Zubair, *Extension of Euler's beta function*, Journal of Computational and Applied Mathematics, 78, (1997)19-32.

[16] M.A. Chaudhry, S.M. Zubair, On a class of incomplete gamma functions with application, Chapman & Hall / CRC, New York, 2002.

[17] U.M. Abubakar, S.R. Kabara, *Some results on the extension of the extended beta function*, IOSR Journal of Mathematics, 15 (5), (2019) 7-12.

[18] M.A. Chaudhry, A. Qadir, H.M. Srivastava, R.B. Paris, *Extended hyper geometric and confluent hyper geometric functions*, Journal of Computational and Applied Mathematics, 159, (2004) 589-602.

[19] D.M. Lee, A.K. Rathie, R.K. Parmar, Y.S. Kim, *Generalization of extended beta function, hypergeometric and confluent hypergeometric functions*, Homam Mathematical Journal, 33 (2), (2011)187-206.

[20] U.M. Abubakar, *A study of extended beta and associated functions connected to Fox-Wright function*, Journal of Fractional Calculus and Applications, 12(3), (2021), No:13, 1-23.

[21] M-J. Luo, G.V. Milovanovic, P. Agarwal, *Some results on the extended beta and extended hypergeometric functions*, Applied Mathematics and Computation, 248, (2014) 631-651.

[22] G.M. Mittag-Leffler, *Sur la nouvelle function* $E_\alpha(x)$, Comptes Rendus de I'Academie des Sciences Paris Series II, 11 (137), (1903) 537-539.

[23] G.M. Mittag-Leffler, *Soprala funzione* $E_\alpha(x)$, Redicoti della Academia dei Lincei, V (13), (1904) 3-5.

[24] G.M. Mittag-Leffler, *Sur larepresentation analytique d'une function monogone (inquieme note),* Acta Mathematica, 29, (1905) 237-252.

[25] A. Wiman, *Uber den fundamenta satz under theorie de function* $E_\alpha(x)$, Acta Mathematica, 29, (1950) 191-201.

[26] A. Wiman, *Uber die nullstellum de funktionen* $E_\alpha(x)$, Acta Mathematica, 29, (1950) 217- 234.

[27] T.R. Prabhakar, *A singular integral equation with a generalized Mittag-Leffler function in the kernel*, Yokohama Mathematical Journal, 19, (1971) 7-15.

[28] A.K. Shukla, J.C. Prajapati, *On a generalization of Mittag-Leffler function and its properties*, Journal of Mathematical Analysis and Applications, 336, (2007) 797-811.

[29] H.M. Srivastava, Z. Tomovski, *Functional calculus with an integral operator containing a generalized Mittag-Leffler function in the kernel*, Applied Mathematics and Computations, 211, (2009) 198-210.

[30] S. Khan, B. Agarwal, M.A. Pathan, F. Muhammad, *Evaluation of Euler type integral*, Applied Mathematics and Computation, 15, (2007), 31-49.

[31] S. Jabee, M. Shadab, R.B. Paris, *Certain results on Euler-type integrals and their applications*, Ramanujan Journal, 54, (2021), 245-260.

[32] M. Ali, W.A. Khan, I.A. Khan, *Study on double integral operator involving generalized Bessel-Maitland function*, Palestine Journal of Mathematics, 9 (2), (2020), 991-998.

[33] W.A. Khan, K.S. Nisar, M. Ahmad, *Euler type integral operator involving K-Mittag-Leffler function*, Boletim da Socidade Paranaense de Matematica, 38 (5), (2020), 165-174.

[34] M. Ghaysauddin, W.A. Khan, L.N. Mishra, *On Hankle type integral transform associated with Whittaker and hypergeometric functions*, Thai Journal of Mathematics, 19 (2), (2021), 521-527.

[35] A.P. Prudniko, Yu.A. Brychkov, O.I. Matichev, Integrals and series, Vol. 1, Gordan and Breach Science Publishers, New York, 1990.

[36] W.A. Khan, M. Ahmad, *Some Euler type beta function involving extended Mittag-Leffler function*, Palestine Journal of Mathematics, 9 (2), (2020) 969-976.

[37] S. Ahmed, M.A. Khan, *Euler type integral involving generalized Mittag-Leffler function*, Communication of Korean Mathematical Society, 29 (3), (2014) 479-487.

Journal of New Results in Science
https://dergipark.org.tr/en/pub/jnrs
Research Article
Open Access

E-ISSN:1304-7981 https://doi.org/10.54187/jnrs.970325

Molecular and morphological investigation of *Cortinarius bulliardii* from Tokat (Turkey)

Meryem Şenay Şengül Demirak[1], İbrahim Türkekul[2]

Keywords: *Cortinariaceae, ITS, LSU, Phylogenetics, Turkey,*

Subject Classification (2020):

Abstract — A macrofungi species, *Cortinarius bulliardii* is collected from Tokat city province during field trips in 2019. It has a smooth, finely light fibrous, brownish-red pileus, whitish to light lilac-brownish flesh, broadly ellipsoidal spores, light brown when young, then dark brown lamellae with age. In addition to morphological analysis, molecular sequence data based on the ITS and LSU rDNA gene regions indicated that the studied species is *Cortinarius bulliardii*.

1. Introduction

The genus *Cortinarius* (Pers.) Gray is the largest genus of the Agaricales in the world [1]. Species of *Cortinarius* have a worldwide distribution and they form ectomycorrhizal associations with some coniferous and broad-leaved trees [2–4].

Species identification in this genus based solely on morphological analysis is very confusing and may lead to false interpretations. Thus, molecular studies are important to better identify and name *Cortinarius* species correctly. The nuclear ribosomal internal transcribed spacer (ITS) is a universal barcode marker for fungal taxonomic studies [5]. It is also the most reliable marker to solve species delimitation problems of the genus *Cortinarius* [6]. Additionally, other marker regions, such as nuclear ribosomal large subunit (LSU) or largest subunits of RNA polymerase II (RPB1, RPB2) may also be used to better resolve infrasubgeneric relationship within the *Cortinarius* species [3].

More than 130 species belonging to this genus have been identified in Turkey [7]. However, molecular studies are lacking in most of these studies. A few species from this genus have been studied including molecular data, some of which are *Cortinarius conicoumbonatus* [2], *Cortinarius caerulescens* [8], *Cortinarius rapaceoides* [9], *Cortinarius rufo-olivaceus* [10] and *Cortinarius lilacinovelatus* [11]. *Cortinarius bulliardii* (Pers.) Fr. / çizik örümcekmantarı has been previously reported as list from

[1]senay.sengul@gop.edu.tr (Corresponding Author); [2]ibrahim.turkekul@gop.edu.tr
[1]Department of Molecular Biology and Genetics, Faculty of Arts & Sciences, Tokat Gaziosmanpasa University, Tokat, Turkey
[2]Department of Biology, Faculty of Arts & Sciences, Tokat Gaziosmanpasa University, Tokat, Turkey
Article History: Received: 12 Jul 2021 — Accepted: 26 Oct 2021 — Published: 31 Dec 2021

Trabzon/Akçaabat [7, 12] and Çanakkale/Bayramiç [13] regions of Turkey. However, these studies lack both molecular data and morphological description of this species.

Cortinarius bulliardii (Pers.) Fr. was first described by Fries [14]. It is characterized with a flesh, rounded, smooth and reddish-colored pileus; bulbous, cinnabar-colored stipe; whitish flesh and reddish brown at the base of the stipe; lamella broad and reddish-brown. *Cortinarius bulliardii* is reported from different regions of Europe, widely distributed within the temperate-Mediterranean Europe, and from America, Asia and north Africa [15, 16]. It usually found in deciduous forests (*Corylus*, *Quercus*, *Tilia*, *Fagus*) on calcareous soil [4, 17].

In this study, we provide description of *C. bulliardii* from Tokat city province (Turkey) based on morphological features and molecular phylogenetic analyses of the ITS and LSU gene regions. With the combination of morphological and molecular analyses, we shed light into the *Cortinarius* distribution in this continent and contribute significantly to the *Cortinarius* mycobiota of Turkey.

2. Materials and methods

2.1. Morphological analysis

The fungal specimens were collected from Tokat province during field trips in December 2019. Ecological and macroscopic features such as sizes of cap and stipe, color, odor, color change upon handle or bruising were noted in the field. Then, specimens were brought to the laboratory for chemical tests and microscopic examinations. Microscopic observations were made from dried fungarium specimens mounted in distilled water, Lactophenol, Congo red, or KOH using a light microscope. Identification of the samples was performed with the help of the literature [18]. The identified collection was deposited in the Fungarium of Department of Biology, Tokat Gaziosmanpaşa University (GOPUF).

2.2. Molecular analysis

Genomic DNA was isolated from lamella of the macrofungi using the ZR Fungal/Bacterial DNA MiniPrep kit (Zymo Research Irvine, CA, USA) as described by the manufacturer's protocol. To amplify ITS1-5.8S-ITS2 and 28S LSU gene regions, primer pairs ITS4: 5′-TCCTCCGCTTATTGATATGC-3′/ITS5: 5′-GGAAGTAAAAGTCGTAACAAGG-3′ [19] and LROR: 5′: ACCCGCTGAACTTAAGC-3′/LR5: 5′: TCCTGAGGGAAACTTCG-3′ [20] were used. The DNA was amplified in a 30 µl volume mixture using Dream Taq DNA polymerase (Thermo) using the conditions described previously [11]. PCR amplifications were verified by using 1 % agarose gel electrophoresis. PCR products were sequenced from both ends using forward and reverse primers (BM Labosis Inc., Ankara).

Chromatograms were checked for errors for each sequence and a final sequence for ITS and LSU regions were generated for further analysis. Homology based searches using Basic Local Alignment Search Tool (BLAST) program was performed to identify best matches. Accordingly, representative ITS and LSU sequences from other *Cortinarius* species were retrieved from GenBank for phylogenetic analysis. Sequence analysis, such as sequence alignments and phylogenetic trees for each genomic region were determined using MEGA 6.0 [21]. Phylogenetic trees were constructed using the maximum likelihood (ML) method where Tamura-Nei model [22] was used to construct the ML tree with bootstrap support of 1000 replicates and default settings. The bootstrap support values $\geq$ 50% were marked on the branches of the tree.

3. Results and Discussion

3.1. Taxonomy

Fungi

Basidiomycota

Cortinariaceae

Cortinarius bulliardii (Pers.) Fr., Epicrisis Systematis Mycologici: 282 (1838) (Figure 1)

Macroscopic and microscopic features:

Pileus 50-80 mm in diameter, hemispherical in youth, then conical to broad bell-shaped, wavy in age, with a long-curled edge. On the surface smooth, finely light fibrous, brownish-red, hygrophane (Figure 1a). Flesh whitish to light lilac-brownish, slightly gray-brown marbled, unchanged by oxidation, odor weak, unpleasant, taste mild, radish. Lamellae in number 45-57, attached to the friction, light brown in youth, then dark brown. Stipe 60-110 × 6-10 mm, at the base up to 25 mm wide. Surface dry, fibrous, grayish-white in the upper part, noticeably in the lower half towards the base orange (Figure 1a). Spores broadly ellipsoidal, on the surface with warty, coarse, and low ornamentation, 8-11 × 5-7 µm, (Figure 1b). Basidia tetrasporic, clavate, 25-35 × 8.5-11 µm, with basal clamp (Figure 1c). Terminal cells 3.5-10 µm across, hyaline to reddish-brown and lightly encrusted in places septa with clamps (Figure 1d).

Specimen examined: TURKEY, Tokat province, Akbelen village, in *Quercus* spp. forests, on calcareous soil. 40°27'55"N, 36°38'24"E, 1079 m, 08.12.2019, GOPUF HIS-23, GenBank MZ291672 and MZ291697.

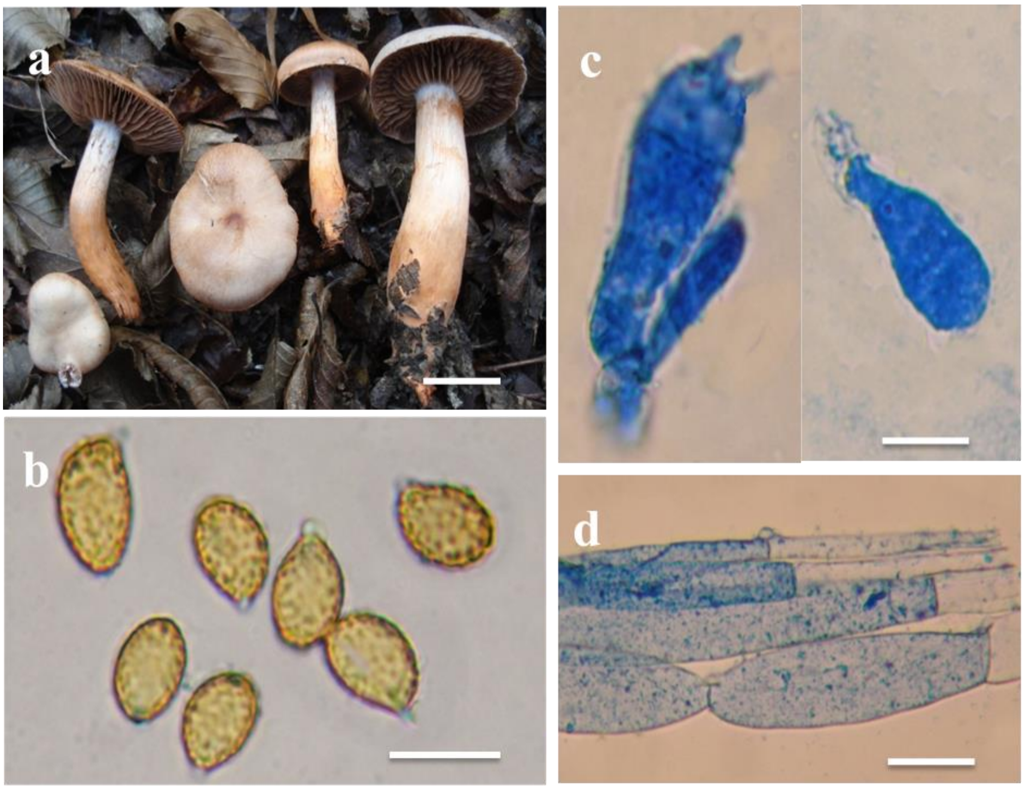

Figure 1. *Cortinarius bulliardii* (Collection HIS-23): a- basidiomata in situ, b- basidiospores, c- basidia, d- pileipellis (Scale bars: a = 30 mm; b-d = 10 µm).

Fries [14] indicated that *Cortinarius colus* Fr. is similar to *Cortinarius bulliardii* (Pers.) Fr. although it has a much pale and decurrent lamellae, a narrow stipe and it is a much smaller fungus when compared to *C. bulliardii*. Moreover, *Cortinarius colus* is a species found in pine forests while *C. bulliardii* is normally associated with *Corylus*, *Quercus* and *Fagus*. Other closely related species to *C. bulliardii* are *C. cinnabarinus* Fr. and *C. coccineus* Reumaux, which are mostly found in mixed forests of hardwoods in Europe [23]. These two species are regarded as the orange-to-orange red species of subgenus *Telamonia* [23]. *Cortinarius cinnabarinus* has a cinnabar red to brownish red whole fruiting body, brownish red flesh, and smaller spores, while *C. bulliardii* is recognized by saturated red brown cap, cinnabar red base of its stipe, grayish brown flesh and larger spores [17]. *Cortinarius coccineus* also differs from *C. bulliardii* by its dull reddish to dark brown or blackish lamellae, strongly orange red stipe, and smaller spores [23, 24].

3.2. Molecular Phylogeny

About 600 bp ITS and 881 bp LSU genomic rDNA sequences were determined from the studied sample and the sequences were deposited at GenBank under the accession numbers, MZ291672 and MZ291697, respectively.

Blast search with ITS sequence showed high sequence similarity (98 %) with *C. bulliardii* (GenBank No. JX114942) from Sweden. Blast search with LSU also gave a high sequence similarity (100 %) *to C. bulliardii* (GenBank No. AF388782). Other sequences that showed significant similarity with our ITS and LSU query sequences were also retrieved for phylogenetic analysis. Maximum likelihood (ML) tree was constructed separately for each gene region (Figure 2 and Figure 3). Each tree clearly showed a well-supported clade for *C. bulliardii* species from different locations. In the ITS tree, *C. cinnabarinus* and *C. coccineus* form a clade with *C. bulliardii*, while *C. californicus*, *C. hesleri* and *C. coracis* form a distant clade to *C. bulliardii* (Figure 2). *Cortinarius neosanguineus* was used as the outgroup species to root the trees.

Molecular phylogenetic analysis showed that *C. cinnabarinus* and *C. bulliardii* are monophyletic and *C. coccineus* was basal to the clade including *C. bulliardii* and *C. cinnabarinus*. *Cortinarius hesleri* is the distant species to *C. bulliardii* but more closely related to *C. californicus*. Although *C. cinnabarinus* is genetically the most closely related species to *C. bulliardii*, they have distinctive morphological features as mentioned above. Our phylogenetic results are also in agreement with that of Ammirati et al. [23].

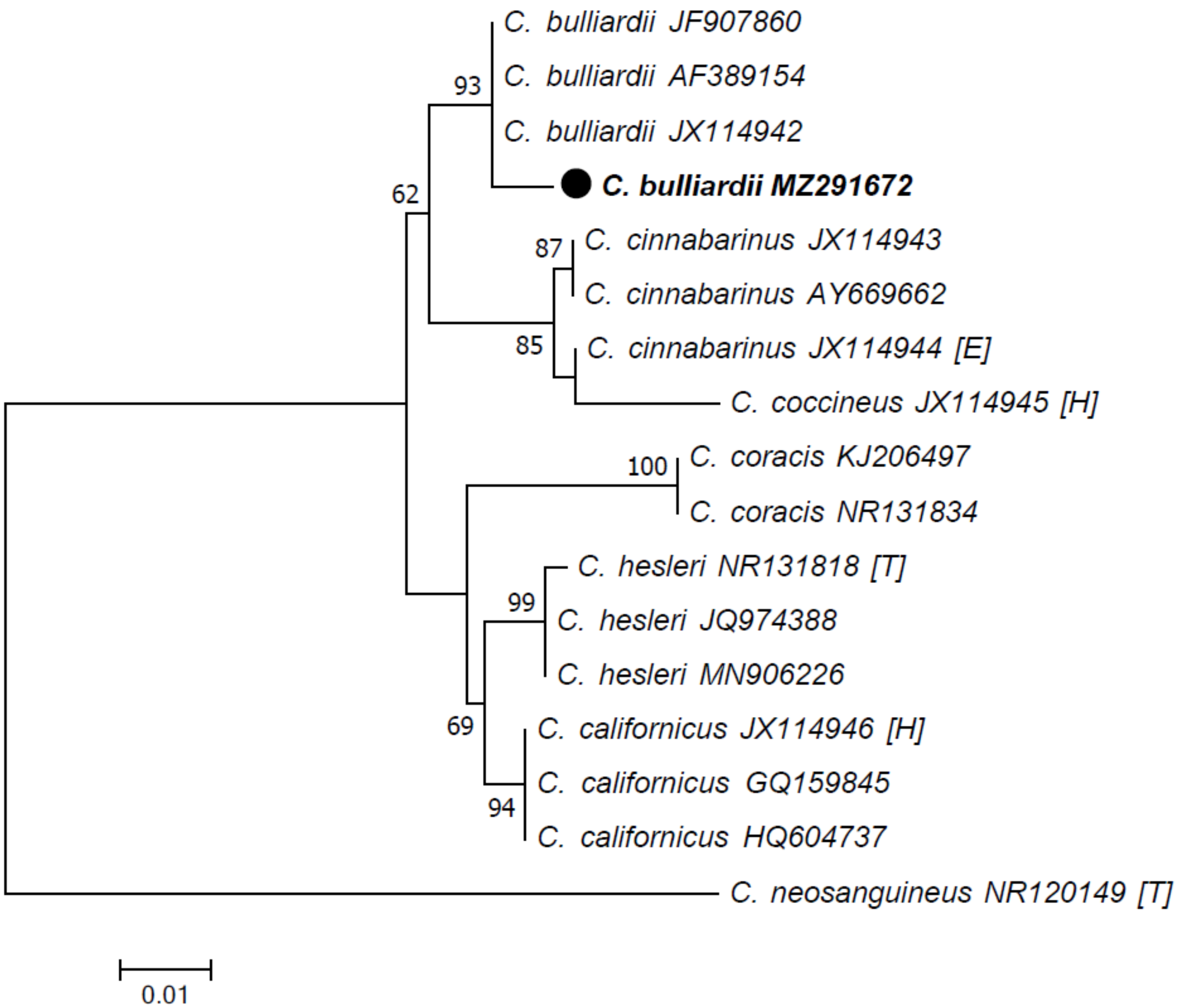

Figure 2. ITS sequence-based phylogeny of *Cortinarius bulliardii* using ML method. The studied specimen is indicated with black circle and in bold. *Cortinarius neocanguineus* was the outgroup species. Bootstrap support values ≥ 50% from ML analysis were shown on the branches. Bar indicates 0.01 expected change per site per branch. E: epitype, H: holotype, T: type

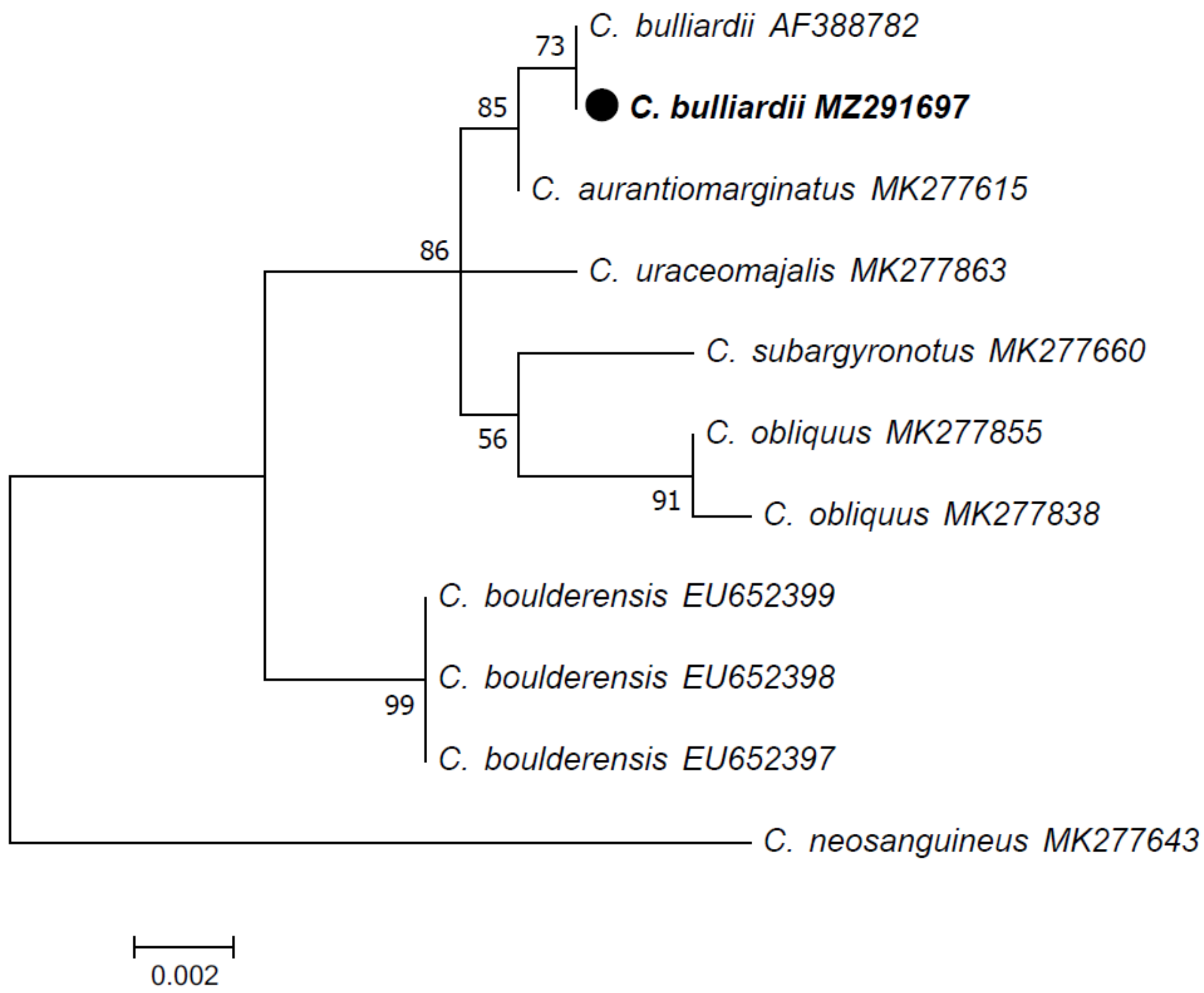

Figure 3. LSU sequence-based phylogeny of *Cortinarius bulliardii* using ML method. The studied specimen is indicated with black circle and in bold. *Cortinarius neocanguineus* was the outgroup species. Bootstrap support values ≥ 50% from ML analysis were shown on the branches. Bar indicates 0.002 expected change per site per branch.

4. Conclusion

Cortinarius bulliardii is described from Tokat city province, Turkey, including both its morphological features and molecular data. The phylogenetic relationship and biogeographical patterns of *C. bulliardii* are discussed. We hope more ITS barcoding data are produced for other *Cortinarius* species from Turkey to better understand speciation in the genus *Cortinarius* and their distribution in this continent which has high biological diversity.

Author Contributions

All authors contributed equally to this work. They all read and approved the final version of the manuscript.

Conflicts of Interest

The authors declare no conflict of interest.

Acknowledgement

This work was supported by the Office of Scientific Research Projects Coordination at Tokat Gaziosmanpaşa University, Grant number: 2019/87.

References

[1] P. M. Kirk, P. F. Cannon, D. W. Minter, J. A. Stalpers, Dictionary of the fungi, 10th edn. CAB International, Wallingford, UK, 2008.

[2] E. Sesli, K. Liimatainen, *Cortinarius conicoumbonatus (Cortinarius subgen. Telamonia sect. Hinnulei): a new species from spruce-beech forests of the East Black Sea Region of Turkey*, Turkish Journal of Botany, 42, (2018) 327–334.

[3] K. Soop, B. Dima, J. A. Cooper, D. Park, B. Oertel, *A phylogenetic approach to a global supraspecific taxonomy of Cortinarius (Agaricales) with an emphasis on the southern mycota*, Persoonia, 42, (2019) 261–290.

[4] K. Liimatainen, T. Niskanen, B. Dima, J. F. Ammirati, P. M. Kirk, I. Kytövuori, *Mission impossible completed: unlocking the nomenclature of the largest and most complicated subgenus of Cortinarius, Telamonia*, Fungal Diversity, 104(1), (2020) 291–331.

[5] C. L. Schoch, K. A. Seifert, S. Huhndorf, V. Robert, J. L. Spouge, C. A. Levesque, W. Chen, *Fungal Barcoding Consortium, Nuclear ribosomal internal transcribed spacer (ITS) region as a universal DNA barcode marker for Fungi*, Proceedings of the National Academy of Sciences USA, 109, (2012) 6241–6246.

[6] S. Garnica, M. E. Schön, K. Abarenkov, K. Riess, K. Liimatainen, T. Niskanen, B. Dima, K. Soop, T. G. Frøslev, T. S. Jeppesen, U. Peintner, R. Kuhnert-Finkernagel, T. E. Brandrud, G. Saar, B. Oertel, J. F. Ammirati, *Determining threshold values for barcoding fungi: lessons from Cortinarius (Basidiomycota), a highly diverse and widespread ectomycorrhizal genus*, FEMS Microbiology Ecology, 92 (4), (2016) fiw045.

[7] E. Sesli , A. Asan, F. Selçuk (eds.) Ö. Abacı Günyar, I. Akata, H. Akgül, S. Aktaş, S. Alkan, H. Allı, H. Aydoğdu, D. Berikten, K. Demirel, R. Demirel, H. H. Doğan, M. Erdoğdu, C. C. Ergül, G. Eroğlu, G. Giray, A. Halikî Uztan, Ş. Kabaktepe, D. Kadaifçiler, F. Kalyoncu, İ. Karaltı, G. Kaşık, A. Kaya, A. Keleş, S. Kırbağ, M. Kıvanç, İ. Ocak, S. Ökten, E. Özkale, C. Öztürk, M. Sevindik, B. Şen, İ. Şen, İ. Türkekul, M. Ulukapı, Ya. Uzun, Yu. Uzun, A. Yoltaş, The Checklist of Fungi of Turkey, Ali Nihat Gökyiğit Vakfı Yayını, İstanbul, 2020.

[8] A. Kalmer, İ. Acar, A. Dizkırıcı Tekpınar, *Phylogenetic and taxonomic studies on Cortinarius caerulescens (Schaeff.) Fr. a new record for Turkish mycota*, The Journal of Fungus 10, (2019) 8–16.

[9] M. S. Sengul Demirak, H. Isik, *Cortinarius rapaceoides, a new record for Turkey*, Mycotaxon, 135, (2020) 559–568.

[10] M. S. Şengül Demirak, H. Işık, İ. Türkekul, İ., *Morphological and Molecular Phylogeny of Cortinarius rufo-olivaceus (Pers.) Fr. (subgenus Phlegmacium sect. Calochroi) Collected from Tokat Region*. KSU Journal of Agriculture and Nature, 23(3), (2020) 600–605.

[11] M. S. Sengul Demirak, I. Turkekul, *Cortinarius lilacinovelatus (Agaricales, Cortinariaceae)–A new record for Turkey*, Nova Hedwigia, (2021) 217–227.

[12] S. Baydar, E. Sesli, *The macromycetes determined in Akçaabat District of Trabzon Province*, Turkish Journal of Botany 18, (1994) 99–101.

[13] N. Adanacıoğlu, Ü. Yıldız, O. Erdinç, L. Aykas, A. Tan, T. Taylan, *Türkiye makromantarı genetik kaynakları I. Ege Bölgesi*, Anadolu Ege Tarımsal Araştırma Enstitüsü Dergisi, 26(1), (2016) 46–61.

[14] E. M. Fries, Epicrisis Systematis Mycologici, 282, Uppsala, Sweden, 1838.

[15] T. Tejklová, J. Kramoliš, Pavučinec Bulliardův-Cortinarius bulliardii, nápadný druh teplomilných dubohabřin, Mykologický Sborník 3, 2016.

[16] G. J. Krieglsteiner, A. Gminder, Die GroGpilze Baden-Wiirttembergs. Band 5: Standerpilze: Blatterpilze III. Eugen Ulmer KG, Stuttgart, 671 p., 2010.

[17] T. Niskanen, I. Kytövuori, E. Bendiksen, K. Bendiksen, T. E. Brandrud, T. G. Frøslev, K. Høiland, T. S. Jeppesen, K. Liimatainen, H. Lindström, *Cortinarius* (Pers) Gray. In: Knudsen H, Vesterholt J (eds). Funga Nordica, 2nd revised edition. Agaricoid, boletoid, clavarioid, cyphelloid and gastroid genera, Nordsvamp, Copenhagen, Denmark, (2012), pp 762–763.

[18] J. Breitenbach, F. Kränzlin, Fungi of Switzerland (Vol. 5), Lucerne, Switzerland: Verlag Mykologia, 2000.

[19] T. J. White, T. Bruns, S. J. Lee, J. Taylor, *Amplification, and direct sequencing of fungal ribosomal RNA genes for phylogenetics*, In: Innis MA, Gelfand DH, Sninsky JJ, White TJ, editors. PCR protocols: a guide to methods and applications. New York, NY, USA: Academic Press, pp. 315–322, 1990.

[20] R. Vilgalys, M. Hester, *Rapid genetic identification, and mapping of enzymatically amplified ribosomal DNA from several Cryptococcus species*, Journal of Bacteriology, 172(8), (1990) 4238–4246.

[21] K. Tamura, G. Stecher, D. Peterson, A. Filipski, S. Kumar, *MEGA6: molecular evolutionary genetics analysis version 6.0.*, Molecular Biology and Evolution, 30, (2013) 2725–2729.

[22] K. Tamura, M. Nei, *Estimation of the number of nucleotide substitutions in the control region of mitochondrial DNA in humans and chimpanzees*, Molecular Biology and Evolution, 10(3), (1993) 512–526.

[23] J. F. Ammirati, K. W. Hughes, K. Liimatainen, T. Niskanen, P. B. Matheny, *Cortinarius hesleri from eastern North America and related species from Europe and western North America*, Botany, 91(2), (2013) 91–98.

[24] A. Bidaud, P. Moënne-Loccoz, P. Reumaux. Atlas des *Cortinaires*, Pars VI, Èditions Fèdération mycologique Dauphiné-Savoie, France, 1994.

Journal of New Results in Science 10(3) (2021) 19-33

Journal of New Results in Science

https://dergipark.org.tr/en/pub/jnrs

Research Article

Open Access

E-ISSN: 1304-7981 https://doi.org/10.54187/jnrs.974667

Local fractional Elzaki transform and its application to local fractional differential equations

Djelloul Ziane[1], **Mountassir Hamdi Cherif**[2]

Keywords
Local fractional calculus, General integral transforms, local fractional differential equations

Abstract — The objective of our work is to couple the Elzaki transform method and the local fractional derivative which is called local fractional Elzaki transform, where we have provided important results of this transformation as local fractional Laplace-Elzaki duality, Elzaki transform of the local fractional derivative and the local fractional integral and the local fractional convolution, also we have presented the properties of some special functions with the local fractional derivative sense. The Elzaki transform was applied to solve some linear local fractional differential equations in order to obtain non-differentiable analytical solutions. The results of the solved examples show the effectiveness of the proposed method.

Subject Classification (2020): 44A05, 44A20.

1. Introduction

The integral transformations play a crucial role in the resolution of ordinary differential equations, partial differential equations and in the resolution of integral differential equations with integer order or fractional order. They are also widely used by engineers to solve the linear differential equations, the systems of linear partial differential equation, and determine the transfer function of a linear system.

The Laplace transform method [1], the Fourier transform method [2], the Hankel transform method [3], and the Mellin transform method [4] are among the most well-known transformations. Other transformations that have recently appeared include for example the Sumudu transform method [5], the Natural transform method [6], the Elzaki transform method [7–10], the Aboodh transform method [11], the ZZ-transform method [12], the Shehu transform method [13], and others.

Tarig M. Elzaki et al. developed the Elzaki transform method in 2011 from the classical Fourier integral [7], based on the Elzaki transform's mathematical simplicity and fundamental features. This transform has been used by many researchers to facilitate the process of solving the ordinary differential equations without and with variable coefficients [14–17], the higher order differential equations [18], the integro-differential

[1]djeloulz@yahoo.com; [2]mountassir27@yahoo.fr(Corresponding Author)
[1]Faculty of exact sciences and informatics, pole of Ouled Fares, Hassiba Benbouali University of Chlef, Algeria.
[2]Laboratory of complex systems, Oran's Hight School of Electrical and Energetics Engineering (ESGEE-Oran), Oran, Algeria.
[1,2]Laboratory of mathematics and its applications (LAMAP), university of Oran1, Oran, Algeria.
Article History: Received: 26 Jul 2021 - Accepted: 06 Dec 2021 - Published: 31 Dec 2021

equations [19–22] and to the partial differential equations [23–27] in the time domain. Several works have been made by using the Elzaki transform method and its combination with other methods to solve the linear and nonlinear differential equations with the concept of fractional operator, for example the fractional order differential equation arising in RLC electrical circuit, the fractional Porous Medium equation, the fractional higher dimensional initial boundary value problems [28–32].

In this work, we will based on the notion of local fractional operator by presented some important results and properties of the local fractional Elzaki transform and we will extend and applied it to solve the linear differential equations with local fractional derivative. We supported our work, with illustrative examples showing how to apply this transformation to the differential equations on Cantor sets.

2. Basic of local fractional calculus

We present the basic definitions and theorems of local fractional derivative, local fractional integral, local fractional Taylor's series and local fractional Laplace transform method.

Definition 2.1. [33–35] Let $f(x) \in C_\sigma(a,b)$, so

$$\left|f(x)-f(x_0)\right| < \epsilon^\sigma, \ \ 0<\sigma\leqslant 1, \tag{2.1}$$

with $|x-x_0|<\delta$, for $\epsilon, \delta \in \mathbb{R}_+^*$. $f(x)$ is local fractional continuous.

Definition 2.2. [33–35] The local fractional derivative of $f(x)$ of order σ at $x = x_0$ is

$$f^{(\sigma)}(x) = \left.\frac{d^\sigma f}{dx^\sigma}\right|_{x=x_0} = \lim_{x\to x_0} \frac{\Delta^\sigma (f(x)-f(x_0))}{(x-x_0)^\sigma}, \ \ 0<\sigma\leqslant 1, \tag{2.2}$$

where

$$\Delta^\sigma (f(x)-f(x_0)) \cong \Gamma(1+\sigma)\left[(f(x)-f(x_0))\right]. \tag{2.3}$$

The local fractional partial differential operator of order σ was given by

$$\frac{\partial^\sigma w(x_0,t)}{\partial t^\sigma} = \lim_{x\to x_0} \frac{\Delta^\sigma (w(x_0,t)-w(x_0,t_0))}{(t-t_0)^\sigma}, \tag{2.4}$$

where

$$\Delta^\sigma (u(x_0,t)-u(x_0,t_0)) \cong \Gamma(1+\sigma)\left[u(x_0,t)-u(x_0,t_0)\right]. \tag{2.5}$$

Definition 2.3. [33–35] The local fractional integral of $f(x)$ of order σ is

$$\begin{aligned} {}_aI_b^{(\sigma)} f(x) &= \frac{1}{\Gamma(1+\sigma)} \int_a^b f(t)(dt)^\sigma \\ &= \frac{1}{\Gamma(1+\sigma)} \lim_{\Delta t\longrightarrow 0} \sum_{j=0}^{N-1} f(t_j)(\Delta t_j)^\sigma, \end{aligned} \tag{2.6}$$

where $\Delta t_j = t_{j+1}-t_j$, $\Delta t = \max\{\Delta t_0,\ \Delta t_1,\ \Delta t_2, \cdots\}$ and $\left[t_j, t_{j+1}\right]$, $t_0 = a$, $t_N = b$, is a partition of the interval $[a,b]$.

Definition 2.4. [35–37] The local fractional Laplace transform of $f(x)$ of order σ is given by

$$L_\sigma\left\{f(x)\right\} = F_\sigma(s) = \frac{1}{\Gamma(1+\sigma)}\int_0^\infty E_\sigma(-s^\sigma x^\sigma)f(x)(dx)^\sigma. \tag{2.7}$$

If $LFL_\sigma\left\{f(x)\right\} = F_\sigma(s)$, so the inverse formula of (2.7) is

$$f(x) = L_\sigma^{-1}\left\{F_\sigma(s)\right\} = \frac{1}{(2\pi)^\sigma}\int_{\beta-i\infty}^{\beta+i\infty} E_\sigma(s^\sigma x^\sigma)F_\sigma(s)(ds)^\sigma, \tag{2.8}$$

$s^\sigma = \beta^\sigma + i^\sigma\infty^\sigma$, i^σ is the fractal imaginary unit and $\mathrm{Re}(s) = \beta > 0$.

Theorem 2.5. [34] If $L_\sigma\left\{f(x)\right\} = F_\sigma(s)$, then one has

$$L_\sigma\left\{f^{(\sigma)}(x)\right\} = s^\sigma L_\sigma\left\{f(x)\right\} - f(0). \tag{2.9}$$

Proof.
see [34]

Theorem 2.6. [34] If $L_\sigma\left\{f(x)\right\} = F_\sigma(s)$, so

$$L_\sigma\left\{{}_0I_x^\sigma f(x)\right\} = \frac{1}{s^\sigma}L_\sigma\left\{f(x)\right\}. \tag{2.10}$$

Proof.
see [34]

Theorem 2.7. [34] If $L_\sigma\left\{f(x)\right\} = F_\sigma(s)$ and $L_\sigma\left\{g(x)\right\} = G_\sigma(s)$, then one has

$$L_\sigma\left\{f(x) * g(x)\right\} = F_\sigma(z)G_\sigma(z), \tag{2.11}$$

where

$$f(x) * g(x) = \frac{1}{\Gamma(1+\sigma)}\int_0^\infty f(t)g(x-t)(dt)^\sigma. \tag{2.12}$$

Proof.
see [34]

Theorem 2.8. [38] Let $f(x) \in C_\sigma[a,b]$, so there is a function

$$\Pi(x) = {}_aI_x^{(\sigma)}f(x),$$

its derivative with respect to $(dx)^\rho$ is

$$\frac{d^\sigma\Pi(x)}{(dx)^\sigma} = f(x),\ a \leqslant x \leqslant b.$$

Proof.
see [38]

3. Main Result

Now, we present the local fractional Elzaki transform method ($LFET$) and some properties are discussed. If there is a new transform operator $LFE_\sigma : f(x) \longrightarrow T_\sigma(v)$, namely

$$LFE_\sigma \left\{f(x)\right\} = LFE_\sigma \left\{\sum_{k=0}^{\infty} a_k x^{k\sigma}\right\} = \sum_{k=0}^{\infty} \Gamma(1+k\sigma)\, a_k v^{k\sigma+2\sigma}. \tag{3.1}$$

For example if $f(x) = E_\sigma(i^\sigma x^\sigma)$, we obtain

$$LFE_\sigma \left\{E_\sigma(i^\sigma x^\sigma)\right\} = LFE_\sigma \left\{\sum_{k=0}^{\infty} \frac{i^{k\sigma} x^{k\sigma}}{\Gamma(1+k\sigma)}\right\} \tag{3.2}$$

$$= \sum_{k=0}^{\infty} i^{k\sigma} v^{k\sigma+2\sigma}, \tag{3.3}$$

and if $f(x) = \frac{x^\sigma}{\Gamma(1+\sigma)}$, we get

$$LFE_\sigma \left\{\frac{x^\sigma}{\Gamma(1+\sigma)}\right\} = v^{3\sigma}. \tag{3.4}$$

These results can be generalized by this definition.

Definition 3.1. The local fractional Elzaki transform of $f(x)$ of order σ is defined as

$$LFE_\sigma \left\{f(x)\right\} = T_\sigma(v) = \frac{1}{\Gamma(1+\sigma)} v^\sigma \int_0^\infty E_\sigma(-\frac{x^\sigma}{v^\sigma}) f(x)(dx)^\sigma,\ 0 < \sigma \leqslant 1. \tag{3.5}$$

The inverse transformation can be obtained as follows

$$LFE_\sigma^{-1}\left\{ T_\sigma(v)\right\} = f(x). \tag{3.6}$$

Theorem 3.2. (linearity).
If $LFE_\sigma \left\{f(x)\right\} = F_\sigma(v)$ and $LFE_\sigma \left\{g(x)\right\} = G_\sigma(v)$, then one has

$$LFE_\sigma \left\{\lambda f(x) + \mu g(x)\right\} = \lambda F_\sigma(v) + \mu G_\sigma(v), \tag{3.7}$$

where λ and μ are constant.

Proof.
Using formula (3.5), we obtain

$$\begin{aligned}
LFE_{\sigma}\left\{\lambda f(x)+\mu g(x)\right\} &= \frac{v^{\sigma}}{\Gamma(1+\sigma)}\int_{0}^{\infty}E_{\sigma}(-\frac{x^{\sigma}}{v^{\sigma}})\left\{\lambda f(x)+\mu g(x)\right\}(dx)^{\sigma} \\
&= \frac{v^{\sigma}}{\Gamma(1+\sigma)}\int_{0}^{\infty}\left[E_{\sigma}(-\frac{x^{\sigma}}{v^{\sigma}})\left(\lambda f(x)\right)+E_{\sigma}(-\frac{x^{\sigma}}{v^{\sigma}})\left(\mu g(x)\right)\right](dx)^{\sigma} \\
&= \lambda\frac{v^{\sigma}}{\Gamma(1+\sigma)}\int_{0}^{\infty}E_{\sigma}(-\frac{x^{\sigma}}{v^{\sigma}})f(x)(dx)^{\sigma}+\mu\frac{v^{\sigma}}{\Gamma(1+\sigma)}\int_{0}^{\infty}E_{\sigma}(-\frac{x^{\sigma}}{v^{\sigma}})g(x)(dx)^{\sigma} \\
&= \lambda LFE_{\sigma}\left\{f(x)\right\}+\ \mu LFE_{\sigma}\left\{g(x)\right\}.
\end{aligned}$$

This ends the proof.

Theorem 3.3. (local fractional Elzaki-Laplace and Laplace-Elzaki duality).
If $L_{\sigma}\left\{f(x)\right\}=F_{\sigma}(s)$ and $LFE_{\sigma}\left\{g(x)\right\}=T_{\sigma}(v)$, then one has

$$LFE_{\sigma}\left\{f(x)\right\}=v^{\sigma}F_{\sigma}\left(\frac{1}{v}\right). \tag{3.8}$$

$$L_{\sigma}\left\{f(x)\right\}=s^{\sigma}T_{\sigma}(\frac{1}{s}). \tag{3.9}$$

Proof.
We show the formula (3.8). Using the formula (3.5) gives

$$\begin{aligned}
LFE_{\sigma}\left\{f(x)\right\} &= v^{\sigma}\frac{1}{\Gamma(1+\alpha)}\int_{0}^{\infty}E_{\sigma}\left(-\frac{x^{\sigma}}{v^{\sigma}}\right)f(x)(dx)^{\sigma} \\
&= v^{\sigma}\frac{1}{\Gamma(1+\sigma)}\int_{0}^{\infty}E_{\sigma}\left(-\left(\frac{1}{v}\right)^{\sigma}x^{\sigma}\right)f(x)(dx)^{\sigma} \\
&= v^{\sigma}F_{\sigma}\left(\frac{1}{v}\right).
\end{aligned}$$

Proof of the formula (3.9). We have

$$T_{\sigma}(v)=v^{\sigma}F_{\sigma}\left(\frac{1}{v}\right).$$

By substituting $v=\frac{1}{s}$, we obtain

$$T_{\sigma}\left(\frac{1}{s}\right)=\frac{1}{s^{\sigma}}F_{\sigma}(s),$$

then

$$F_{\sigma}(s)=s^{\sigma}T_{\sigma}\left(\frac{1}{s}\right),$$

therefore, we get

$$L_{\sigma}\left\{f(x)\right\}=s^{\sigma}T_{\sigma}\left(\frac{1}{s}\right).$$

This ends the proof.

Theorem 3.4. (Elzaki transform of local fractional derivative).
If $LFE_{\sigma}\left\{f(x)\right\} = T_{\sigma}(v)$, so

$$LFE_{\sigma}\left\{D_{0+}^{\sigma}f(x)\right\} = \frac{1}{v^{\sigma}}T_{\sigma}(v) - v^{\sigma}f(0),\ 0<\sigma\leqslant 1, \tag{3.10}$$

and

$$LFE_{\sigma}\left\{D_{0+}^{n\sigma}f(x)\right\} = \frac{1}{v^{n\sigma}}T_{\sigma}(v) - \sum_{k=0}^{n-1} v^{(k-n+2)\sigma}f^{(k\sigma)}(0),\ 0<\sigma\leqslant 1. \tag{3.11}$$

Proof.
We proof the formula (3.10). Using the formula (3.8) and the integration by parts [41], we get the following

$$\begin{aligned}
LFE_{\sigma}\left\{f^{(\sigma)}(x)\right\} &= v^{\sigma}F_{\sigma}\left(\frac{1}{v}\right) = \frac{v^{\sigma}}{\Gamma(1+\sigma)}\int_{0}^{\infty}E_{\sigma}(-\frac{x^{\sigma}}{v^{\sigma}})f^{(\sigma)}(x)(dx)^{\sigma}\\
&= \frac{v^{\sigma}}{\Gamma(1+\sigma)}\left(\left[-\Gamma(1+\sigma)f(0)\right] + \frac{1}{v^{\sigma}}\lim_{t\longrightarrow\infty}\int_{0}^{t}E_{\sigma}(-\frac{x^{\sigma}}{v^{\sigma}})f(x)(dx)^{\sigma}\right)\\
&= -v^{\sigma}f(0) + \frac{1}{v^{\sigma}}\left(\frac{v^{\sigma}}{\Gamma(1+\sigma)}\int_{0}^{\infty}E_{\sigma}(-\frac{x^{\sigma}}{v^{\sigma}})f(x)(dx)^{\sigma}\right)\\
&= \frac{1}{v^{\sigma}}T_{\sigma}(v) - v^{\sigma}f(0).
\end{aligned}$$

To demonstrate the validity of (3.11), we use the mathematical induction.

If $n=1$ and according to (3.11), we have

$$LFE_{\sigma}\left\{D_{0+}^{\sigma}f(x)\right\} = \frac{1}{v^{\sigma}}T_{\sigma}(v) - v^{\sigma}f(0),$$

so, according to (3.10), we note that the formula holds when $n=1$.

Assume inductively that the formula holds for n, we get

$$LFE_{\sigma}\left\{D_{0+}^{n\sigma}f(x)\right\} = \frac{1}{v^{n\sigma}}T_{\sigma}(v) - \sum_{k=0}^{n-1} v^{(k-n+2)\sigma}f^{(k\sigma)}(0). \tag{3.12}$$

It remains to show that (3.11) is true for $n+1$. Let $D_{0+}^{n\sigma}f(x) = g(x)$ and according to (3.10) and (3.12), we have

$$\begin{aligned}
LFE_{\sigma}\left[D_{0+}^{(n+1)\sigma}f(x)\right] &= LFE_{\sigma}\left[D_{0+}^{\sigma}g(x)\right] = \frac{1}{v^{\sigma}}G_{\sigma}(v) - v^{\sigma}g(0)\\
&= \frac{1}{v^{\sigma}}\left[\frac{1}{v^{n\sigma}}T_{\sigma}(v) - \sum_{k=0}^{n-1} v^{(k-n+2)\sigma}f^{(k\sigma)}(0)\right] - v^{\sigma}g(0)\\
&= \frac{1}{v^{(n+1)\sigma}}T_{\sigma}(v) - \sum_{k=0}^{n-1} v^{(k-n+1)\sigma}f^{(k\sigma)}(0) - v^{\sigma}f^{(n\sigma)}(x)\\
&= \frac{1}{v^{(n+1)\sigma}}T_{\sigma}(v) - \sum_{k=0}^{n} v^{(k-n+1)\sigma}f^{(k\sigma)}(0).
\end{aligned}$$

Therefore the formula (3.11) is true for $n+1$. Thus by the principle of mathematical induction, for all $n \geqslant 1$ the formula (3.11) holds.

Theorem 3.5. (Elzaki transform of local fractional integral).
If $LFE_\sigma\left\{f(x)\right\} = T_\sigma(v)$, so

$$LFE_\alpha\left\{{}_0I_x^{(\sigma)} f(x)\right\} = v^\sigma T_\sigma(v). \tag{3.13}$$

Proof.
Let $H(x) = {}_0I_x^{(\sigma)} f(x)$. According to the (theorem 3.2.9, [38]), we get

$$D_{0+}^\sigma H(x) = f(x), \tag{3.14}$$

and $H(0) = 0$.

Taking the local fractional Elzaki transform on both sides of (3.14), we have

$$LFE_\sigma\left\{D_{0+}^\sigma H(x)\right\} = LFE_\sigma\left\{f(x)\right\}.$$

Which give

$$\frac{1}{v^\sigma} LFE_\sigma\left\{H(x)\right\} = T_\sigma(v),$$

because $H(0) = 0$, and $LFE_\sigma\left\{f(x)\right\} = T_\sigma(v)$.

Thus we get

$$LFE_\sigma\left\{{}_0I_x^{(\sigma)} f(x)\right\} = v^\sigma T_\sigma(v).$$

Theorem 3.6. (local fractional convolution).
If $LFE_\sigma\left\{f(x)\right\} = T_\sigma(v)$ and $LFE_\sigma\left\{g(x)\right\} = G_\sigma(v)$,

then one has

$$LFE_\sigma\left\{\left(f(x) * g(x)\right)_\sigma\right\} = \frac{1}{v^\sigma} T_\sigma(v) G_\sigma(v), \tag{3.15}$$

where

$$\left(f(x) * g(x)\right)_\sigma = \frac{1}{\Gamma(1+\sigma)} \int_0^\infty f(\theta) g(r-\theta) (dr)^\sigma.$$

Proof.
The Laplace transform of fractional order of the function $\left(f(x)*g(x)\right)_{\sigma}$ is

$$L_{\sigma}\left\{\left(f(x)*g(x)\right)_{\sigma}\right\}=L_{\sigma}\left\{f(x)\}L_{\sigma}\{g(x)\right\}.$$

Using the formula (3.8) gives

$$\begin{aligned}
LFE_{\sigma}\left\{\left(f(x)*g(x)\right)_{\sigma}\right\} &= v^{\sigma}L_{\sigma}\{f(x)*g(x)\} \\
&= v^{\sigma}L_{\sigma}\{f(x)\}L_{\sigma}\{g(x)\} \\
&= \frac{1}{v^{\sigma}}\left(v^{\sigma}L_{\sigma}\{f(x)\}v^{\sigma}L_{\sigma}\{g(x)\}\right) \\
&= \frac{1}{v^{\sigma}}T_{\sigma}(v)G_{\sigma}(v).
\end{aligned}$$

This completes the proof.

3.1. Local fractional Elzaki transform of somes special functions

In the all following results, we relied on the formula (3.5), and some of the results found in the references [39–41].

1) If $f(x)=1$, we get

$$\begin{aligned}
LFE_{\sigma}\{1\} &= \frac{1}{\Gamma(1+\sigma)}v^{\sigma}\int_0^{\infty}E_{\sigma}\left(-\frac{x^{\sigma}}{v^{\sigma}}\right)(dx)^{\sigma} \\
&= v^{\sigma}\lim_{t\longrightarrow\infty}\left[-v^{\sigma}E_{\sigma}\left(-\frac{x^{\sigma}}{v^{\sigma}}\right)\right]_0^t \\
&= v^{2\sigma}.
\end{aligned}$$

2) If $f(x)=\frac{x^{\sigma}}{\Gamma(1+\sigma)}$ $(0<\sigma\leqslant 1)$, by using the integration by parts [41], we obtain the following

$$\begin{aligned}
LFE_{\sigma}\left\{\frac{x^{\sigma}}{\Gamma(1+\sigma)}\right\} &= \frac{1}{\Gamma(1+\sigma)}v^{\sigma}\int_0^{\infty}E_{\sigma}\left(-\frac{x^{\sigma}}{v^{\sigma}}\right)\frac{x^{\sigma}}{\Gamma(1+\sigma)}(dx)^{\sigma} \\
&= \frac{v^{\sigma}}{\Gamma(1+\sigma)}\lim_{t\longrightarrow\infty}\left(\int_0^t\left(-v^{\sigma}E_{\sigma}\left(-\frac{x^{\sigma}}{v^{\sigma}}\right)\right)^{(\sigma)}\frac{x^{\sigma}}{\Gamma(1+\sigma)}(dx)^{\sigma}\right) \\
&= v^{\sigma}\lim_{t\longrightarrow\infty}\left(\left[-v^{\sigma}E_{\sigma}\left(-\frac{x^{\sigma}}{v^{\sigma}}\right)\frac{x^{\sigma}}{\Gamma(1+\sigma)}\right]_0^t+\frac{v^{\sigma}}{\Gamma(1+\sigma)}\int_0^tE_{\sigma}\left(-\frac{x^{\sigma}}{v^{\sigma}}\right)(dx)^{\sigma}\right) \\
&= \lim_{t\longrightarrow\infty}\left(v^{2\sigma}\left[-v^{\sigma}E_{\sigma}\left(-\frac{x^{\sigma}}{v^{\sigma}}\right)\right]_0^t\right).
\end{aligned}$$

Because $\lim_{t\longrightarrow\infty}\left[-v^{\sigma}E_{\sigma}\left(-\frac{x^{\sigma}}{v^{\sigma}}\right)\frac{x^{\sigma}}{\Gamma(1+\sigma)}\right]_0^t=0.$

Therefore,

$$\begin{aligned} LFE_{\sigma}\left\{\frac{x^{\sigma}}{\Gamma(1+\sigma)}\right\} &= \lim_{t\longrightarrow\infty}\left(v^{2\sigma}\left[-v^{\sigma}E_{\sigma}\left(-\frac{x^{\sigma}}{v^{\sigma}}\right)\right]_{0}^{t}\right) \\ &= v^{3\sigma}. \end{aligned}$$

3) If $f(x) = E_{\sigma}\left((ax)^{\sigma}\right)$, using the formula (3.5) gives

$$\begin{aligned} LFE_{\sigma}\left\{E_{\sigma}\left((ax)^{\sigma}\right)\right\} &= \frac{v^{\sigma}}{\Gamma(1+\sigma)}\int_{0}^{\infty}E_{\sigma}(-\frac{x^{\sigma}}{v^{\sigma}})E_{\sigma}\left((ax)^{\sigma}\right)(dx)^{\sigma} \\ &= \frac{v^{\sigma}}{\Gamma(1+\sigma)}\int_{0}^{\infty}E_{\sigma}\left(-\frac{1-(av)^{\sigma}}{v^{\sigma}}x^{\sigma}\right)(dx)^{\sigma} \\ &= v^{\sigma}\lim_{t\longrightarrow\infty}\left[\frac{-v^{\sigma}}{1-(av)^{\sigma}}E_{\sigma}\left(-\frac{1-(av)^{\sigma}}{v^{\sigma}}x^{\sigma}\right)\right]_{0}^{t} \\ &= \frac{v^{2\sigma}}{1-(av)^{\sigma}}. \end{aligned}$$

4) If $f(x) = \frac{x^{\sigma}}{\Gamma(1+\sigma)}E_{\sigma}\left((ax)^{\sigma}\right)$, by using the definition, and the integration by parts [41], we have

$$\begin{aligned} LFE_{\sigma}\left\{\frac{x^{\sigma}}{\Gamma(1+\sigma)}E_{\sigma}\left((ax)^{\sigma}\right)\right\} &= \frac{v^{\sigma}}{\Gamma(1+\sigma)}\int_{0}^{\infty}E_{\sigma}\left(-\frac{x^{\sigma}}{v^{\sigma}}\right)\frac{x^{\sigma}}{\Gamma(1+\sigma)}E_{\sigma}\left((ax)^{\sigma}\right)(dx)^{\sigma} \\ &= \frac{v^{\sigma}}{\Gamma(1+\sigma)}\lim_{t\longrightarrow\infty}\int_{0}^{t}\left(\frac{-v^{\sigma}}{1-(av)^{\sigma}}E_{\sigma}\left(-\frac{1-(av)^{\sigma}}{v^{\sigma}}x^{\sigma}\right)\right)^{(\sigma)}\frac{x^{\sigma}}{\Gamma(1+\sigma)}(dx)^{\sigma} \\ &= v^{\sigma}\lim_{t\longrightarrow\infty}\left[\frac{-v^{\sigma}}{1-(av)^{\sigma}}E_{\sigma}\left(-\frac{1-(av)^{\sigma}}{v^{\sigma}}x^{\sigma}\right)\frac{x^{\sigma}}{\Gamma(1+\sigma)}\right]_{0}^{t} \\ &\quad +\frac{v^{\sigma}}{\Gamma(1+\sigma)}\lim_{t\longrightarrow\infty}\int_{0}^{t}\frac{v^{\sigma}}{1-(av)^{\sigma}}E_{\sigma}\left(-\frac{1-(av)^{\sigma}}{v^{\sigma}}x^{\sigma}\right)(dx)^{\sigma} \\ &= v^{\sigma}\lim_{t\longrightarrow\infty}\left[\frac{-v^{2\sigma}}{(1-(av)^{\sigma})^{2}}E_{\sigma}\left(-\frac{1-(av)^{\sigma}}{v^{\sigma}}x^{\sigma}\right)\right]_{0}^{t}, \end{aligned}$$

because $\lim_{t\longrightarrow\infty}\left[\frac{-v^{\sigma}}{1-(av)^{\sigma}}E_{\sigma}\left(-\frac{1-(av)^{\sigma}}{v^{\sigma}}x^{\sigma}\right)\frac{x^{\sigma}}{\Gamma(1+\sigma)}\right]_{0}^{t} = 0.$

Therefore, we get

$$LFE_{\sigma}\left\{\frac{x^{\sigma}}{\Gamma(1+\sigma)}E_{\sigma}\left((ax)^{\sigma}\right)\right\} = \frac{v^{3\sigma}}{(1-(av)^{\sigma})^{2}}. \tag{3.16}$$

5) If $f(x) = \sin_{\sigma}((ax)^{\sigma})$ $(0 < \sigma \leqslant 1)$, by using the formula (3.5), we get

$$\begin{aligned} LFE_{\sigma}\left\{\sin_{\sigma}((ax)^{\sigma})\right\} &= \frac{v^{\sigma}}{\Gamma(1+\sigma)}\int_{0}^{\infty}E_{\sigma}\left(-\frac{x^{\sigma}}{v^{\sigma}}\right)\frac{E_{\sigma}\left(i^{\sigma}(ax)^{\sigma}\right)-E_{\eta}\left(-i^{\sigma}(ax)^{\sigma}\right)}{2i^{\sigma}}(dx)^{\sigma} \\ &= \frac{1}{2i^{\sigma}}\frac{v^{\sigma}}{\Gamma(1+\sigma)}\int_{0}^{\infty}\left[E_{\sigma}\left(-\frac{1-(av)^{\sigma}i^{\sigma}}{v^{\sigma}}x^{\sigma}\right)-E_{\sigma}\left(-\frac{1+(av)^{\sigma}i^{\sigma}}{v^{\sigma}}x^{\sigma}\right)\right](dx)^{\sigma} \\ &= \frac{v^{\sigma}}{2i^{\sigma}}\lim_{t\longrightarrow\infty}\left[-\frac{v^{\sigma}}{1-(av)^{\sigma}i^{\sigma}}E_{\sigma}\left(-\frac{1-(av)^{\sigma}i^{\sigma}}{v^{\sigma}}x^{\sigma}\right)+\frac{v^{\sigma}}{1+(av)^{\sigma}i^{\sigma}}E_{\sigma}\left(-\frac{1+(av)^{\sigma}i^{\sigma}}{v^{\sigma}}x^{\sigma}\right)\right]_{0}^{t}. \end{aligned}$$

After calculations, we find

$$LFE_\sigma\left\{\sin_\sigma((ax)^\sigma)\right\}=\frac{a^\sigma v^{3\sigma}}{1+(av)^{2\sigma}}. \tag{3.17}$$

6) If $f(x)=\cos_\sigma((ax)^\sigma)$ $(0<\sigma\leqslant 1)$, the use of the formula (3.5) gives

$$\begin{aligned}
LFE_\sigma\left\{\cos_\sigma((ax)^\sigma)\right\}&=\frac{v^\sigma}{\Gamma(1+\sigma)}\int_0^\infty E_\sigma\left(-\frac{x^\sigma}{v^\sigma}\right)\frac{E_\sigma\left(i^\sigma(ax)^\sigma\right)+E_\eta\left(-i^\sigma(ax)^\sigma\right)}{2}(dx)^\sigma\\
&=\frac{1}{2}\frac{v^\sigma}{\Gamma(1+\sigma)}\int_0^\infty\left[E_\sigma\left(-\frac{1-(av)^\sigma i^\sigma}{v^\sigma}x^\sigma\right)+E_\sigma\left(-\frac{1+(av)^\sigma i^\sigma}{v^\sigma}x^\sigma\right)\right](dx)^\sigma\\
&=\frac{v^\sigma}{2}\lim_{t\longrightarrow\infty}\left[-\frac{v^\sigma}{1-(av)^\sigma i^\sigma}E_\sigma\left(-\frac{1-(av)^\sigma i^\sigma}{v^\sigma}x^\sigma\right)-\frac{v^\sigma}{1+(av)^\sigma i^\sigma}E_\sigma\left(-\frac{1+(av)^\sigma i^\sigma}{v^\sigma}x^\sigma\right)\right]_0^t.
\end{aligned}$$

After calculations, we find

$$LFE_\sigma\left\{\cos_\sigma((ax)^\sigma)\right\}=\frac{v^{2\sigma}}{1+(av)^{2\sigma}}. \tag{3.18}$$

7) If $f(x)=\sinh_\sigma((ax)^\sigma)$ $(0<\sigma\leqslant 1)$, we obtain

$$\begin{aligned}
LFE_\sigma\left\{\sinh_\sigma((ax)^\sigma)\right\}&=\frac{v^\sigma}{\Gamma(1+\sigma)}\int_0^\infty E_\sigma\left(-\frac{x^\sigma}{v^\sigma}\right)\frac{E_\sigma\left((ax)^\sigma\right)-E_\sigma\left(-(ax)^\sigma\right)}{2}(dx)^\sigma\\
&=\frac{1}{2}\frac{v^\sigma}{\Gamma(1+\sigma)}\int_0^\infty\left[E_\sigma\left(-\frac{1-(av)^\sigma}{v^\sigma}x^\sigma\right)-E_\sigma\left(-\frac{1+(av)^\sigma}{v^\sigma}x^\sigma\right)\right](dx)^\sigma\\
&=\frac{v^\sigma}{2}\lim_{t\longrightarrow\infty}\left[-\frac{v^\sigma}{1-(av)^\sigma}E_\sigma\left(-\frac{1-(av)^\sigma}{v^\sigma}x^\sigma\right)+\frac{v^\sigma}{1+(av)^\sigma}E_\sigma\left(-\frac{1+(av)^\sigma}{v^\sigma}x^\sigma\right)\right]_0^t.
\end{aligned}$$

By performing simple operations, we find

$$LFE_\sigma\left\{\sinh_\sigma((ax)^\sigma)\right\}=\frac{a^\sigma v^{3\sigma}}{1-(av)^{2\sigma}}. \tag{3.19}$$

8) If $f(x)=\cosh_\sigma((ax)^\sigma)$ $(0<\sigma\leqslant 1)$, we obtain

$$\begin{aligned}
LFE_\sigma\left\{\sinh_\sigma((ax)^\sigma)\right\}&=\frac{v^\sigma}{\Gamma(1+\sigma)}\int_0^\infty E_\sigma\left(-\frac{x^\sigma}{v^\sigma}\right)\frac{E_\sigma\left((ax)^\sigma\right)+E_\sigma\left(-(ax)^\sigma\right)}{2}(dx)^\sigma\\
&=\frac{1}{2}\frac{v^\sigma}{\Gamma(1+\sigma)}\int_0^\infty\left[E_\sigma\left(-\frac{1-(av)^\sigma}{v^\sigma}x^\sigma\right)+E_\sigma\left(-\frac{1+(av)^\sigma}{v^\sigma}x^\sigma\right)\right](dx)^\sigma\\
&=\frac{v^\sigma}{2}\lim_{t\longrightarrow\infty}\left[-\frac{v^\sigma}{1-(av)^\sigma}E_\sigma\left(-\frac{1-(av)^\sigma}{v^\sigma}x^\sigma\right)-\frac{v^\sigma}{1+(av)^\sigma}E_\sigma\left(-\frac{1+(av)^\sigma}{v^\sigma}x^\sigma\right)\right]_0^t.
\end{aligned}$$

By performing simple operations, we get

$$LFE_\sigma\left\{\sinh_\sigma((ax)^\sigma)\right\}=\frac{v^{2\sigma}}{1-(av)^{2\sigma}}. \tag{3.20}$$

4. Illustrative examples

Finally, we'll use the local fractional Elzaki transform to solve the local fractional differential equations that have been suggested.

Example 4.1. We consider the local fractional differential equation of order σ

$$\frac{d^{\sigma}U(x)}{dx^{\sigma}} - U(x) = 1, \quad 0 < \sigma \leqslant 1, \tag{4.1}$$

with the initial condition $U(0) = 0$.

On both sides of (4.1), the local fractional Elzaki transform yields

$$\frac{1}{v^{\sigma}} LFE_{\sigma}\{U(x)\} - v^{\sigma}U(0) - LFE_{\sigma}\{U(x)\} = LFE_{\sigma}\{1\}. \tag{4.2}$$

Then

$$\left(\frac{1}{v^{\sigma}} - 1\right) LFE_{\sigma}\{U(x)\} = v^{2\sigma}. \tag{4.3}$$

Which give

$$\begin{aligned} LFE_{\sigma}\{U(x)\} &= \frac{v^{3\sigma}}{1-v^{\sigma}} \\ &= \frac{v^{2\sigma}}{1-v^{\sigma}} - v^{2\sigma}. \end{aligned} \tag{4.4}$$

We get (4.4) by doing the inverse transformation on both sides

$$U(x) = E_{\sigma}(-x^{\sigma}) - 1, \tag{4.5}$$

which is the exact solution of the equation (4.1). E_{σ} is the Mittag-Leffler function.

Example 4.2. Next, we consider the following local fractional differential equation of order σ, $(0 < \sigma \leqslant 1)$

$$\frac{d^{\sigma}U(x)}{dx^{\sigma}} - 2U(x) = 4, \tag{4.6}$$

with the initial condition

$$U(0) = 0. \tag{4.7}$$

Taking local fractional Elzaki transform on both sides of (4.6), we have

$$\frac{1}{v^{\sigma}} LFE_{\sigma}\{U(x)\} - 2LFE_{\sigma}\{U(x)\} = 4v^{2\sigma}. \tag{4.8}$$

By following the same steps as the previous example, we obtain

$$LFE_\sigma\left\{U(x)\right\} = -2v^{2\sigma} + 2\frac{v^{2\sigma}}{1-2v^\sigma}. \tag{4.9}$$

Take the inverse transformation on both sides of (4.9), we get

$$U(x) = 2E_\sigma(2x^\sigma) - 2. \tag{4.10}$$

The result (4.10) represents the exact solution of (4.6) – (4.7).

Example 4.3. We consider the local fractional differential equation of order 2σ, $(0 < \sigma \leqslant 1)$

$$\frac{d^{2\sigma}U(x)}{dx^{2\sigma}} + U(x) = -\frac{x^\sigma}{\Gamma(1+\sigma)}, \tag{4.11}$$

with to the initial conditions

$$U(0) = 0,\ U^{(\sigma)}(0) = 0. \tag{4.12}$$

Taking local fractional Elzaki transform on both sides of (4.11), we get

$$\frac{1}{v^{2\sigma}}\,LFE_\sigma\left\{U(x)\right\} + LFE_\sigma\left\{U(x)\right\} = -v^{3\sigma}. \tag{4.13}$$

We get the same result as the previous example by following the same steps

$$LFE_\sigma\left\{U(x)\right\} = -v^{3\sigma} + \frac{v^{3\sigma}}{1+v^{2\sigma}}. \tag{4.14}$$

Take the inverse transformation on both sides of (4.14), we get

$$U(x) = \sin_\sigma(x^\sigma) - \frac{x^\sigma}{\Gamma(1+\sigma)}, \tag{4.15}$$

so this result (4.15) represents the exact solution to the equation (4.11) – (4.12).

5. Conclusion

The idea that we presented in this paper is based on combining the Elzaki transform with the local fractional derivative, where we present some important results of this combination which called: Local fractional Elzaki transform of the Mittag-Leffler function, the hyperbolic sine and the hyperbolic cosine in fractal space and also we provide its properties of some non-differentiable functions were presented. This method was used to solve several linear local fractional differential equations, where we have seen that the non-differential solutions are precise and these results lead us to say that the local fractional Elzaki transform is powerful and effective in solving this type of equation, and thus can be applied to other linear local fractional partial differential equations with variable coefficients, to the linear systems of differential equations and to the other linear problems in Cantor sets.

Author Contributions

All authors contributed equally to this work. They all read and approved the final version of the manuscript.

Conflicts of Interest

The authors declare no conflict of interest.

Acknowledgement

We thank Dr. Ali YAKAR for technical support. The authors would like to thank editor and the reviewers for the reading carefully of the manuscript and the detail comments and valuable suggestions which has helped us to improve this paper.

References

References

[1] M. R. Spiegel, Theory and problems of Laplace transform, McGraw Hill, New York, 1965.

[2] S. Benzoni, Analyse de Fourier, Universite de Lyon, Lyon 1, Camille Jordan Institute, Saint-Étienne, 2011.

[3] N. T. Negero, *Zero-Order Hankel Transform Method for Partial Differential Equations,* International Journal of Modern Science and Engineering Technology, 3(10), (2016) 24-36.

[4] D. Lomen, *Application of the Mellin Transforin to Boundary Value Problems,* Proceedings of the Iowa Academy of Science, 69(1), (1962) 436-442.

[5] G. K. Watugala, *Sumudu transform: a new integral transform to solve differentia lequations and control engineering problems,* International Journal of Mathematical Education in Science and Technology, 24(1), (1993) 35-43.

[6] Z. H. Khan, W. A. Khan, *N-transform properties and applications*, NUST Journal of Engineering Sciences, 1, (2008) 127-133.

[7] T. M. Elzaki, *The New Integral Transform "ELzaki Transform"*, Global Journal of Pure and Applied Mathematics, 7(1), (2011) 57-64.

[8] H. J. Kim, *The time shifting theorem and the convolution for Elzaki transform*, Global Journal of Pure and Applied Mathematics, 87, (2013) 261-271.

[9] A. Devi, P. Roy, V. Gill, *Solution of ordinary differential equations with variable coefficients using Elzaki transform*, Asian Journal of Applied Science and Technology, 1, (2017) 186-194.

[10] A. Kalavathi, T. Kohila, L. M. Upadhyaya, *On the degenerate Elzaki transform*, Bulletin of Pure and Applied Sciences Section -E- Mathematics & Statistics, 40E(1), (2021) 99-107.

[11] K. S. Aboodh, *The new integrale transform "Aboodh transform"*, Global Journal of Pure and Applied Mathematics, 9(1), (2013) 35-43.

[12] Z. U. Zafar, *ZZ Transform Method*, International Journal of Advanced Engineering and Global Technoloy, 4(1), (2016) 1605-1611.

[13] S. Maitama, W. Zhao, *New Integral Transform: Shehu Transform a Generalization of Sumudu and Laplace Transform for Solving differential equations,* International Journal of Analysis and Applications, 17(2), (2019) 167-190.

[14] M. S. Archana, V. J. Pratibha, *Elzaki Transform: A Solution of Differential Equations,* International Journal of Scientific Engineering & Technology Research, 4(4), (2015) 1006-1008.

[15] P. P. Chopade, S. B. Devi, *Applications of Elzaki Transform to Ordinary Differential Equations and Partial Differential Equations,* International Journal Advanced Research in Computer Science Software Engineering, 5(3), (2015) 38-41.

[16] M. Eslaminasab, S. Abbasbandy, *Study on usage of Elzaki transform for the ordinary differential equations with non-constant coefficients,* International Journal of Industrial Mathematics, 7(3), (2015) 277-281.

[17] T. M. Elzaki, S. M. Ezaki, *On the ELzaki Transform and Ordinary Differential Equation with Variable Coefficients*, Advances in Theoretical and Applied Mathematics, 6(1), (2011) 41-46.

[18] T. M. Elzaki, S. M. Ezaki, *On the ELzaki Transform and Higher Order Ordinary Differential Equations*, Advances in Theoretical and Applied Mathematics, 6(1), (2011) 107-113.

[19] T. M. Elzaki, S. M. Ezaki, *Solution of Integro-Differential Equations by Using ELzaki Transform,* Global Journal of Mathematical Sciences: Theory & Practical , 3(1), (2011) 1-11.

[20] M. M. A. Mahgob, *Elzaki Transform and a Bulge Function on Volterra Integral Equations of the Second Kind*, IOSR Journal of Mathematics, 11(2), (2012) 68-70.

[21] M. M. A. Mahgob, T.M. Elzaki, *Solution of Partial Integro-Differential Equations by Elzaki Transform Method,* Applied Mathematical Sciences, 9(6), (2015) 295-303.

[22] M. M. A. Mahgob, T. M. Elzaki, *Elzaki Transform and Integro-Differential Equation with a Bulge Function,* IOSR Journal of Mathematics, 11(2), (2015) 25-28.

[23] P. G. Bhadane, V. H. Pradhan, S. V. Desale, *Elzaki Transform Solution of One Dimensional Ground Water Recharge through Spreading,* International Journal of Engineering Research and Applications, 3(6), (2013) 1607-1610.

[24] T. M. Elzaki, E. M. A. Hilal, *Analytical Solution for Telegraph Equation by Modified of Sumudu Transform "Elzaki Transform",* Mathematical Theory and Modeling, 2(4), (2012) 104-111.

[25] T. M. Elzaki, S. M. Ezaki, *On the ELzaki Transform and System of Partial Differential Equations,* Advances in Theoretical and Applied Mathematics, 6(1), (2011) 115-123.

[26] D. Ziane, M. Hamdi Cherif, *Resolution of Nonlinear Partial Differential Equations by Elzaki Transform Decomposition Method*, Journal of Approximation Theory and Applied Mathematics, 5, (2015) 17-30.

[27] T. M. Elzaki, S. M. Elzaki, *Applications of New Transform "ELzaki Transform" to Partial Differential Equations,* Global Journal of Pure and Applied Mathematics, 7(1), (2011) 65-70.

[28] A. Devi, M. Jakhar, *Analytic solution of fractional order differential equation arising in RLC electrical circuit*, Malaya Journal of Matematik, 8(2), (2020) 421-426.

[29] D. Ziane, *Application of Homotopy Analysis Method Combined with Elzaki Transform for Fractional Porous Medium Equation*, Journal of Approximation Theory and Applied Mathematics, 6, (2019) 1-19.

[30] D. Ziane, *Elzaki transform and the decomposition method for nonlinear fractional partial differential equations,* International Journal of Open Problems in Computer Science and Mathematics, 9(4), (2016) 25-39.

[31] D. Ziane, M. Hamdi Cherif, K. Belghaba, *Fractional higher dimensional initial boundary value problems via variational iteration method coupled with Elzaki transform*, Nonlinear Studies, 24(4), (2017) 1-17.

[32] D. Ziane, T. M. Elzaki, M. Hamdi Cherif, *Elzaki transform combined with variational iteration method for partial differential equations of fractional order*, Fundamental Journal of Mathematics and Applications, 1(1), (2018) 102-108.

[33] H. M. Srivastava, A. K. Golmankhaneh, D. Baleanu, X. J. Yang, *Local Fractional Sumudu Transform with Application to IVPs on Cantor Sets*, Abstract and Applied Analysis, 2014, (2014) Article ID: 176395, 1-7.

[34] X. J. Yang, Fractional Functional Analysis and Its Applications, Asian Academic, Hong Kong, 2011.

[35] X. J. Yang, Local Fractional Calculus and Its Applications, World Scientific Publishing, New York, 2012.

[36] J. H. He, *Asymptotic Methods for Solitary Solutions and Compactons,* Abstract and Applied Analysis, 2012, (2012) Article ID: 916793, 1-130.

[37] C. G. Zhao, A. M. Yang, H. Jafari, A. Haghbin, *The Yang-Laplace Transform for Solving the IVPs with Local Fractional Derivative,* Abstract and Applied Analysis, 2014, Article ID: 386459, (2014) 1-5.

[38] X. J. Yang, L. Li, R. Yang, *Problems of local fractional definite integral of the one-variable non-differentiable function*, World Science and Technology R&D, 31(4), (2009) 722-724.

[39] J. Ahmad, S. T. Mohyud-Din, H. M. Srivastava, X-J. Yang, *Analytic solutions of the Helmholtz and Laplace equations by using local fractional derivative operators*, Waves, Wavelets and Fractals - Advanced Analysis, 1, (2015) 22-26.

[40] X. J. Yang, *Generalized Sampling Theorem for Fractal Signals*, Advances in Digital Multimedia, 1(2), (2012) 88-92.

[41] G. Jumarie, *Table of some basic fractional calculus formulae derived from a modified Riemann-Liouville derivative for non-differentiable functions*, Applied Mathematics Letters, 22, (2009) 378-385.

Journal of New Results in Science
https://dergipark.org.tr/en/pub/jnrs
Research Article
Open Access

E-ISSN: 1304-7981 https://doi.org/10.54187/jnrs.979984

Properties of invertible elements in complete intuitionistic fuzzy pseudo normed algebra

Bivas Dinda[1], **Santanu Kumar Ghosh**[2], **Tapas Kumar Samanta**[3]

Keywords
IFPNA,
Invertible element,
Intuitionistic fuzzy continuity

Abstract — In this paper, we deal with the invertible elements in a complete intuitionistic fuzzy pseudo normed algebra(in short, IFPNA) with respect to Archimedean t-norm and Archimedean t-conorm. It is done by studying the continuity of algebraic operations in a complete IFPNA and investigating the condition for existence of inverse of an element in a complete IFPNA. Also some properties of invertible elements are studied. It is observed that the set of invertible elements in a complete IFPNA is an open set.

Subject Classification (2020): 08A72, 46S40.

1. Introduction

For dealing with uncertainty, Zadeh extended the classical set theory and initiated the idea of fuzzy set theory [1]. In 1986, K.T. Atanassov extended the notion of fuzzy set and proposed intuitionistic fuzzy set [2]. Fuzzy norm was first studied by A.K. Katsaras [3, 4]. Thereafter the concept of fuzzy normed spaces were presented in succession by C. Felbin [5] in 1992, S.C. Cheng and J.N. Morderson [6] in 1994, T. Bag and S.K. Samanta [7] in 2003, R. Saadati and S.M. Vaezpour [8] in 2005, I. Golet [9] in 2010 and many other researchers [10–12] in past years.

Fuzzy Banach algebra was first introduced by I. Sadeqi and A. Amiripour [12] in 2007. Dinda et. al. [13] in 2011, proposed a notion of intuitionistic fuzzy Banach algebra. Fuzzy Menger normed algebra was studied by A.K. Mirmostaface [14] in 2012. Following the concept of Mirmostaface [14], B$\hat{i}$nzar et. al. [15] in 2016 studied condition for continuous product in fuzzy normed algebra, N. Konwar and P. Debnath [16] in 2018 studied condition for continuous product in intuitionistic fuzzy n-normed algebra. J.R. Kider and A.H. Ali [17] in 2019 proposed some properties of complete fuzzy normed algebra.

In 2016, S. Nădăban [18] introduced fuzzy pseudo norm and showed that fuzzy pseudo norm is a generalization of fuzzy norm. Following the works S. Nădăban [18] and Bag-Samanta [7, 19], Dinda et. al. [20–23] extended the concept of intuitionistic fuzzy norm and developed intuitionistic fuzzy pseudo norm.

[1]rs.bivas@knu.ac.in (Corresponding Author); [2]santanu_96@yahoo.co.in; [3] mumpu_tapas5@yahoo.co.in
[1,2]Department of Mathematics, Kazi Nazrul University, Asansol, WB 713340, India.
[3]Department of Mathematics, Uluberia College, Uluberia, WB 711315, India.
Article History: Received: 07 Aug 2021 - Accepted: 29 Nov 2021 - Published: 31 Dec 2021

While solving differential equation, linear algebraic equation, or integral equation, in intuitionistic fuzzy environment there is a problem related to inverse operation. In this paper, we investigate the inverse of an element and properties of the set of invertible elements of a complete IFPNA with respect to Archimedean t-norm and Archimedean t-conorm.
The structure of this paper is as follows: In section 2, we give some preliminary results which were known before and used in the subsequent sections. In section 3, we propose the definition of intuitionistic fuzzy pseudo normed algebra (IFPNA) with respect to Archimedean t-norm and Archimedean t-conorm and prove that the algebraic operations are continuous in a complete IFPNA. We also prove a result giving the condition for the existence of the inverse of an element in a complete IFPNA. In section 4, we show that the set of all invertible elements (I) is an open set and the map $a \to a^{-1}$ from I into I is strongly intuitionistic fuzzy continuous(IFC).

2. Preliminaries

Definition 2.1. [24] A function $* : [0,1] \times [0,1] \to [0,1]$ is called a t-norm if and only if (iff) the following four conditions are satisfied:
(1.1) $e_1 * e_2 = e_2 * e_1, \ \forall e_1, e_2 \in [0,1]$,
(1.2) $e_1 * e_2 \le e_1 * e_3$ if $e_2 \le e_3, \ \forall e_1, e_2, e_3 \in [0,1]$,
(1.3) $e_1 * (e_2 * e_3) = (e_1 * e_2) * e_3, \ \forall e_1, e_2, e_3 \in [0,1]$,
(1.4) $e_1 * 1 = e_1, \ \forall e_1 \in [0,1]$.

Definition 2.2. [24, 25] A function $\diamond : [0,1] \times [0,1] \to [0,1]$ is called a t-conorm iff the following four conditions are satisfied:
(2.1) $e_1 \diamond e_2 = e_2 \diamond e_1, \ \forall e_1, e_2 \in [0,1]$,
(2.2) $e_1 \diamond e_2 \le e_1 \diamond e_3$ if $e_2 \le e_3, \ \forall e_1, e_2, e_3 \in [0,1]$,
(2.3) $e_1 \diamond (e_2 \diamond e_3) = (e_1 \diamond e_2) \diamond e_3, \ \forall e_1, e_2, e_3 \in [0,1]$,
(2.4) $e_1 \diamond 0 = e_1, \ \forall e_1 \in [0,1]$.

Definition 2.3. [25] A t-norm $*$ is called Archimedean iff
(1.5) $*$ is continuous, and
(1.6) $e_1 * e_1 < e_1, \ \forall e_1 \in (0,1)$.

Definition 2.4. [25] A t-conorm $\diamond$ is called Archimedean iff
(2.5) $\diamond$ is continuous, and
(2.6) $e_1 \diamond e_1 > e_1, \ \forall e_1 \in (0,1)$.

In the subsequent theorems, we use $*$ as Archimedean t-norm and $\diamond$ as Archimedean t-conorm.

Definition 2.5. [20] Let V be linear space over the field $\mathbb{K} (= \mathbb{R}$ or $\mathbb{C})$. An intuitionistic fuzzy subset (μ, ν) of $(V \times \mathbb{R}, V \times \mathbb{R})$ is said to be an intuitionistic fuzzy pseudo norm on V if $\forall v_1, v_2 \in V$
(IFP.1) $\forall s \in \mathbb{R}, \ \mu(v_1, s) + \nu(v_1, s) \le 1$;
(IFP.2) $\forall s \in \mathbb{R}$ with $s \le 0, \ \mu(v_1, s) = 0$;
(IFP.3) $\forall s \in \mathbb{R}^+, \ \mu(v_1, s) = 1$ iff $v_1 = \theta$;
(IFP.4) $\forall s \in \mathbb{R}^+, \ \mu(cv_1, s) \ge \mu(v_1, s)$ if $|c| \le 1, \forall c \in \mathbb{K}$;
(IFP.5) $\mu(v_1 + v_2, s + t) \ge \min\{\mu(v_1, s), \mu(v_2, t)\}, \ \forall s, t \in \mathbb{R}^+$;
(IFP.6) $\lim_{s \to \infty} \mu(v_1, s) = 1$;
(IFP.7) if $\exists \ \alpha \in (0,1)$ such that $\mu(v_1, s) > \alpha, \forall s \in \mathbb{R}^+$ then $v_1 = \theta$;

(IFP.8) $\forall\, v_1 \in V,\ \mu(v_1, \cdot)$ is left continuous on $\mathbb{R}$;
(IFP.9) $\forall s \in \mathbb{R}$ with $s \leq 0,\ \nu(v_1, s) = 1$;
(IFP.10) $\forall s \in \mathbb{R}^+,\ \nu(v_1, s) = 0$ iff $v_1 = \theta$;
(IFP.11) $\forall s \in \mathbb{R}^+,\ \nu(cv_1, s) \leq \nu(v_1, s)$ if $|c| \leq 1, \forall c \in \mathbb{K}$;
(IFP.12) $\nu(v_1 + v_2, s + t) \leq \max\{\nu(v_1, s), \nu(v_2, t)\},\ \forall s, t \in \mathbb{R}^+$;
(IFP.13) $\lim_{s \to \infty} \nu(v_1, s) = 0$;
(IFP.14) if $\exists\, \alpha \in (0,1)$ such that $\nu(v_1, s) < \alpha, \forall s \in \mathbb{R}^+$ then $v_1 = \theta$;
(IFP.15) $\forall\, v_1 \in V,\ \nu(v_1, \cdot)$ is left continuous on $\mathbb{R}$.

Here (V, μ, ν) is called intuitionistic fuzzy pseudo normed linear space (IFPNLS).

Definition 2.6. [22] Let (V, μ_1, ν_1), (U, μ_2, ν_2) be two IFPNLS. A mapping $P : (V, \mu_1, \nu_1) \to (U, \mu_2, \nu_2)$ is said to be strongly IFC at $v_0 \in V$ if for any given $\epsilon > 0$ there exists $\delta(\epsilon) > 0$ such that for all $v \in V$,

$$\mu_2(P(v) - P(v_0), \epsilon) \geq \mu_1(v - v_0, \delta),\ \nu_2(P(v) - P(v_0), \epsilon) \leq \nu_1(v - v_0, \delta).$$

Definition 2.7. [21] Let (V, μ, ν) be an IFPNLS. An open ball $B(v, r, s)$ with center at x, radius $0 < r < 1$ and $s \in \mathbb{R}^+$ is defined by

$$B(v, r, s) = \{a \in V : \mu(v - a, s) > 1 - r,\ \nu(v - a, s) < r\}.$$

3. Condition for existence of invertible element in complete IFPNA

Throughout this paper unless otherwise stated we take $*$ as Archimedean t-norm and $\diamond$ as Archimedean t-conorm. In this section we endeavor to investigate the condition for existence of an invertible element in a complete IFPNA.

Definition 3.1. Let V be an algebra over the field of complex numbers, $*$ be the Archimedean t-norm and $\diamond$ be the Archimedean t-conorm. By an intuitionistic fuzzy pseudo normed algebra(in short, IFPNA) we mean an intuitionistic fuzzy subset (μ, ν) of $(V \times \mathbb{R}^+, V \times \mathbb{R}^+)$ such that
(IFPNA.1) (V, μ, ν) is an IFPNLS.
(IFPNA.2) $\mu(v_1 v_2, st) \geq \mu(v_1, s) \diamond \mu(v_2, t),\ \nu(v_1 v_2, st) \leq \nu(v_1, s) * \nu(v_2, t),\ \forall\, v_1 v_2 \in V$, and for each $s, t \in \mathbb{R}^+$.

If (V, μ, ν) be a complete IFPNLS then the normed algebra $(V, \mu, \nu, *, \diamond)$ will be complete IFPNA.

Example 3.2. Let $(V, \|\cdot\|)$ be a pseudo normed algebra, and consider $a \diamond b = \max\{a, b\}$ and $a * b = \min\{a, b\}$. Define $\mu, \nu : V \times \mathbb{R} \to [0,1]$ by

$$\mu(v, s) = \begin{cases} \dfrac{s}{s + \|v\|} & \text{if } s > \|v\|, \\ 0 & \text{if } s \leq \|v\|. \end{cases}$$

$$\nu(v, s) = \begin{cases} \dfrac{\|v\|}{s + \|v\|} & \text{if } s > \|v\|, \\ 1 & \text{if } s \leq \|v\|. \end{cases}$$

We will show that $(V, \mu, \nu, \diamond, *)$ is an IFPNA on V.
From the Example 3.2 of [20] it is easy to verify the conditions of (IFPNA.1). Now we show (IFPNA.2).
Clearly $* = \min$, and $\diamond = \max$ are Archimedean t-norm and Archimedean t-conorm.
Let $v_1, v_2 \in V$ and $s \in \mathbb{R}^+$. Without loss of generality let us assume $\mu(v_1, s) \geq \mu(v_2, s)$. Then $\|v_1\| \leq \|v_2\|$. Now

we have the following cases for consideration.
Case-1:

$$\begin{aligned} s > \|v_2\| \geq \|v_1\| &\Rightarrow s\|v_1\| > \|v_1\|\|v_2\| \geq \|v_1 v_2\| \\ &\Rightarrow s^2\|v_1\| > s\|v_1 v_2\| \\ &\Rightarrow s^3 + s^2\|v_1\| > s^3 + s\|v_1 v_2\| \\ &\Rightarrow s^2(s + \|v_1\|) > s(s^2 + \|v_1 v_2\|) \\ &\Rightarrow \frac{s^2}{s^2 + \|v_1 v_2\|} > \frac{s}{s + \|v_1\|} \\ &\Rightarrow \mu(v_1 v_2, s^2) > \max\{\mu(v_1, s), \mu(v_2, s)\}. \end{aligned}$$

Case-2:

$$\begin{aligned} s \leq \|v_1\| \leq \|v_2\| &\Rightarrow \mu(v_1, s) = 0,\ \mu(v_2, s) = 0 \\ &\Rightarrow \mu(v_1 v_2, s^2) \geq \max\{\mu(v_1, s), \mu(v_2, s)\}. \end{aligned}$$

Also, Without loss of generality let us assume $\nu(v_1, s) \geq \nu(v_2, s)$. Now we have the following cases.
Case-1:

$$\begin{aligned} s > \|v_2\| \geq \|v_1\| &\Rightarrow s\|v_2\| > \|v_1\|\|v_2\| \geq \|v_1 v_2\| \\ &\Rightarrow s^2\|v_2\| > s\|v_1 v_2\| \\ &\Rightarrow s^2\|v_2\| + \|v_2\|\|v_1 v_2\| > s\|v_1 v_2\| + \|v_2\|\|v_1 v_2\| \\ &\Rightarrow \|v_2\|(s^2 + \|v_1 v_2\|) > \|v_1 v_2\|(s + \|v_2\|) \\ &\Rightarrow \frac{\|v_1 v_2\|}{s^2 + \|v_1 v_2\|} < \frac{\|v_2\|}{s + \|v_2\|} \\ &\Rightarrow \nu(v_1 v_2, s^2) < \min\{\nu(v_1, s), \nu(v_2, s)\}. \end{aligned}$$

Case-2:

$$\begin{aligned} s \leq \|v_1\| \leq \|v_2\| &\Rightarrow \nu(v_2, s) = 1,\ \nu(v_1, s) = 1 \\ &\Rightarrow \nu(v_1 v_2, s^2) \leq \min\{\nu(v_1, s), \nu(v_2, s)\}. \end{aligned}$$

Therefore, (IFPNA.2) is satisfied and hence $(V, \mu, \nu, \diamond, *)$ is an IFPNA.

Example 3.3. Let $(V, \|\cdot\|)$ be a pseudo normed linear space. Define $\mu, \nu : V \times \mathbb{R} \to [0, 1]$ by

$$\mu(v, s) = \begin{cases} 1 & \text{if } s > \|v\|, \\ 0 & \text{if } s \leq \|v\|. \end{cases}$$

$$\nu(v, s) = \begin{cases} 0 & \text{if } s > \|v\|, \\ 1 & \text{if } s \leq \|v\|. \end{cases}$$

Then $(V, \mu, \nu, \diamond, *)$ is an IFPNA on V.

From the Example 3.1 of [20] and from Example 3.2, the proof follows.

Theorem 3.4. In an IFPNA $(V, \mu, \nu, \diamond, *)$, the algebraic operations " + " and " · " are continuous.

Proof.

Let $\{a_n\}_n$ and $\{b_n\}_n$ be two sequences in V converges to a and b respectively. Then for every $s \in \mathbb{R}^+$, $\lim_{n\to\infty} \mu(a_n - a, s) = 1$, $\lim_{n\to\infty} \nu(a_n - a, s) = 0$ and $\lim_{n\to\infty} \mu(b_n - b, s) = 1$, $\lim_{n\to\infty} \nu(b_n - b, s) = 0$.
Now, $\mu((a_n + b_n) - (a + b), s) \geq \min\{\mu(a_n - a, \frac{s}{2}), \mu(b_n - b, \frac{s}{2})\}$. Hence

$$\begin{aligned}
&\lim_{n\to\infty} \mu((a_n + b_n) - (a + b), s) \\
&\geq \min\left\{\lim_{n\to\infty} \mu(a_n - a, \frac{s}{2}), \lim_{n\to\infty} \mu(b_n - b, \frac{s}{2})\right\} \\
&\geq \min\{1, 1\} = 1.
\end{aligned}$$

This proves the continuity of addition in $(V, \mu, \nu, \diamond, *)$.

$$\begin{aligned}
\text{Again, } \mu(a_n b_n - ab, s) &= \mu(a_n b_n - a_n b + a_n b - ab, s) \\
&= \mu(a_n(b_n - b) + b(a_n - a), s) \\
&\geq \min\left\{\mu(a_n(b_n - b), \frac{s}{2}), \mu(b(a_n - a), \frac{s}{2})\right\} \\
&\geq \min\left\{\mu(a_n, \sqrt{\frac{s}{2}}) \diamond \mu(b_n - b, \sqrt{\frac{s}{2}}), \mu(b, \sqrt{\frac{s}{2}}) \diamond \mu(a_n - a, \sqrt{\frac{s}{2}})\right\}.
\end{aligned}$$

$$\begin{aligned}
&\text{Therefore, } \lim_{n\to\infty} \mu(a_n b_n - ab, s) \\
&\geq \min\left\{\lim_{n\to\infty} \mu(a_n, \sqrt{\frac{s}{2}}) \diamond 1, \lim_{n\to\infty} \mu(b, \sqrt{\frac{s}{2}}) \diamond 1\right\} \\
&\geq \min\{1, 1\} \\
&= 1.
\end{aligned}$$

Hence multiplication is also continuous in $(V, \mu, \nu, \diamond, *)$.

Theorem 3.5. Let $(V, \mu, \nu, \diamond, *)$ be a complete IFPNA. If $a \in B(0, r, s)$, $s \in \mathbb{R}^+$ and $0 < r < 1$ then the inverse of $(i - a)$ exists and

$$(i - a)^{-1} = i + \sum_{n=1}^{\infty} a^n$$

where i and 0 are the identity and the zero of V respectively.

Proof.

Since $a \in B(0, r, s)$ we have $\mu(a, s) > 1 - r$, $\nu(a, s) < r$, for each $s \in \mathbb{R}^+$ and $0 < r < 1$.
First we verify the convergence of the series $\sum_{n=1}^{\infty} a^n$ in V.

Let $u_n = \sum_{j=1}^{n} a^j$ then it is enough to verify that $\mu(u_{n+p} - u_n, s) > 1 - r$ and $\nu(u_{n+p} - u_n, s) < r$. Now,

$$\begin{aligned}
&\mu(u_{n+p} - u_n, s)\\
&= \mu\left(a^{n+1} + a^{n+2} + \cdots + a^{n+p}, s\right)\\
&\geq \min\left\{\mu(a^{n+1}, \frac{s}{p}),\ \mu(a^{n+2}, \frac{s}{p}),\ \cdots, \mu(a^{n+p}, \frac{s}{p})\right\}\\
&\geq \min\{\mu\left(a,\ \sqrt[n+1]{\frac{s}{p}}\right) \diamond \mu(a,\ \sqrt[n+1]{\frac{s}{p}}) \diamond \cdots \diamond \mu(a,\ \sqrt[n+1]{\frac{s}{p}}),\ \mu(a,\ \sqrt[n+2]{\frac{s}{p}}) \diamond \mu(a,\ \sqrt[n+2]{\frac{s}{p}}) \diamond \cdots \diamond \mu(a,\ \sqrt[n+2]{\frac{s}{p}}),\\
&\cdots, \mu(a,\ \sqrt[n+p]{\frac{s}{p}}) \diamond \mu(a,\ \sqrt[n+p]{\frac{s}{p}}) \diamond \cdots \diamond \mu(a,\ \sqrt[n+p]{\frac{s}{p}})\}\\
&> \min\{(1-r) \diamond (1-r) \diamond \cdots \diamond (1-r),\ (1-r) \diamond (1-r) \diamond \cdots \diamond (1-r),\ \cdots,\ (1-r) \diamond (1-r) \diamond \cdots \diamond (1-r)\}\\
&> \min\{(1-r),\ (1-r),\ \cdots,\ (1-r)\}, \text{ [By (2.6) of Definition 2.4]}\\
&= 1 - r.
\end{aligned}$$

$$\begin{aligned}
&\nu(u_{n+p} - u_n, s)\\
&= \nu\left(a^{n+1} + a^{n+2} + \cdots + a^{n+p}, s\right)\\
&\leq \max\left\{\nu(a^{n+1}, \frac{s}{p}),\ \nu(a^{n+2}, \frac{s}{p}),\ \cdots, \nu(a^{n+p}, \frac{s}{p})\right\}\\
&\leq \max\{\nu\left(a,\ \sqrt[n+1]{\frac{s}{p}}\right) * \nu(a,\ \sqrt[n+1]{\frac{s}{p}}) * \cdots * \nu(a,\ \sqrt[n+1]{\frac{s}{p}}),\ \nu(a,\ \sqrt[n+2]{\frac{s}{p}}) * \nu(a,\ \sqrt[n+2]{\frac{s}{p}}) * \cdots * \nu(a,\ \sqrt[n+2]{\frac{s}{p}}),\\
&\cdots, \nu(a,\ \sqrt[n+p]{\frac{s}{p}}) * \nu(a,\ \sqrt[n+p]{\frac{s}{p}}) * \cdots * \nu(a,\ \sqrt[n+p]{\frac{s}{p}})\}\\
&< \max\{r * r * \cdots * r,\ r * r * \cdots * r,\ \cdots,\ r * r * \cdots * r\}\\
&< \max\{r,\ r,\ \cdots,\ r\}, \text{ [By (1.6) of Definition 2.3]}\\
&= r.
\end{aligned}$$

Hence the series $\sum_{n=1}^{\infty} a^n$ is convergent in V.
Now $(i - a)(i + a + a^2 + \cdots + a^n) = (i + a + a^2 + \cdots + a^n)(i - a) = i - a^{n+1}$.
Also,

$$\begin{aligned}
\mu(a^{n+1}, s) &\geq \mu(a,\ \sqrt[n+1]{s}) \diamond \mu(a,\ \sqrt[n+1]{s}) \diamond \cdots \diamond \mu(a,\ \sqrt[n+1]{s})\\
&> (1-r) \diamond (1-r) \diamond \cdots \diamond (1-r)\\
&> (1-r), \text{ [By (2.6) of Definition 2.4].}
\end{aligned}$$

$$\begin{aligned}
\nu(a^{n+1}, t) &\leq \nu(a,\ \sqrt[n+1]{s}) * \nu(a,\ \sqrt[n+1]{s}) * \cdots * \nu(a,\ \sqrt[n+1]{s})\\
&< r * r * \cdots * r\\
&< r, \text{ [By (1.6) of Definition 2.3].}
\end{aligned}$$

Hence a^{n+1} converges to 0 as $n \to \infty$. Therefore taking $n \to \infty$ we obtain

$$(i-a)(i+\sum_{n=1}^{\infty} a^n) = (i+\sum_{n=1}^{\infty} a^n)(i-a) = e$$

Thus $(i-a)^{-1} = i + \sum_{n=1}^{\infty} a^n$.

Corollary 3.6. Let $(V, \mu, \nu, \diamond, *)$ be a complete IFPNA. If $i-a \in B(0,r,s)$, for each $s \in \mathbb{R}^+$ and $0 < r < 1$ then the inverse of a exists and

$$a^{-1} = i + \sum_{n=1}^{\infty} (i-a)^n$$

Corollary 3.7. Let $(V, \mu, \nu, \diamond, *)$ be a complete IFPNA. If $\lambda (\neq 0)$ be a scalar such that $\frac{a}{\lambda} \in B(0,r,s)$, for each $s \in \mathbb{R}^+$ and $0 < r < 1$ then the inverse of $(\lambda i - a)$ exists and

$$(\lambda i - a)^{-1} = \sum_{n=1}^{\infty} \lambda^{-n} a^{n-1}$$

Proof.
Since $\frac{a}{\lambda} \in B(0,r,s)$ for each $s \in \mathbb{R}^+$ and $0 < r < 1$, then

$$\mu(\frac{a}{\lambda}, s) > 1-r,\ \nu(\frac{a}{\lambda}, s) < r\ \Rightarrow \mu\left(i-(i-\frac{a}{\lambda}), s\right) > 1-r,\ \nu\left(i-(i-\frac{a}{\lambda}), s\right) < r$$

Hence by Corollary 3.6, the inverse of $(i - \frac{a}{\lambda})$ exists i.e., the inverse of $(\lambda i - a)$ exists.

$$\begin{aligned}
\text{Also, } (\lambda i - a)^{-1} &= \lambda^{-1}(i - \lambda^{-1} a)^{-1} \\
&= \lambda^{-1}\left[i + \sum_{n=1}^{\infty} \{i - (i - \lambda^{-1} a)\}^n\right], \text{ [by Corollary 3.6]} \\
&= \lambda^{-1}\left[i + \sum_{n=1}^{\infty} \lambda^{-n} a^n\right] \\
&= \sum_{n=1}^{\infty} \lambda^{-n} a^{n-1}.
\end{aligned}$$

4. Properties of invertible elements in IFPNA

Theorem 4.1. Let $(V, \mu, \nu, \diamond, *)$ be a complete IFPNA. Then set of invertible elements of V is an open set.

Proof.
Let I be the set of invertible elements of V. Let $a_0 \in I$, then we have to show that $B(a_0, r, s) \subseteq I$ for each $s \in \mathbb{R}^+$ with $0 < r < 1$.
Let $a \in B(a_0, r, s)$ then $\mu(a - a_0, s) > 1 - r$ and $\nu(a - a_0, s) < r$.
Let us take $r \in (0,1)$ such that $r < \min\{1 - \mu(a_0^{-1}, s), \nu(a_0^{-1}, s)\}$. Then

$$\mu(a - a_0, s) > 1 - r > \mu(a_0^{-1}, s),\ \nu(a - a_0, s) < r < \nu(a_0^{-1}, s). \tag{4.1}$$

Let $b = a_0^{-1} a$, and $c = i - b$, where i is the identity of V. Then for all $s \in \mathbb{R}^+$,
$\mu(c, s) = \mu(i - b, s)$
$\quad = \mu(b - i, s)$, [by (IFP.4)]

$$
\begin{aligned}
&= \mu(a_0^{-1}a - a_0^{-1}a_0, s)\\
&= \mu(a_0^{-1}(a-a_0), s)\\
&\geq \mu(a_0^{-1}, \sqrt{s}) \diamond \mu(a-a_0, \sqrt{s}), \text{ [by (IFPNA.2)]}\\
&> \mu(a-a_0, \sqrt{s}) \diamond \mu(a-a_0, \sqrt{s}), \text{ [by Equation 4.1, and (2.2) of Definition 2.2]}\\
&> \mu(a-a_0, \sqrt{s}), \text{ [by (2.6) of Definition 2.4]}\\
&> 1-r, \text{ since } a \in B(a_0, r, s) \text{ for all } s \in \mathbb{R}^+ \text{ with } 0<r<1.
\end{aligned}
$$

$$
\begin{aligned}
\nu(c,s) &= \nu(i-b, s)\\
&= \nu(b-i, s), \text{ [by (IFP.11)]}\\
&= \nu(a_0^{-1}a - a_0^{-1}a_0, s)\\
&= \nu(a_0^{-1}(a-a_0), s)\\
&\leq \nu(a_0^{-1}, \sqrt{s}) * \nu(a-a_0, \sqrt{s}), \text{ [by (IFPNA.2)]}\\
&< \nu(a-a_0, \sqrt{s}) * \nu(a-a_0, \sqrt{s}), \text{ [by Equation 4.1, and (1.2) of Definition 2.1]}\\
&< \nu(a-a_0, \sqrt{s}), \text{ [by (1.6) of Definition 2.3]}\\
&< r, \text{ since } a \in B(a_0, r, s) \text{ for all } s \in \mathbb{R}^+ \text{ with } 0<r<1.
\end{aligned}
$$

Hence $c \in B(0, r, s)$ and therefore by Theorem 3.5, $(i-c)$ is invertible; i.e., b is invertible. Hence $b \in I$. Now $a_0 \in I$ and $b \in I$. Hence $a_0.b \in I$; i.e., $a_0 a_0^{-1} a \in I$; i.e., $a \in I$.
Thus $B(a_0, r, s) \subseteq I$ and hence I is an open in V.

Corollary 4.2. Let $(V, \mu, \nu, \diamond, *)$ be a complete IFPNA. Then set of non-invertible elements of V is a closed set.

Theorem 4.3. Let I be the set of invertible elements of a complete IFPNA $(V, \mu, \nu, \diamond, *)$. Then the mapping P from a to a^{-1} of I into I is strongly IFC.

Proof.
Let $a_0 \in I$, then by Theorem 4.1, $B(a_0, r, s) \subseteq I$, where $s \in \mathbb{R}^+$ and $0<r<1$.
Let $r < \min\{1-\mu(a_0^{-1}, t), \nu(a_0^{-1}, t)\}$, and $a \in I$ be such that $a \in B(a_0, r, s)$. Then we have the Equation 4.1.
Now by Corollary 3.6, $a^{-1}a_0 = \left(a_0^{-1}a\right)^{-1} = i + \sum_{n=1}^{\infty}\left(i - a_0^{-1}a\right)^n$. Therefore,

$$
\begin{aligned}
&\mu\left(a^{-1}a_0 - i, \frac{\pi^2}{6}\right)\\
&= \mu\left(\sum_{n=1}^{\infty}(i-a_0^{-1}a)^n, 1+\frac{1}{4}+\frac{1}{9}+\frac{1}{16}+\cdots\right)\\
&\geq \min\left\{\mu((i-a_0^{-1}a),1), \mu\left((i-a_0^{-1}a)^2, \frac{1}{4}\right), \cdots, \mu\left((i-a_0^{-1}a)^n, \frac{1}{n^2}\right), \cdots\right\}, \text{ [by (IFP.5)]}\\
&\geq \min\left\{\mu\left(a_0^{-1}(a_0-a),1\right), \mu\left(a_0^{-1}(a_0-a), \frac{1}{2}\right) \diamond \mu\left(a_0^{-1}(a_0-a), \frac{1}{2}\right), \cdots\right\}, \text{ [by (IFPNA.2)]}\\
&\geq \min\left\{\mu\left(a_0^{-1},1\right) \diamond \mu((a_0-a),1), \mu\left(a_0^{-1}, \frac{1}{\sqrt{2}}\right) \diamond \mu\left((a_0-a), \frac{1}{\sqrt{2}}\right) \diamond \mu\left(a_0^{-1}, \frac{1}{\sqrt{2}}\right) \diamond \mu\left((a_0-a), \frac{1}{\sqrt{2}}\right), \cdots\right\}, \text{ [by (IFPNA.2)]}\\
&> \min\left\{\mu((a_0-a),1) \diamond \mu((a_0-a),1), \mu\left((a_0-a), \frac{1}{\sqrt{2}}\right) \diamond \mu\left((a_0-a), \frac{1}{\sqrt{2}}\right) \diamond \mu\left((a_0-a), \frac{1}{\sqrt{2}}\right) \diamond \mu\left((a_0-a), \frac{1}{\sqrt{2}}\right), \cdots\right\},\\
&\qquad\qquad \text{[by Equation 4.1, and (2.2) of Definition 2.2]}\\
&> \min\left\{\mu((a_0-a),1), \mu\left((a_0-a), \frac{1}{\sqrt{2}}\right), \cdots\right\}, \text{ [by (2.6) of Definition 2.4]}\\
&\geq \mu\left((a_0-a), \lim_{n\to\infty}\left(\frac{1}{n^2}\right)^{\frac{1}{2n}}\right), \text{ since } \mu(a,\cdot) \text{ is a non decreasing function and } 1 > \frac{1}{4^{\frac{1}{4}}} > \frac{1}{9^{\frac{1}{6}}} > \frac{1}{16^{\frac{1}{8}}} > \cdots > \frac{1}{n^{2\frac{1}{2n}}} > \cdots.
\end{aligned}
$$

$$= \mu\left((a_0 - a), \lim_{n\to\infty} \frac{1}{n^{\frac{1}{n}}}\right)$$
$$= \mu\left((a_0 - a), 1\right)$$
$$\geq \mu(a - a_0, 1), \text{ [by (IFP.4)].}$$

Hence

$$\mu\left(a^{-1}a_0 - i, \frac{\pi^2}{6}\right) > \mu\left((a - a_0), 1\right) \tag{4.2}$$

Also,

$$\nu\left(a^{-1}a_0 - e, \frac{\pi^2}{6}\right)$$
$$= \nu\left(\sum_{n=1}^{\infty}(i - a_0^{-1}a)^n, 1 + \frac{1}{4} + \frac{1}{9} + \frac{1}{16} + \cdots\right)$$
$$\leq \max\left\{\nu((i - a_0^{-1}a), 1), \nu\left((i - a_0^{-1}a)^2, \frac{1}{4}\right), \cdots, \nu\left((i - a_0^{-1}a)^n, \frac{1}{n^2}\right), \cdots\right\}, \text{ [by (IFP.12)]}$$
$$\leq \max\left\{\nu\left(a_0^{-1}(a_0 - a), 1\right), \nu\left(a_0^{-1}(a_0 - a), \frac{1}{2}\right) * \nu\left(a_0^{-1}(a_0 - a), \frac{1}{2}\right), \cdots\right\}, \text{ [by (IFPNA.2)]}$$
$$\leq \max\left\{\nu\left(a_0^{-1}, 1\right) * \nu((a_0 - a), 1), \nu\left(a_0^{-1}, \frac{1}{\sqrt{2}}\right) * \nu\left((a_0 - a), \frac{1}{\sqrt{2}}\right) * \nu\left(a_0^{-1}, \frac{1}{\sqrt{2}}\right) * \nu\left((a_0 - a), \frac{1}{\sqrt{2}}\right), \cdots\right\}, \text{ [by (IFPNA.2)]}$$
$$< \max\left\{\nu((a_0 - a), 1) * \nu((a_0 - a), 1), \nu\left((a_0 - a), \frac{1}{\sqrt{2}}\right) * \nu\left((a_0 - a), \frac{1}{\sqrt{2}}\right) * \nu\left((a_0 - a), \frac{1}{\sqrt{2}}\right) * \nu\left((a_0 - a), \frac{1}{\sqrt{2}}\right), \cdots\right\},$$

[by Equation 4.1 and (1.2) of Definition 2.1]

$$< \max\left\{\nu((a_0 - a), 1), \nu\left((a_0 - a), \frac{1}{\sqrt{2}}\right), \cdots\right\}, \text{ [by (1.6) of Definition 2.3]}$$
$$\leq \nu\left((a_0 - a), \lim_{n\to\infty}\left(\frac{1}{n^2}\right)^{\frac{1}{2n}}\right), \text{ since } \nu(a, \cdot) \text{ is a non increasing function and } 1 > \frac{1}{4^{\frac{1}{4}}} > \frac{1}{9^{\frac{1}{6}}} > \frac{1}{16^{\frac{1}{8}}} > \cdots > \frac{1}{n^{2\frac{1}{2n}}} > \cdots.$$
$$= \nu\left((a_0 - a), \lim_{n\to\infty} \frac{1}{n^{\frac{1}{n}}}\right)$$
$$= \nu((a_0 - a), 1)$$
$$\leq \nu(a - a_0, 1), \text{ [by (IFP.11)].}$$

Hence

$$\nu\left(a^{-1}a_0 - e, \frac{\pi^2}{6}\right) < \nu((a - a_0), 1) \tag{4.3}$$

Let $a \in I$ and $P(a) = a^{-1}$. Let us take $\epsilon = \frac{\pi^4}{36} > 0$,

$$\mu(P(a) - P(a_0), \epsilon)$$
$$= \mu(a^{-1} - a_0^{-1}, \tfrac{\pi^4}{36})$$
$$= \mu\left((a^{-1}a_0 - i)a_0^{-1}, \tfrac{\pi^4}{36}\right)$$
$$\geq \mu\left((a^{-1}a_0 - i), \tfrac{\pi^2}{6}\right) \diamond \mu\left(a_0^{-1}, \tfrac{\pi^2}{6}\right), \text{ [by (IFPNA.2)]}$$
$$> \mu((a - a_0), 1) \diamond \mu\left(a_0^{-1}, \tfrac{\pi^2}{6}\right), \text{ [by Equation 4.2]}$$
$$> \mu((a - a_0), 1) \diamond \mu\left((a - a_0), \tfrac{\pi^2}{6}\right), \text{ [by Equation 4.1]}$$

$\geq \mu((a-a_0),1) \diamond \mu((a-a_0),1)$, since $\mu(a,\cdot)$ is a non decreasing function and $1 < \frac{\pi^2}{6}$ and by (2.2) of Definition 2.2.

$> \mu((a-a_0),1)$, [by (2.6) of Definition 2.4]

$= \mu((a-a_0),\delta)$.
Also, $\nu(P(a)-P(a_0),\epsilon)$
$= \nu(a^{-1}-a_0^{-1},\frac{\pi^4}{36})$
$= \nu\left((a^{-1}a_0-i)a_0^{-1},\frac{\pi^4}{36}\right)$
$\leq \nu\left((a^{-1}a_0-i),\frac{\pi^2}{6}\right) * \nu\left(a_0^{-1},\frac{\pi^2}{6}\right)$, [by (IFPNA.2)]
$< \nu((a-a_0),1) * \nu\left(a_0^{-1},\frac{\pi^2}{6}\right)$, [by Equation 4.3]
$< \nu((a-a_0),1) * \nu\left((a-a_0),\frac{\pi^2}{6}\right)$, [by Equation 4.1]
$\leq \nu((a-a_0),1) * \nu((a-a_0),1)$, since $\nu(a,\cdot)$ is a non increasing function and $1<\frac{\pi^2}{6}$ and by (1.2) of Definition 2.1.
$< \nu((a-a_0),1)$, [by (1.6) of Definition 2.3]
$= \nu((a-a_0),\delta)$.
Thus for every $\epsilon>0$ there exists $\delta=\frac{\epsilon}{\frac{\pi^4}{36}}$ such that

$$\mu(P(a)-P(a_0),\epsilon)\geq \mu(a-a_0,\delta)\,,\ \nu(P(a)-P(a_0),\epsilon)\leq \nu(a-a_0,\delta).$$

Hence the mapping P from a to a^{-1} of I into I is strongly IFC.

Corollary 4.4. Let I be the set of invertible elements of a complete IFPNA $(V,\mu,\nu,\diamond,*)$. Then the mapping P from a to a^{-1} of I into I is strongly IFB.

Proof.
From Theorem 4.6 of [22] and Theorem 4.3 the corollary follows.

5. Conclusion

In this paper, we have proposed a notion of intuitionistic fuzzy pseudo normed algebra and investigated on inverse of an element in a complete IFPNA. With suitable adaptation, the notion of IFPNA deserves attention in the study of spectrum of a bounded linear operator in intuitionistic fuzzy pseudo normed linear space.

Author Contributions

All authors contributed almost equally to this work. The manuscript has been read and approved for submission by all the named authors.

Conflicts of Interest

The authors know of no conflict of interest associated with this publication and there has been no financial support for this work that could have influenced its outcome.

Acknowledgement

The authors are grateful to the referees and the Editor for their fruitful comments, valuable suggestions and careful corrections to improve this paper.

References

[1] L. A. Zadeh, *Fuzzy sets*, Information and control, 8(3), (1965) 338–353.

[2] K. T. Atanassov, *Intuitionistic fuzzy sets*, Fuzzy Sets and Systems, 20(1), (1986) 87–96.

[3] A. K. Katsaras, *Fuzzy topological vector spaces i*, Fuzzy sets and systems, 6(1), (1981) 85–95.

[4] A. K. Katsaras, *Fuzzy topological vector spaces ii*, Fuzzy sets and systems, 12(2), (1984) 143–154.

[5] C. Felbin, *Finite dimensional fuzzy normed linear space*, Fuzzy sets and Systems, 48(2), (1992) 239–248.

[6] S. C. Cheng, J. N. Mordeson, *Fuzzy linear operators and fuzzy normed linear spaces*, Bulletin of the Calcutta Mathematical Society, 86, (1994) 429–436.

[7] T. Bag, S. K. Samanta, *Finite dimensional fuzzy normed linear spaces*, Journal of Fuzzy Mathematics, 11(3), (2003) 687–706.

[8] R. Saadati, S. Vaezpour, *Some results on fuzzy banach spaces*, Journal of Applied Mathematics and Computing, 17(1), (2005) 475–484.

[9] I. Goleţ, *On generalized fuzzy normed spaces and coincidence point theorems*, Fuzzy sets and Systems, 161(8), (2010) 1138–1144.

[10] B. Dinda, T. K. Samanta, *Intuitionistic fuzzy continuity and uniform convergence*, International Journal of Open Problems in Computer Science and Mathematics, 3(1), (2010) 8–26.

[11] R. Saadati, J. H. Park, *On the intuitionistic fuzzy topological spaces*, Chaos, Solitons & Fractals, 27(2), (2006) 331–344.

[12] I. Sadeqi, F. S. Kia, *Fuzzy normed linear space and its topological structure*, Chaos, Solitons & Fractals, 40(5), (2009) 2576–2589.

[13] B. Dinda, T. K. Samanta, I. H. Jebril, *Fuzzy anti-norm and fuzzy α-anti-convergence*, Demonstratio Mathematica, 45(4), (2012) 739–754.

[14] A. K. Mirmostafaee, *Perturbation of generalized derivations in fuzzy menger normed algebras*, Fuzzy sets and systems, 195, (2012) 109–117.

[15] T. Bınzar, F. Pater, S. Nadaban, *On fuzzy normed algebras*, Journal of Nonlinear Sciences and Applications, 9(9), (2016) 5488–5496.

[16] N. Konwar, P. Debnath, *Intuitionistic fuzzy n-normed algebra and continuous product*, Proyecciones (Antofagasta), 37(1), (2018) 68–83.

[17] J. R. Kider, A. H. Ali, *Properties of a complete fuzzy normed algebra*, Baghdad Science Journal, 16(2), (2019) 382–388.

[18] S. Nădăban, *Fuzzy pseudo-norms and fuzzy f-spaces*, Fuzzy Sets and Systems, 282, (2016) 99–114.

[19] T. Bag, S. K. Samanta, *Fuzzy bounded linear operators*, Fuzzy sets and Systems, 151(3), (2005) pp. 513–547.

[20] B. Dinda, S. K. Ghosh, T. K. Samanta, *Intuitionistic fuzzy pseudo-normed linear spaces*, New Mathematics and Natural Computation, 15(1), (2019) 113–127.

[21] B. Dinda, S. K. Ghosh, T. K. Samanta, *On w-convergence and s-convergence in intuitionistic fuzzy pseudo normed spaces*, New Mathematics and Natural Computation, 17(3), (2021) 623–632.

[22] B. Dinda, S. K. Ghosh, T. K. Samanta, *Relations on continuities and boundedness in intuitionistic fuzzy pseudo normed linear spaces*, arXiv preprint, arXiv:2102.06519, 2021.

[23] B. Dinda, S. K. Ghosh, T. K. Samanta, *An introduction to spectral theory of bounded linear operators in intuitionistic fuzzy pseudo normed linear space*, Sahand Communications in Mathematical Analysis, (2021) 12 pages (accepted), doi:10.22130/SCMA.2021.531698.942.

[24] B. Schweizer, A. Sklar, *Statistical metric spaces.*, Pacific Journal of Mathematics, 10(1), (1960) 313 – 334.

[25] M. M. Gupta, J. Qi, *Theory of t-norms and fuzzy inference methods*, Fuzzy sets and systems, 40(3), (1991) 431–450.

Journal of New Results in Science 10(3) (2021) 46-59

Journal of New Results in Science

https://dergipark.org.tr/en/pub/jnrs

Research Article

Open Access

E-ISSN:1304-7981 https://doi.org/10.54187/jnrs.986038

A study on radiation shielding potentials of green and red clayey soils in Turkey reinforced with marble dust and waste tire

Zeynep Aygün[1], **Murat Aygün**[2], **Necmi Yarbaşı**[3]

Keywords:
Green and red clayey soil,
Radiation shielding,
EpiXS,
Marble dust,
Waste tire

Abstract: The increasing radiation applications in our daily life makes it essential to protect ourselves from the harms of radiation by using alternative, cheap and natural materials. The present study aimed to analyze the radiation shielding abilities of green and red clayey soils from Oltu/Erzurum in Turkey, reinforced with waste tires and marble dust. For the purpose to investigate the shielding features of the samples, radiation attenuation parameters were determined by using EpiXS software, which can calculate partial or total cross-sections, partial or total mass attenuation coefficients, electron densities, effective atomic numbers, and buildup factors for energy absorption and exposure between 1keV and 1GeV. We compared the obtained mass attenuation coefficients and total atomic cross-section values of the samples with those of a widely used shielding material, ordinary concrete, to make a meaningful evaluation about the shielding potentials of the samples. To validate obtained values by EpiXS, we also calculated the mass attenuation coefficients of the samples by XCOM code, and compatible results were obtained. Among all the studied clayey soil samples, green clay reinforced with marble dust and waste tire has the highest shielding capability. It can also be mentioned that reinforcement with marble dust and waste tire improves the shielding ability of the clayey soils.

Subject Classification (2020):

1. Introduction

Soil materials such as clayey soils are essential in geologic, construction, and environmental applications. Soil performances for some purposes can be improved by reinforcing with natural resources and types of waste based on their environment-friendly and cost-effectiveness aspects. Marble dust (MD) and waste tire (WT) were commonly chosen for reinforcing the soil materials and attracts the attention of researchers for different purposes [1-4]. Reusing waste materials is also important and can make it possible to reduce environmental problems. However, these kinds of natural and cheap materials are also significant for radiation shielding. Radiation is widely used in energy production (nuclear reactors), space exploration, medical imaging and treatment, material investigations, archaeology, military etc. [5]. Due to the increase of radiation applications in daily lives, protection from the harms of radiation has become more important nowadays. It is also important to

[1]zeynepyarbasi@hotmail.com (Corresponding author); [2]maygun@beu.edu.tr; [3]nyarbasi@atauni.edu.tr
[1]Vocational School of Technical Sciences, Bitlis Eren University, Bitlis, Turkey
[2]Department of Physics, Faculty of Science and Arts, Bitlis Eren University, Bitlis, Turkey
[3]Department of Geotechnics, Faculty of Engineering, Atatürk University, Erzurum, Turkey
Article History: Received: 23 Aug 2021 — Accepted: 05 Oct 2021 — Published: 31 Dec 2021

use alternative materials as building materials for shielding purposes. There are many studies about these kinds of materials in the literature [6-11]. Clay is one of the eco-friendly and cost-effective materials which can be used as a shielding material in construction and building purposes in many nations [11]. Important knowledge about the shielding properties of the materials can be obtained by determining radiation attenuation parameters. Radiation interaction coefficients of materials can be calculated by widely used codes such as XCOM [12], GEANT4 [13], WinXCom [14,15], and XMuDat [16], and recently Phy-X/PSD [17] and Py-MLBUF [18]. Among the lately reported codes, EpiXS makes it possible to determine the radiation shielding parameters such as mass attenuation coefficient, effective atomic number, electron density, atomic cross-section and buildup factors without knowing the density [19]. This feature takes the program one step ahead in terms of usability. Several research is done by using EpiXS recently [20-23].

The present study aimed to investigate the photon attenuation parameters; mass attenuation coefficients (MAC), effective atomic number (Z_{eff}), electron density (N_{eff}), total atomic cross-section (ACS) and buildup factors of green clayey (GC) and red clayey (RC) soils reinforced with WT and MD to learn the radiation shielding potentials of the samples. In this regard, we used EpiXS code which can perform in the energy range of 1keV-1GeV. The studied clay materials show the characteristics of the Oltu/Erzurum region consisting of Oligocene lower upper sedimentary units, volcanic rocks and upper sedimentary units. The lower sedimentary unit consists of silt-clay layers, conglomerate sandstone, and gypsum-limestone band. The upper sedimentary unit has high clay content [1,24]. To the best of our knowledge, there is no paper about the shielding potentials of the used materials in the literature. By this investigation, the determination of radiation-matter interaction parameters of unreinforced and reinforced (with MD and WT) clayey soils from Oltu/Erzurum region can contribute to the literature.

2. Materials and Methods

2.1. Samples

In this study, the used samples were taken from literature reported by Aygun and Yarbasi [1]. GC and RC samples were obtained from Oltu (Erzurum) in Turkey. WT fragments were obtained from the Erzurum industry region. Obtained shredded waste tire pieces were shaken in the sieve machine. MD was provided from the Afyon region (Turkey) by polishing, scraping, and carving the marbles. The clay samples were also prepared by reinforcing with 5% MD and 5% MD with 0.5% WT.

2.2. Calculation Process

The MAC, a quantity that defines the interaction possibility between incident photons and the mass per unit area, can be calculated by the Beer-Lambert formulated as:

$$I = I_0 e^{-\mu t} \tag{2.1}$$

$$\mu_m = \frac{\mu}{\rho} = ln(I_0/I)/\rho t = ln(I_0/I)/t_m \tag{2.2}$$

where I_0 and I are incidents and attenuated photon intensities, ρ (g/cm^3) is the density of a material, μ_m(cm^2/g) and μ(cm^{-1}) are mass, and linear attenuation coefficients, t_m (g/cm^2) and t (cm) are sample mass thickness (the mass per unit area) and the thickness, respectively.

We can write the total MAC for any compound as follows [25];

$$\mu/\rho = \sum_i w_i (\mu/\rho)_i \tag{2.3}$$

where w_i and $(\mu/\rho)_i$ are the weight fraction and the MAC of the ith constituent element, respectively.

ACS (σ_T) is defined as the sum of partial cross-sections in Eq. 2.4,

$$\sigma_T = \sigma_{PE} + \sigma_{coh} + \sigma_{incoh} + \sigma_{PP-N} + \sigma_{PP-E} \tag{2.4}$$

where σ_{PE}, σ_{coh}, σ_{incoh}, σ_{PP-N}, and σ_{PP-E} are cross sections for photoelectric, coherent, incoherent, pair production in the nuclear field, and pair production in an electron field, respectively [19].

Z_{eff} can be calculated by Eq. 2.5 where σ_e is the electronic cross-section given by Eq. 2.6 [26]. Z_{eff} can also be determined by an interpolation given in Eq. 2.7. In this equation, σ_1 and σ_2 are the elemental cross-sections of two successive elements Z_1 and Z_2.

$$Z_{eff} = \sigma_T \sigma_e \tag{2.5}$$

$$\sigma_e = \sum \frac{f_i}{Z_i} (\sigma_T)_i \tag{2.6}$$

$$Z_{eff} = \frac{Z_1(\log\sigma_2 - \log\sigma_T) + Z_2(\log\sigma_T - \log\sigma_1)}{\log\sigma_2 - \log\sigma_1} \tag{2.7}$$

N_{eff} (elctrs/g) parameter is directly proportional to its Z_{eff} as given in Eq. 2.8 [27],

$$N_{eff} = Z_{eff}\left(\frac{N_A}{\sum f_i A_i}\right) \tag{2.8}$$

Energy absorption buildup factors (EABF) or exposure buildup factors (EBF) are calculated by the given formulas below [28,29]. G-P fitting parameters for the material can be calculated by using fitting parameters in the ANSI/ANS 6.4.3 [30] in Eq. 2.9 Buildup factors are calculated using Eq. 2.11 or 12 by determining $K(E,x)$ in Eq. 2.13. The distance from the source in mfp (cm) is given as x.

$$Z_{eq} = \frac{Z_1(\log R_2 - \log R) + Z_2(\log R - \log R_1)}{\log R_2 - \log R_1} \tag{2.9}$$

$$F = \frac{F_1(\log Z_2 - \log Z_{eq}) + F_2(\log Z_{eq} - \log Z_1)}{\log Z_2 - \log Z_1} \tag{2.10}$$

$$B(E,x) = 1 + \frac{(b-1)(K^x - 1)}{(K-1)} \qquad \text{for } K \neq 1 \tag{2.11}$$

$$B(E,x) = 1 + (b-1)x \qquad \text{for } K = 1 \tag{2.12}$$

$$K(E,x) = cx^a + d\frac{\tanh\left(\frac{x}{X_k} - 2\right) - \tanh(-2)}{1 - \tanh(-2)} \qquad \text{for } x \leq 40 \text{ mfp} \tag{2.13}$$

3. Results and discussion

The chemical compositions of the used samples are given in Table 1 [1]. To validate the calculated values of unreinforced and reinforced clay materials by EpiXS, MAC values of the samples were also determined by XCOM [12], a well-known code, and a good agreement is obtained between the results.

Table 1. Chemical compositions (wt%) of the studied samples.

Samples	O	Si	Al	Fe	Ca	Mg	Na	K	C	Ti	Mn	S
GC	53.63	18.74	8.13	3.78	4.46	3.53	3.33	2.61	1.32	0.48	-	-
RC	52.69	20.49	8.60	5.74	3.53	3.05	1.29	2.68	1.26	0.68	-	-
MD	53.63	0.07	-	-	34.49	0.59	-	-	9.57	0.16	-	1.49
WT	50.10	14.59	7.64	8.85	6.86	1.76	1.21	1.65	4.20	0.59	2.55	-
GC+MD	49.20	20.95	8.71	4.94	5.02	3.77	2.92	2.91	1.10	0.47	-	-
RC+MD	53.59	20.00	8.31	4.60	4.48	3.04	1.82	2.03	1.57	0.55	-	-
GC+MD+WT	51.19	17.26	7.27	4.05	9.46	3.18	2.69	3.12	1.30	0.47	-	-
RC+MD+WT	52.51	22.73	8.89	5.14	0.94	3.74	1.48	2.67	1.30	0.61	-	-

Variations of the calculated total MAC values of the samples versus photon energies (1keV-1GeV) are shown in Fig. 1. In the low-energy range of 1-100keV, the photoelectric process is predominant and total MAC values are directly affected by this process. It was seen that MAC values decreased sharply with increasing energy in this region. In the mid-energy range of 100keV–5MeV, the Compton scattering (incoherent scattering) is dominant, and MAC values slightly changed in this region. At high energies, above 5MeV, the Pair production process (nuclear field) starts, and an increase in MAC values was observed with increasing energy. As seen in Fig. 1, it can be noticed that the MAC values of the samples determined by both EpiXS and XCOM are in good agreement. This agreement is also seen obviously in Table 2 in the range of 1-200keV (above 200 keV, the values are almost the same). To make a detailed comparison about the shielding potentials of the samples, calculated MAC values of the clays were compared with those of other reported shielding materials and the data are given in Table 3. It can be said that the studied samples have more shielding abilities than the other given shielding materials. GC has lower MAC values than RC. GC reinforced with MD (GCMD) has higher MAC values than those of RC reinforced with MD (RCMD). After adding WT to the samples, it was observed that GC reinforced with MD and WT (GCMDWT) has higher MAC values than RC reinforced with MD and WT (RCMDWT). Among the reinforced samples, the best shielding capability is obtained for GCMDWT.

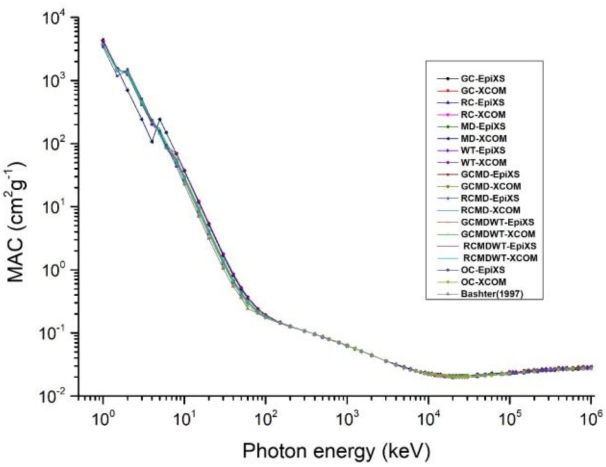

Figure 1. The changes of obtained MAC values of GC, RC, MD, WT, GCMD, RCMD, GCMDWT, RCMDWT and OC as a function of incident photon energies by EpiXS and XCOM.

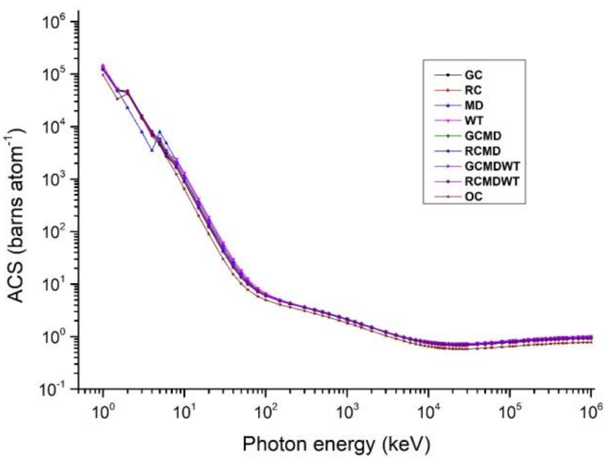

Figure 2. The changes of obtained ACS values of GC, RC, MD, WT, GCMD, RCMD, GCMDWT, RCMDWT and OC as a function of incident photon energies

The changes of total atomic cross-sections versus incident photon energies are given in Fig. 2. The sample with higher ACS values can be defined as a better shielding material. RC has higher ACS values than GC in low, mid and high energy regions. By the addition of MD, GC show higher ACS values than RC. After being reinforced with WT, higher ACS values are still observed for the GC sample. Among the reinforced materials, it can be noticed that GCMDWT has more shielding ability than the others. ACS values of the samples were also compared with those of ordinary concrete (OC), a widely used shielding material [31]; it is observed that all the studied samples have higher protection features than OC.

Table 2. Obtained MAC values of the unreinforced and reinforced samples and ordinary concrete determined by EpiXS and XCOM in the energy range of 1-200keV

Energy	GC		RC		MD		WT		GCMD		RCMD		GCMDWT		RCMDWT		OC		
(keV)	EpiXS	XCOM	EpiXS	XCOM	EpiXS	XCOM	EpiXS	XCOM	EpiXS	XCOM	EpiXS	XCOM	EpiXS	XCOM	EpiXS	XCOM	EpiXS	XCOM	[31]
1	3630	3630	3749	3748	4402	4403	4184	4182	3608	3608	3698	3698	3765	3765	3602	3602	3407	-	-
1,5	1471	1472	1439	1440	1527	1528	1553	1554	1465	1466	1434	1435	1490	1491	1417	1418	1175	-	-
2	1317	1319	1356	1358	697.8	698.2	1242	1243	1384	1386	1335	1337	1271	1273	1409	1411	1489	-	-
3	445.4	445.5	459.9	459.9	242.0	242.4	418.8	418.9	470.0	470.0	452.1	452.1	429.3	429.4	478.7	478.8	509.9	-	-
4	222.5	222.6	230.1	230.2	106.8	107.4	202.6	202.8	236.6	236.8	221.0	221.1	219.4	219.6	238.7	238.8	234.3	-	-
5	145.9	146.1	146.4	146.5	242.0	242.7	148.7	149.0	156.7	156.9	145.6	145.8	171.2	171.5	136.7	136.9	155.7	-	-
6	87.86	87.85	88.09	88.09	149.1	149.1	89.88	89.91	94.47	94.46	87.64	87.63	103.7	103.7	81.95	81.94	93.67	-	-
8	48.99	49.00	54.31	54.34	68.31	68.24	69.78	69.86	55.09	55.11	51.08	51.10	57.18	57.19	49.76	49.79	43.10	-	-
10	26.18	26.18	29.16	29.17	36.75	36.71	37.91	37.92	29.53	29.53	27.36	27.36	30.66	30.66	26.63	26.64	22.74	23.10	22.56
15	8.279	8.271	9.285	9.276	11.69	11.67	12.25	12.24	9.370	9.360	8.679	8.670	9.734	9.722	8.446	8.439	7.063	7.150	7.079
20	3.672	3.667	4.124	4.118	5.165	5.155	5.466	5.457	4.153	4.147	3.852	3.847	4.311	4.304	3.751	3.745	3.110	3.141	3.105
30	1.229	1.228	1.372	1.370	1.684	1.680	1.796	1.792	1.378	1.375	1.287	1.285	1.425	1.423	1.256	1.254	1.049	1.056	1.048
40	0.620	0.619	0.682	0.680	0.813	0.811	0.865	0.863	0.684	0.682	0.645	0.643	0.704	0.702	0.632	0.630	0.542	0.544	0.541
50	0.398	0.397	0.430	0.429	0.498	0.496	0.525	0.524	0.431	0.430	0.411	0.410	0.441	0.440	0.404	0.404	0.359	0.359	0.358
60	0.297	0.297	0.316	0.315	0.355	0.355	0.371	0.370	0.316	0.316	0.305	0.304	0.322	0.322	0.301	0.300	0.275	0.275	0.241
80	0.212	0.212	0.220	0.220	0.237	0.237	0.243	0.243	0.220	0.220	0.215	0.215	0.223	0.222	0.214	0.213	0.204	0.204	0.204
100	0.177	0.177	0.181	0.181	0.191	0.190	0.193	0.193	0.181	0.181	0.179	0.179	0.183	0.182	0.178	0.178	0.174	0.174	0.172
150	0.142	0.142	0.143	0.143	0.147	0.147	0.146	0.146	0.143	0.143	0.142	0.142	0.143	0.144	0.142	0.142	0.142	0.142	0.142
200	0.125	0.125	0.126	0.126	0.128	0.128	0.127	0.127	0.126	0.126	0.126	0.126	0.126	0.126	0.125	0.125	0.127	0.126	0.127

The energy dependence of Z_{eff} is given in Figs. 3-4. In the low energy region, due to the photoelectric effect, maximum Z_{eff} values were obtained. By increasing energy, these values decreased sharply. Then the values gradually increased and remained constant in high energies. As can be seen from the figures, Z_{eff} values of RC are higher than those of GC. By reinforced with MD, GC has higher Z_{eff} values than RC. The addition of WT again kept GCMDWT showing its more shielding potential than the other reinforced materials.

Table 3. Obtained MAC values of the unreinforced and reinforced samples and other shielding materials

Energy (keV)	GC	RC	MD	WT	GCMD	RCMD	GCMDWT	RCMDWT	Silica Sand [6]	WI [20]	Pumice [20]	IO [22]	OC [31]
10	26.18	29.16	36.75	37.91	29.53	27.36	30.66	26.63	19.88	26.09	25.01	23.40	22.74
15	8.279	9.285	11.69	12.25	9.370	8.679	9.734	8.446	6,110	8.215	7.846	7.439	7.063
20	3.672	4.124	5.165	5.466	4.153	3.852	4.311	3.751	2,685	3.635	3.468	3.265	3.110
30	1.229	1.372	1.684	1.796	1.378	1.287	1.425	1.256	0.916	1.215	1.162	1.094	1.049
40	0.620	0.682	0.813	0.865	0.684	0.645	0.704	0.632	0.484	0.614	0.591	0.560	0.542
50	0.398	0.430	0.498	0.525	0.431	0.411	0.441	0.404	0.328	0.395	0.383	0.367	0.359
60	0.297	0.316	0.355	0.371	0.316	0.305	0.322	0.301	0.257	0.295	0.288	0.279	0.275
80	0.212	0.220	0.237	0.243	0.220	0.215	0.223	0.214	0.195	0.211	0.208	0.204	0.204
100	0.177	0.181	0.191	0.193	0.181	0.179	0.183	0.178	0.169	0.177	0.175	0.182	0.174
150	0.142	0.143	0.147	0.146	0.143	0.142	0.143	0.142	0.140	0.142	0.141	0.143	0.142

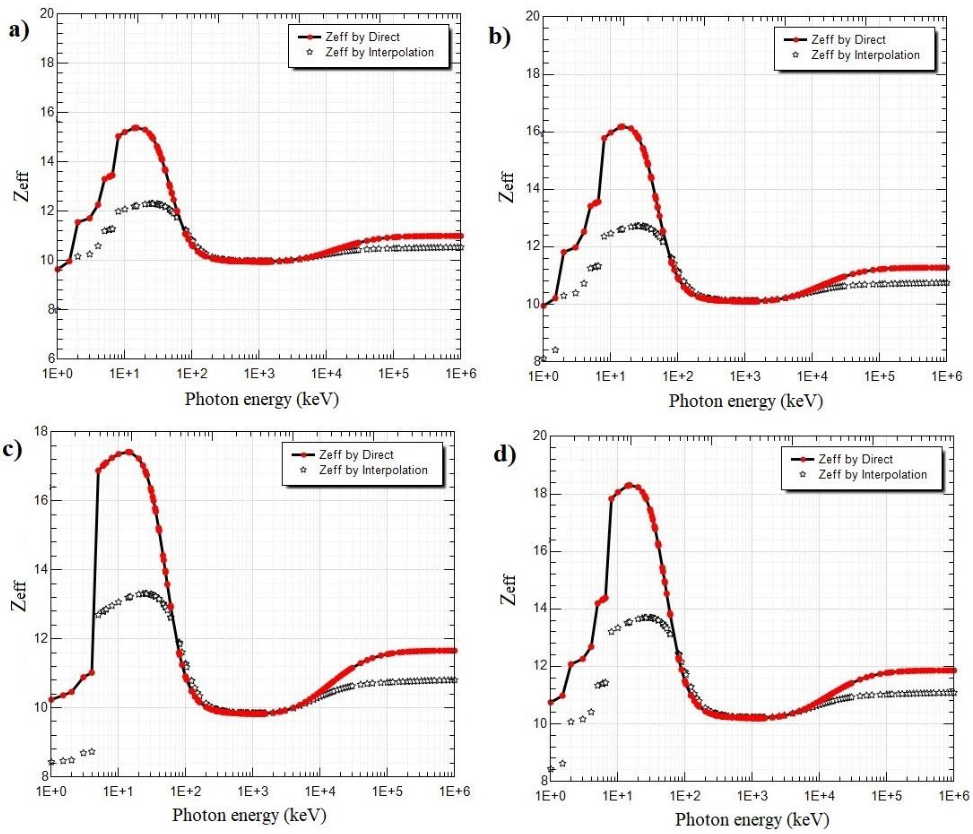

Figure 3. The changes of Z_{eff} values of GC (a) RC (b) MD (c) WT (d) as a function of incident photon energies.

Variation of N_{eff} values versus photon energies is shown in Figs. 5-6. N_{eff} is one of the most critical parameters that represents the effective conductivity of the compound depending on the excitatory photon energy. As seen in the figures, the variation of N_{eff} values versus incident photon energies is similar to that of Z_{eff} values. The interactions between photons and material with the photoelectric effect, Compton scattering, and pair production processes cause changes in the number of free electrons in the material.

EABF and EBF of the samples were calculated in 1-40 mfp depth range in the photon energy range of 0.015-15MeV. The changes of EABF and EBF versus incident photon energies were given in Figs. 7-10. As low-energy photons are absorbed by their all energies due to the photoelectric effect, buildup factor values are small in low photon energies. Compton scattering is the dominant effect in the mid-energy region, so the photons are not completely disappearing; only the energy decreases in this process. As a result, a large number of scattered photons are observed, and this causes an increase in the accumulation of photons. Thus, EABF and EBF values reach great values at medium energies. The dominant effect in high energy region is pair production, and this causes a strong absorption of photons. Therefore, the buildup factors again decrease in the high energy region [32]. As seen in Figs. 7-10, in the 1-40 mfp depth region of the samples, the buildup factors increase with increasing penetration depth. The maximum values of the buildup factors were obtained at 40 mfp.

It was observed that the buildup factors change significantly with the change of photon energies, depth of penetration and different chemical compositions of the samples. According to the obtained values of EABF and EBF, it can be mentioned that the photons cluster slightly more for GC than RC before reinforcing. By the addition of MD, RCMD has higher EABF and EBF values than GCMD. After WT addition, the RCMDWT sample gives higher EABF and EBF values. Among all samples, the highest buildup factors are observed for the GC sample. Therefore, it can be said that the maximum Compton scattering effect is observed for GC.

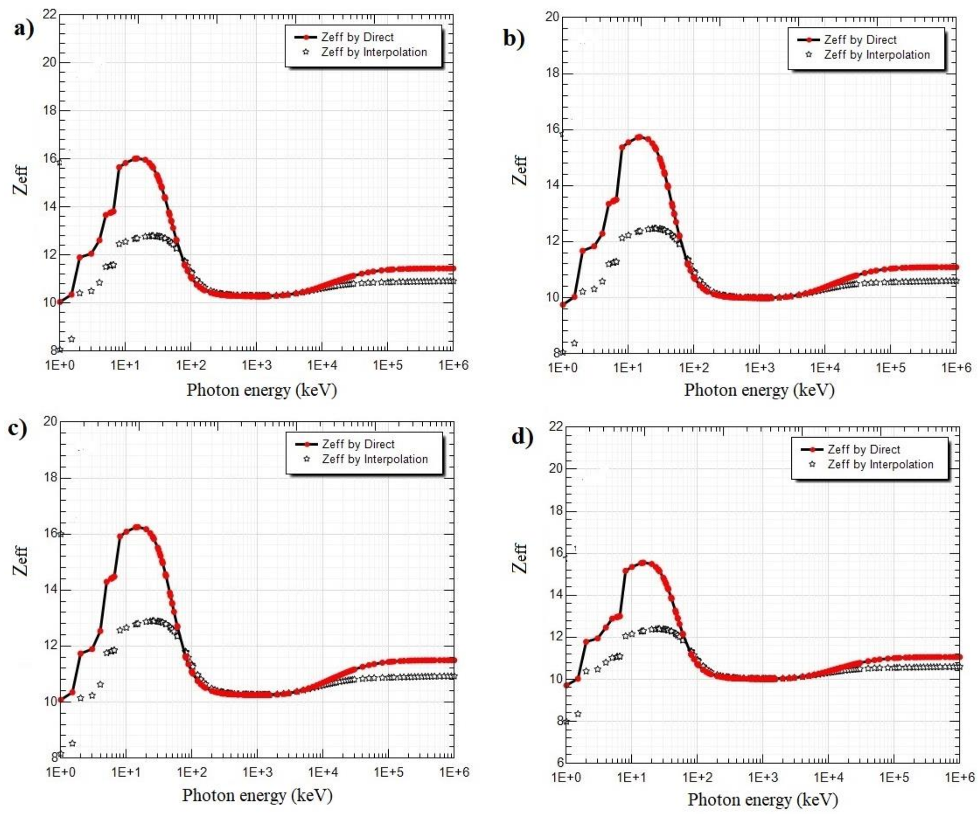

Figure 4. The changes of Z_{eff} values of GCMD (a) RCMD (b) GCMDWT (c) RCMDWT (d) as a function of incident photon energies.

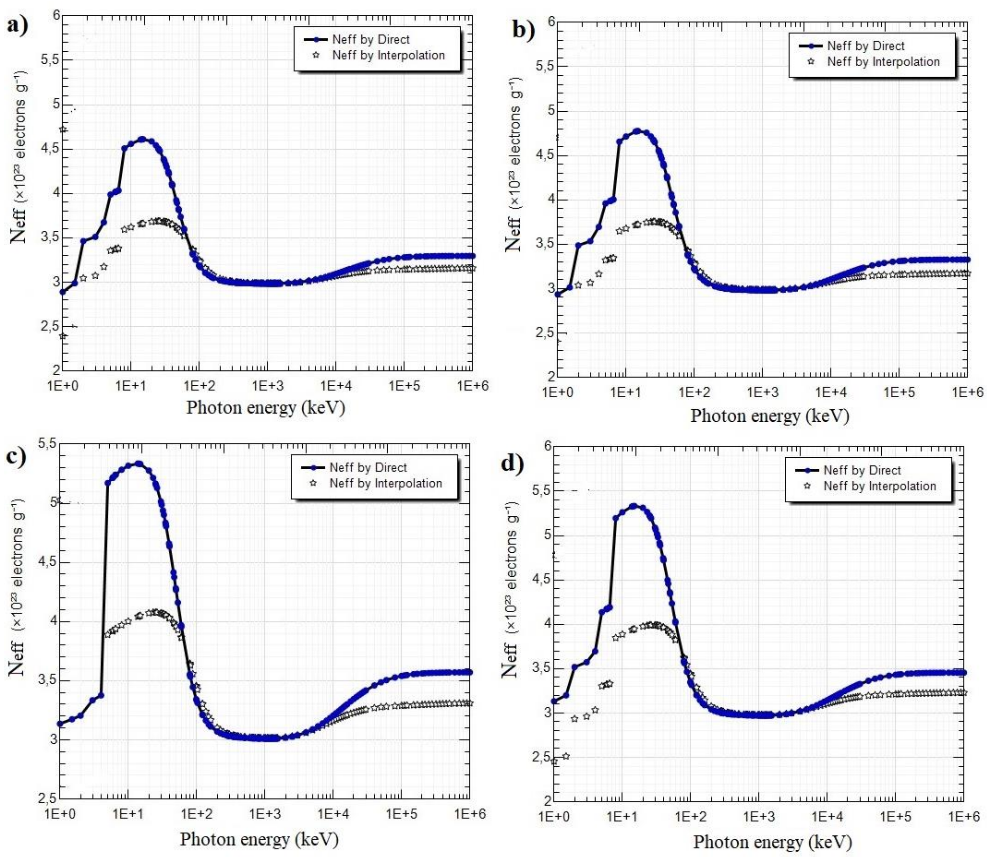

Figure 5. The variations of N_{eff} values of GC (a) RC (b) MD (c) WT (d) versus incident photon energies.

Equivalent atomic number (Z_{eq}) is the parameters that correspond to the interaction between radiation and matter. Z_{eq} is evaluated for the determination of absorbed dose, buildup factor, and energy absorption calculation. While Z_{eff} is calculated by adding all partial photon interaction processes, Compton scattering is the main process in determining Z_{eq} [33]. The obtained Z_{eq} values of the samples are listed in Table 4. As mentioned above, for Z_{eff}, Z_{eq} of RC is higher than GC, while GCMD has higher Z_{eq} values than RCMD. Z_{eq} values of RCMDWT are still lower than those of GCMDWT after WT addition.

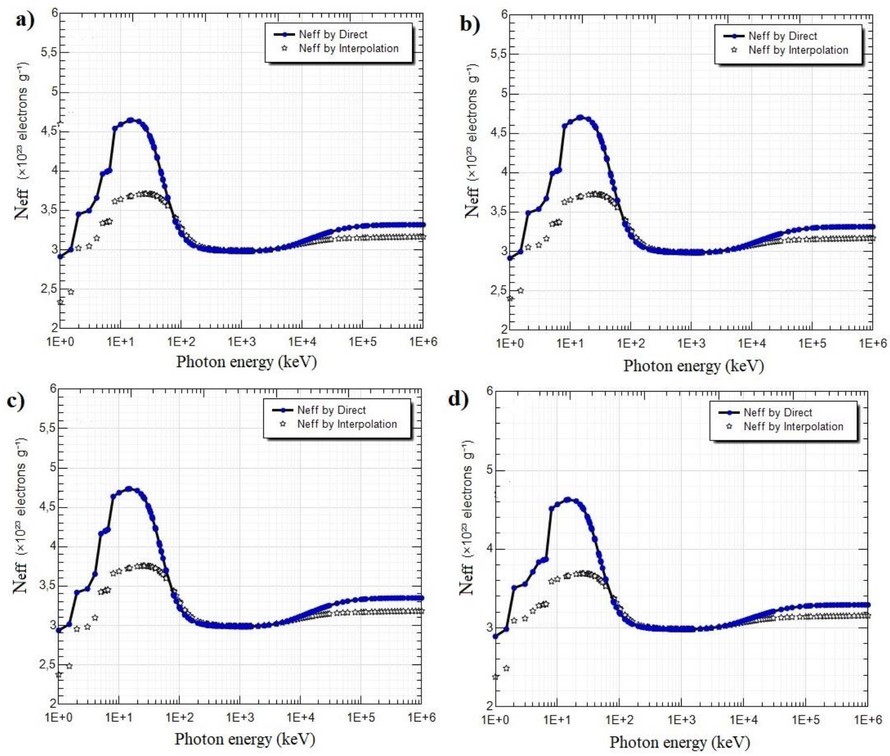

Figure 6. The variations of N_{eff} values of GCMD (a) RCMD (b) GCMDWT (c) RCMDWT (d) versus incident photon energies.

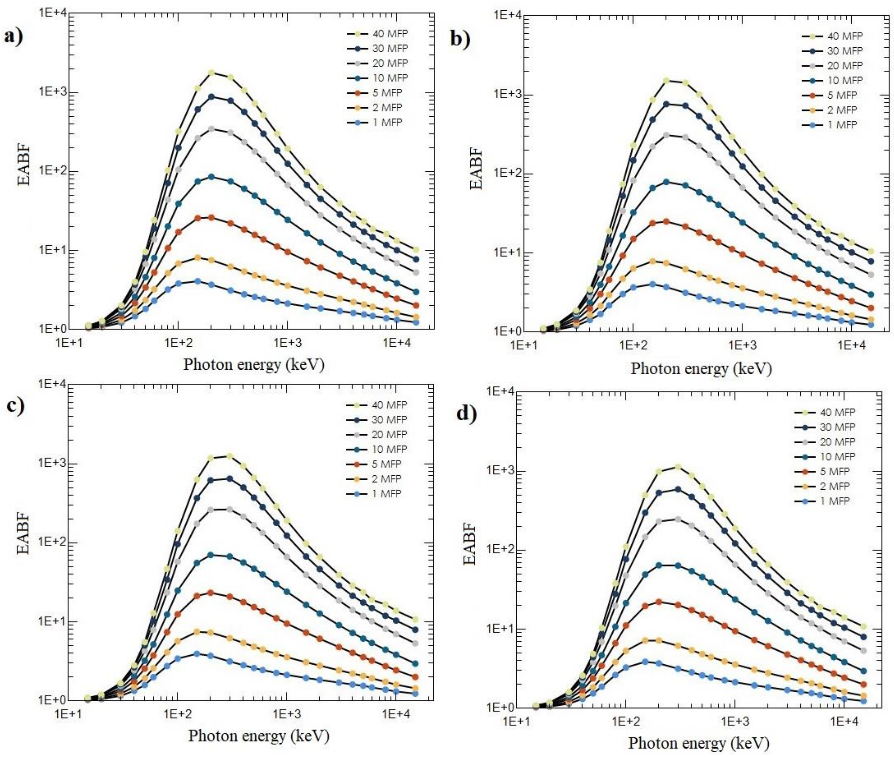

Figure 7. The changes of EABF of GC (a) RC (b) MD (c) WT (d) versus incident photon energies.

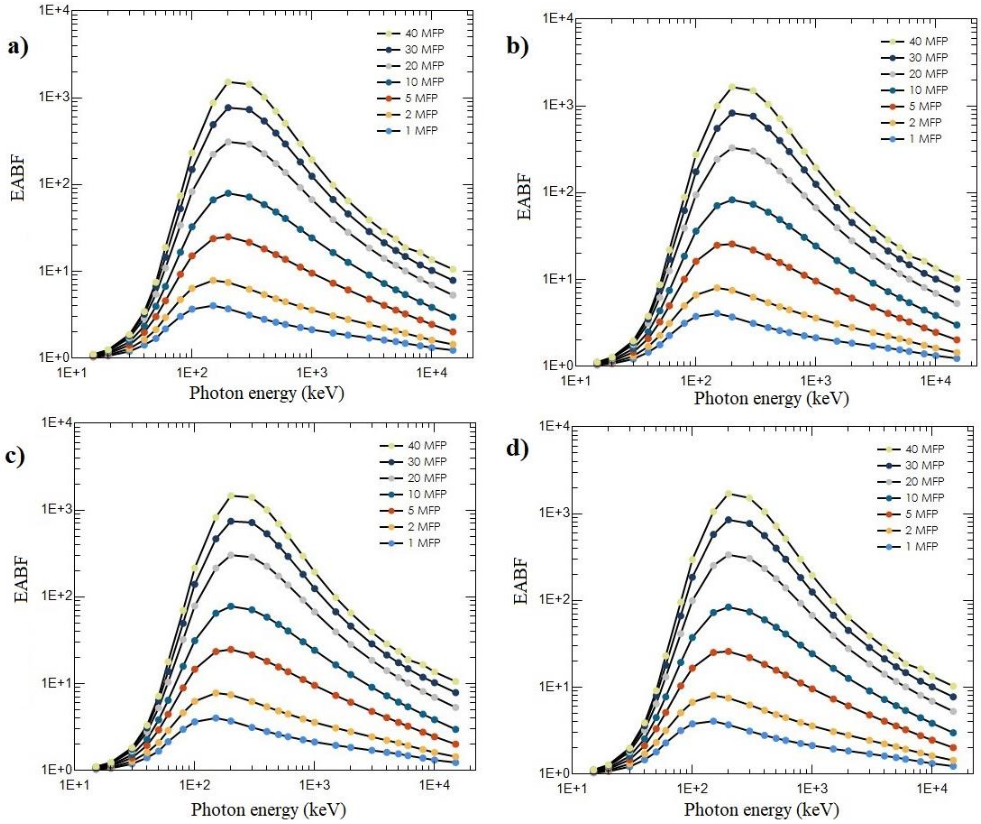

Figure 8. The changes of EABF of GCMD (a) RCMD (b) GCMDWT (c) RCMDWT (d) versus incident photon energies.

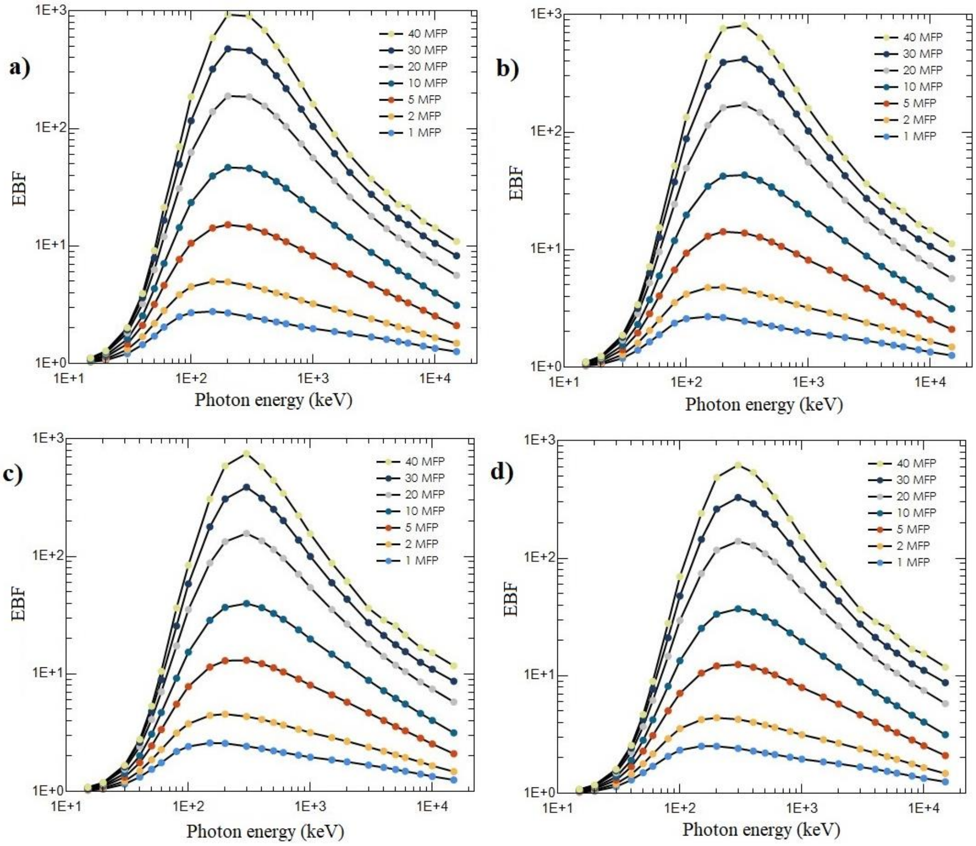

Figure 9. The variations of EBF of GC (a) RC (b) MD (c) WT (d) as a function of incident photon energies.

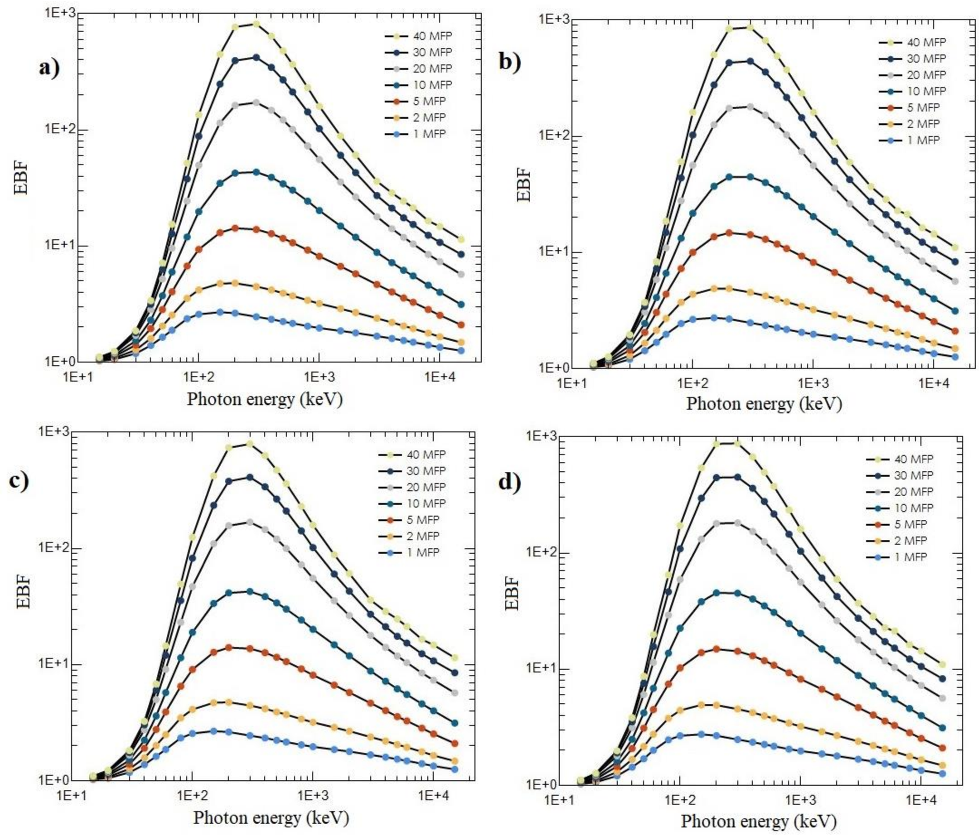

Figure 10. The variations of EBF of GCMD (a) RCMD (b) GCMDWT (c) RCMDWT (d) as a function of incident photon energies.

4. Conclusions

The present paper determined the radiation-matter interaction parameters of unreinforced and reinforced GC and RC obtained from Oltu/Erzurum in Turkey. For this purpose, we used EpiXS software to calculate the photon attenuation parameters, MAC, ACS, Z_{eff}, N_{eff}, buildup factors and Z_{eq}. MAC values of the studied samples were also calculated by XCOM software to validate the determined EpiXS results. A good agreement was obtained between the values. According to the obtained results, we can conclude that RC has more shielding features than GC. However, GCMDWT show more shielding ability than RCMDWT among reinforced samples. This result indicates that adding MD and WT increase the shielding feature of the GC. It is clear that the increase of Ca content in reinforced GC improves the shielding potential of the sample. Therefore, it can be said that chemical composition is one of the factors which affect the shielding property of the materials. Among all the studied clayey soil samples, GCMDWT has the highest shielding capability. It can be said that the maximum Compton scattering effect is observed for GC due to the obtained highest buildup factors. As a result of comparing MAC and ACS values of the samples with ordinary concrete, we can conclude that all the studied samples have more shielding potential than a widely preferred shielding material, ordinary concrete. Therefore, the studied clayey (both unreinforced and reinforced) materials can be used as building materials for shielding purposes in many places related to radiation.

Table 4. Z_{eq} values of the unreinforced and reinforced samples determined by EpiXS.

Energy (keV)	GC	RC	M	W	GCM	RCM	GCMW	RCMW
15	12.89694	13.37959	14.31205	14.60366	13.42975	13.08630	13.58021	12.98012
20	13.05550	13.56008	14.50558	14.83670	13.59793	13.26079	13.74937	13.15151
30	13.23567	13.75602	14.69286	15.08732	13.77945	13.44850	13.92991	13.33993
40	13.35366	13.88703	14.81830	15.25659	13.90104	13.57192	14.05380	13.46337
50	13.43449	13.98435	14.91022	15.37267	13.99203	13.65885	14.14408	13.54863
60	13.49492	14.05589	14.98193	15.46018	14.05823	13.72450	14.20851	13.61318
80	13.58402	14.15710	15.07118	15.58434	14.15203	13.82381	14.29917	13.71033
100	13.64202	14.22010	15.12996	15.66524	14.21049	13.88902	14.35745	13.77365
150	13.73860	14.32201	15.20895	15.79824	14.30425	13.99865	14.44930	13.88156
200	13.79929	14.38330	15.25712	15.87674	14.36087	14.05458	14.50563	13.94790
300	13.87079	14.45799	15.31306	15.97470	14.42956	14.12087	14.57360	14.02296
400	13.91459	14.49992	15.34185	16.02170	14.46838	14.16017	14.61134	14.06281
500	13.93404	14.52353	15.36084	16.04983	14.48993	14.17899	14.63327	14.08116
600	13.94705	14.53786	15.36967	16.06470	14.50298	14.19129	14.64596	14.09362
800	13.95293	14.54443	15.37210	16.07471	14.50861	14.19672	14.65102	14.09938
1000	13.96343	14.55146	15.37628	16.07892	14.51544	14.20494	14.65731	14.10801
1500	11.94591	12.38245	13.10451	13.49454	12.48925	12.10903	12.59738	12.04416
2000	11.44070	11.78642	12.40171	12.61042	11.93270	11.56173	12.02207	11.51112
3000	11.31237	11.63247	12.19695	12.37299	11.78646	11.42222	11.86702	11.37830
4000	11.27695	11.59001	12.14171	12.30958	11.74566	11.38376	11.82390	11.34142
5000	11.26036	11.57239	12.11927	12.28483	11.72984	11.36658	11.80725	11.32484
6000	11.25366	11.56218	12.10295	12.26577	11.71913	11.35857	11.79549	11.31743
8000	11.24021	11.54825	12.08636	12.24656	11.70645	11.34481	11.78233	11.30388
10000	11.23472	11.54181	12.07684	12.23664	11.70026	11.33895	11.77559	11.29831
15000	11.22824	11.53492	12.06371	12.22419	11.69371	11.33228	11.76818	11.29210

Author Contributions

All authors contributed equally to this work. They all read and approved the last version of the manuscript.

Conflicts of Interest

The authors declare no conflict of interest.

References

[1] Z. Aygun, N. Yarbasi, *A Spectroscopic Analysis of Clay Types and Silty Sand from Oltu/Erzurum (Turkey) Region Reinforcing with Marble Dust and Waste Tire,* Karaelmas Science and Engineering Journal, 9(2), (2019) 215-226.

[2] M. Jafari, M. Esnaashari, *Effect of waste tire cord reinforcement on unconfined compressive strength of lime stabilized clayey soil under freeze-thaw condition*, Cold Regions Science and Technology, 82, (2012) 21-29.

[3] R. T. Erdem, A. U. Oztürk, *Effect of Marble Powder Additive on Freezing-Thawing Properties of Cement Mortar*, BEU Journal of Science, 1(2), (2012) 85-91.

[4] N. Yarbasi, E. Kalkan, *The Mechanical Performance of Clayey Soils Reinforced with Waste PET Fibers*, International Journal of Earth Science and Knowledge Applications, 2(1), (2020) 19-26.

[5] B. Aygün, *Neutron and gamma radiation shielding properties of high-temperature-resistant heavy concretes including chromite and wolframite*, Journal of Radiation Research and Applied Sciences, 12, (2019) 352-359.

[6] R. S. M. Rashid, S. M. Salem, N. M. Azreen, Y. L. Voo, M. Haniza, A. A. Shukri, M. S. Yahya, *Effect of elevated temperature to radiation shielding of ultra-high-performance concrete with silica sand or magnetite,* Construction and Building Materials, 262, (2020) 120567

[7] O. Gencel, A. Bozkurt, E. Kam, T. Korkut, *Determination and calculation of gamma and neutron shielding characteristics of concretes containing different hematite proportions*, Annals of Nuclear Energy, 38, (2011) 2719–2723.

[8] A. Gür, B. Artıg, T. Cakır, *Photon attenuation properties of concretes containing magnetite and limonite ores*, Physicochemical Problems of Mineral Process, 53(1), (2017) 184−191.

[9] I. Akkurt, H. Canakci, *Radiation attenuation of boron-doped clay for 662, 1173 and 1332 keV gamma rays*, Iranian Journal of Radiation Research, 9(1), (2011) 37-40.

[10] H. S. Mann, G. S. Brar, G. S. Mudahar, *Gamma-ray shielding effectiveness of novel light-weight clay-flyash bricks*, Radiation Physics and Chemistry, 127, (2016) 97-101.

[11] S. F. Olukotun, S. T. Gbenu, F. I. Ibitoye, O. F. Oladejo, H. O. Shittu, M. K. Fasasi, F. A. Balogun, *Investigation of gamma radiation shielding capability of two clay materials*, Nuclear Engineering and Technology, 50, (2018) 957-962.

[12] M. J. Berger, J. H. Hubbell, *XCOM: Photon Cross Sections Database*, Web Version 1.2. National Institute of Standards and Technology Gaithersburg, MD, (1987) 20899, USA, available at. http://physics.nist.gov/xcom.

[13] S. Agostinelli, J. Allison, K. Amako, J. Apostolakis, H. Araujo, et al., *Geant4-a simulation toolkit*, Nuclear Instrumentation and Methods Physics Research Section A, 506, (2003) 250-303.

[14] L. Gerward, N. Guilbert, K. B. Jensen, H. Levring, *X-ray absorption in matter. Reengineering XCOM*, Radiation Physics and Chemistry, 60, (2001) 23–24.

[15] L. Gerward, N. Guilbert, K. B. Jensen, H. Levring, *WinXCom-a program for calculating X-ray attenuation coefficients*, Radiation Physics and Chemistry, 71, (2004) 653–654.

[16] R. Nowotny, *XMuDat: Photon attenuation data on PC*, IAEA Report IAEA-NDS, (1998) 195.

[17] E. Sakar, Ö. F. Özpolat, B. Alım, M.I. Sayyed, M. Kurudirek, *Phy-X / PSD: Development of a user friendly online software for calculation of parameters relevant to radiation shielding and dosimetry*, Radiation Physics and Chemistry, 166, (2020) 1-12.

[18] K. S. Mann, S. S. Mann, *Py-MLBUF: Development of an online-platform for gamma-ray shielding calculations and investigations*, Annals of Nuclear Energy, 150, (2021) 107845.

[19] F. C. Hila, A. A. Astronomo, C. A. M. Dingle, J. F. M. Jecong, A. M. V. Javier-Hila, et al., *EpiXS: A Windows-based program for photon attenuation, dosimetry and shielding based on EPICS2017 (ENDF/B-VIII) and EPDL97 (ENDF/B-VI8)*, Radiation Physics and Chemistry, 182, (2021) 109331.

[20] Z. Aygun, M. Aygun, A *study on usability of Ahlat ignimbrites and pumice as radiation shielding materials, by using EpiXS code*, International Journal of Environmental Science and Technology, (2021). https://doi.org/10.1007/s13762-021-03530-9.

[21] M. B. Z. Gili, F. C. Hila, *Investigation of Gamma-ray Shielding Features of Several Clay Materials Using the EPICS2017 Library*, Philippine Journal of Science, 150 (5), (2021) 1017-1026.

[22] Z. Aygun, N. Yarbasi, M. Aygun *Spectroscopic and radiation shielding features of Nemrut, Pasinler, Sarıkamıs and Ikizdere obsidians in Turkey: Experimental and theoretical study,* Ceramics International, (2021). https://doi.org/10.1016/j.ceramint.2021.08.330.

[23] A. H. Almuqrin, M. I. Sayyed, J. F. M. Jecong, A. Kumar, M. M. AlShammari, B. Albarzan, *SrO-SiO2-B2O3-ZrO2 glass system: Effects of varying SrO and BaO compositions to physical and optical properties, and radiation shielding using EPDL2017 photoatomic library*, Optik, 245, (2021) 167670.

[24] N. Yarbasi, *Geotechnical mapping of Oltu (Erzurum) residential area and its vicinity*, Pamukkale University Journal of Engineering and Science, 22, (2016) 538-545.

[25] D. F. Jackson, D.J. Hawkes, *X-ray attenuation coefficients of elements and mixtures*, Physics Reports, 70, (1981) 169–233.

[26] L. F. Pires, *Soil analysis using nuclear techniques: a literature review of the gamma ray attenuation method*, Soil Tillage Research, 184, (2018) 216–234.

[27] S. Prabhu, A. C. Sneha, P. P. Shetty, A. A. Narkar, S. G. Bubbly, S. B. Gudennavar, *Effective atomic number and electron density of some biologically important lipids for electron, proton, alpha particle and photon interactions*, Applied Radiation and Isotopes, 160, (2020) 109137.

[28] Y. Harima, *An historical review and current status of buildup factor calculations and applications*, Radiation Physics and Chemistry, 41(4–5), (1993) 631–672.

[29] Y. Harima, Y. Sakamoto, S. Tanaka, M. Kawai, *Validity of the geometric-progression formula in approximating gamma-ray buildup factors*, Nuclear Science and Engineering, 94(1), (1986) 24–35.

[30] ANSI/ANS 643, *Gamma-ray Attenuation Coefficients and Buildup Factors for Engineering Materials*, American Nuclear Society La Grange Park Illinois (1991).

[31] I. I. Bashter, *Calculation of radiation attenuation coefficients for shielding concretes*, Annals of Nuclear Energy, 24(17), (1997) 1389-1401.

[32] N. Kücük, O. Gezer, *Determination of Build-up Factors for Natural Black Obsidian Ores*, AKU Journal of Science and Engineering, 17, (2017) 872-880.

[33] S. S. Obaid, M. I. Sayyed, D. K. Gaikwad, P. P. Pawara, *Attenuation coefficients and exposure buildup factor of some rocks for gamma ray shielding applications*, Radiation Physics and Chemistry, 148, (2018) 86-94.

Journal of New Results in Science 10(3) (2021) 60-66

Journal of New Results in Science
https://dergipark.org.tr/en/pub/jnrs
Research Article
Open Access

E-ISSN: 1304-7981 https://doi.org/10.54187/jnrs.989508

On some identities and Hankel matrices norms involving new defined generalized modified pell numbers

Gül Özkan Kızılırmak[1]

Keywords
Modified Pell Numbers, Hankel Matrices, Matrix Norms

Abstract — The aim of this paper is to introduce a generalization of Modified Pell numbers. Some identities about this new sequence are obtained and also investigated some relationships with another sequence. Finally, using these sequences the row and column norms of the Hankel matrices are presented.

Subject Classification (2020): 11B37, 11K31.

1. Introduction

In the literature, there are many integer sequences defined by a recurrence relation [1–3]. These sequences have been studied in many areas. One of the mentioned sequences is the Pell sequence. Pell sequence can be defined as [4]:

$$P_{n+1} = 2P_n + P_{n-1} \tag{1.1}$$

for $n \geq 1$ with initial conditions $P_0 = 0$ and $P_1 = 1$.

The Pell-Lucas $\{Q_n\}$ and Modified Pell $\{q_n\}$ sequences are defined by the same recurrence but the initial conditions such as $Q_0 = Q_1 = 2$ and $q_0 = q_1 = 1$ respectively [5].

There are a lot of studies on the generalization of these sequences [6–10]. A generalization of the Pell and Pell-Lucas numbers are defined as follows [11]:

$$P_{k,n} = kP_{k,n-1} + (k-1)P_{k,n-2} \tag{1.2}$$

for $n \geq 2$ and with initial conditions $P_{k,0} = 0$ and $P_{k,1} = 1$.

$Q_{k,n} = kQ_{k,n-1} + (k-1)Q_{k,n-2}$, for $n \geq 2$ with initial conditions $Q_{k,0} = Q_{k,1} = 2$.

[1]gulozkan@gazi.edu.tr (Corresponding Author)
[1]Department of Mathematics, Faculty of Science, Gazi University, Ankara,Turkey
Article History: Received: 01 Sep 2021 - Accepted: 30 Nov 2021 - Published: 31 Dec 2021

If $k=2$ in (1.2), we get Pell and Pell-Lucas numbers. $P_{k,n}$ and $Q_{k,n}$ have characteristic equation as follow:

$$r^2 - kr + 1 - k = 0 \tag{1.3}$$

Since $k \geq 2$, the characteristic equation has two roots

$$r_1 = \frac{1}{2}\left(k - \sqrt{k^2+4k-4}\right), r_2 = \frac{1}{2}\left(k + \sqrt{k^2+4k-4}\right). \tag{1.4}$$

$P_{k,n}$ and $Q_{k,n}$ have Explicit formulas for their general terms as follows:

$$P_{k,n} = \frac{r_1^n - r_2^n}{r_1 - r_2}, Q_{k,n} = \frac{2(1-r_2)\, r_1^n + 2(r_1-1)\, r_2^n}{r_1 - r_2}. \tag{1.5}$$

In addition, the expression of the sum of the first terms of the $P_{k,n}$ and $Q_{k,n}$ series is as follows:

$$\sum_{r=0}^{n} P_{k,r} = \frac{1}{2(k-1)}((k-1)P_{k,n} + P_{k,n+1} - 1), \sum_{r=0}^{n} Q_{k,r} = \frac{1}{2(k-1)}((k-1)Q_{k,n} + Q_{k,n+1} + 2k - 4). \tag{1.6}$$

A Hankel matrix [12] is an $n \times n$ symmetric matrix $H_n = \left(h_{ij}\right)$, where $h_{ij} = h_{i+j-1}$, that is a matrix of the form

$$H_n = \begin{bmatrix} h_1 & h_2 & h_3 & \cdots & h_n \\ h_2 & h_3 & h_4 & \cdots & h_{n+1} \\ \vdots & \vdots & \vdots & \ddots & \vdots \\ h_n & h_{n+1} & h_{n+2} & \cdots & h_{2n-1} \end{bmatrix}.$$

Column norm $\|H_n\|_1$ and row norm $\|H_n\|_\infty$ of Hankel matrix are equivalent and defined as follows:

$$\|H_n\|_1 = \begin{matrix} \max \\ i \leq j \leq 1 \end{matrix} \sum_{i=1}^{n} \left|h_{ij}\right| = \|H_n\|_\infty . \tag{1.7}$$

In this paper, a new generalization of Modified Pell numbers is defined. Then,the generating function, Binet formula, and some identities are obtained. Finally, some special cases of Hankel matrices involving $P_{k,n}$ and $q_{k,n}$ are studied.

2. One-Parameter Generalization of Modified Pell Numbers

In this section, the Modified Pell numbers $q_{k,n}$ is defined. Then, the generating function, the Binet Formula and some identities are obtained.

Definition 2.1. Let $k \geq 2$ be an integer. Then, we define generalized Modified Pell Numbers $q_{k,n}$ as follows:

$$q_{k,n} = kq_{k,n-1} + (k-1)q_{k,n-2} \tag{2.1}$$

for $n \geq 2$ and with initial conditions $q_{k,0} = q_{k,1} = 1$.

The characteristic equation associated to (2.1) is

$$r^2 - kr + 1 - k = 0 \tag{2.2}$$

This equation has two roots

$$r_1 = \frac{1}{2}\left(k - \sqrt{k^2 + 4k - 4}\right), r_2 = \frac{1}{2}\left(k + \sqrt{k^2 + 4k - 4}\right). \tag{2.3}$$

Moreover, the following equations hold true:

$$r_1 + r_2 = k \tag{2.4}$$

$$r_1 r_2 = 1 - k. \tag{2.5}$$

Theorem 2.2. The generating function for the generalized modified pell numbers is

$$H\left(q_{k,n}; x\right) = h_k\left(x\right) = \sum_{n=0}^{\infty} q_{k,n} x^n = q_{k,0} + q_{k,1} x + q_{k,2} x^2 + \ldots + q_{k,n} x^n + \ldots. \tag{2.6}$$

Proof.
Using the initial conditions, we get

$$h_k\left(x\right) = 1 + x + \sum_{n=2}^{\infty} \left(k q_{k,n-1} + \left(k-1\right) q_{k,n-2}\right) x^n \tag{2.7}$$

By doing some calculations on the right side of the equation (2.7) , we get

$$\begin{aligned} 1 + x + \sum_{n=2}^{\infty} \left(k q_{k,n-1} + \left(k-1\right) q_{k,n-2}\right) x^n &= 1 + x + kx \sum_{n=2}^{\infty} q_{k,n-1} x^{n-1} + \left(k-1\right) x^2 \sum_{n=2}^{\infty} q_{k,n-2} x^{n-2} \\ &= 1 + x + kx \sum_{n=1}^{\infty} q_{k,n} x^n + \left(k-1\right) x^2 \sum_{n=0}^{\infty} q_{k,n} x^n. \end{aligned}$$

By using equation (2.6), we obtain

$$h_k\left(x\right) = 1 + x - kx + kx h_k\left(x\right) + \left(k-1\right) x^2 h_k\left(x\right).$$

Hence, we have

$$h_k\left(x\right) = \frac{1 + x - kx}{1 - kx - \left(k-1\right) x^2}$$

Theorem 2.3. (Binet's Formula) The nth Generalized Modified Pell Number is given by

$$q_{k,n} = \frac{\left(1 - r_2\right) r_1^n + \left(r_1 - 1\right) r_2^n}{r_1 - r_2} \tag{2.8}$$

where r_1,r_2 are given in (2.3).

Proof.
Since the equation (2.2) has two distinct roots, the sequence

$$q_{k,n} = e r_1^n + f r_2^n \tag{2.9}$$

is the solution of the equation (2.1). Putting $q_{k,0} = q_{k,1} = 1$ we get $e + f$ and $e r_1 + f r_2 = 1$. If we solve this system of linear equations, we obtain $e = \frac{1 - r_2}{r_1 - r_2}$ and $f = \frac{r_1 - 1}{r_1 - r_2}$.

Using these values and (2.9) we obtain (2.8) as required.

Corollary 2.4. Let k and n be integers and $k \geq 2$ and $n \geq 0$. Then, we get

$$2q_{k,n} = Q_{k,n}.$$

Proof.

By using (1.5), we can prove it.

Corollary 2.5. Let k and n be integers and $k \geq 2$ and $n \geq 0$. Then, we get

$$q_{k,n} = P_{k,n} + (k-1)P_{k,n-1}$$

Proof.

By using (2.8) we get

$$q_{k,n} = \frac{(1-r_2)\,r_1^n + (r_1-1)\,r_2^n}{r_1-r_2} = \frac{r_1^n - r_2^n}{r_1-r_2} + \frac{r_2^n r_1 - r_1^n r_2}{r_1-r_2} = \frac{r_1^n - r_2^n}{r_1-r_2} - r_1 r_2 \frac{r_1^{n-1} - r_2^{n-1}}{r_1-r_2}.$$

Using (2.5), we have

$$q_{k,n} = P_{k,n} + (k-1)P_{k,n-1}.$$

Corollary 2.6. Let k and n be integers and $k \geq 2$ and $n \geq 0$. Then, we obtain

$$q_{k,n} = P_{k,n+1} - (k-1)P_{k,n}.$$

Proof.

By using Corollary 2.5, we can proof it.

Theorem 2.7. (Catalan's Identitiy) For any positive integer r, we get

$$q_{k,n-r}\,q_{k,n+r} - q_{k,n}^2 = -2(1-k)^{n-r+1}P_{k,r}^2.$$

Proof.

Using (2.8), we have

$$\begin{aligned}
q_{k,n-r}\,q_{k,n+r} - q_{k,n}^2 &= \frac{(1-r_2)r_1^{n-r}+(r_1-1)r_2^{n-r}}{r_1-r_2}\,\frac{(1-r_2)r_1^{n+r}+(r_1-1)r_2^{n+r}}{r_1-r_2} - \left(\frac{(1-r_2)r_1^{n}+(r_1-1)r_2^{n}}{r_1-r_2}\right)^2 \\
&= \frac{(1-r_2)r_1^{n-r}(r_1-1)r_2^{n+r}+(1-r_2)r_1^{n+r}(r_1-1)r_2^{n-r}-2(1-r_2)r_1^{n}(r_1-1)r_2^{n}}{(r_1-r_2)^2} \\
&= \frac{(1-r_2)(r_1-1)(r_1r_2)^n}{(r_1-r_2)^2}(r_1^{-r}r_2^{r}+r_1^{r}r_2^{-r}-2) \\
&= \frac{(1-r_2)(r_1-1)(r_1r_2)^n}{(r_1-r_2)^2}\,\frac{(r_1^{-2r}+r_2^{2r}-2(r_1r_2)^r)}{(r_1r_2)^r} \\
&= \frac{(1-r_2)(r_1-1)(r_1r_2)^n}{(r_1-r_2)^2}(r_1^{-r}-r_2^{r})^2 \\
&= (r_1r_2)^{n-r}(r_1-r_1r_2-1+r_2)\left(\frac{r_1^{-r}-r_2^{r}}{r_1-r_2}\right)^2
\end{aligned}.$$

By using (2.5) and (1.5), we get

$$\begin{aligned}
q_{k,n-r}\,q_{k,n+r} - q_{k,n}^2 &= (1-k)^{n-r}(2k-2)P_{k,r}^2 \\
&= -2(1-k)^{n-r+1}P_{k,r}^2.
\end{aligned}$$

Theorem 2.8. Let m, n be positive integers and $m \geq n$. Then, we get

$$q_{k,m} q_{k,n+1} - q_{k,m+1} q_{k,n} = (1-k)^{n+1} P_{k,m-n}.$$

Proof.

By using (2.8), we have

$$\begin{aligned} q_{k,m} q_{k,n+1} - q_{k,m+1} q_{k,n} &= \frac{(r_2-1)r_1^m+(1-r_1)r_2^m}{r_2-r_1} \frac{(r_2-1)r_1^{n+1}+(1-r_1)r_2^{n+1}}{r_2-r_1} \\ &- \frac{(r_2-1)r_1^{m+1}+(1-r_1)r_2^{m+1}}{r_2-r_1} \frac{(r_2-1)r_1^{n}+(1-r_1)r_2^{n}}{r_2-r_1} \\ &= (r_2-1)(1-r_1) \frac{(r_1 r_2)^n (r_1^{m-n} r_2 + r_2^{m-n} r_1 - r_1^{m-n+1} - r_2^{m-n+1})}{(r_2-r_1)^2} \\ &= (r_2-1)(1-r_1)(r_1 r_2)^n \frac{r_1^{m-n}-r_2^{m-n}}{r_2-r_1}. \end{aligned}$$

Using (2.5), we get

$$q_{k,m} q_{k,n+1} - q_{k,m+1} q_{k,n} = (1-k)^{n+1} P_{k,m-n}.$$

Theorem 2.9. For all integers $k \geq 2$ and $n \geq 0$ we obtain

$$\sum_{i=0}^{n} q_{k,i} = \frac{1}{2(1-k)}((1-k)q_{k,n} - q_{k,n+1} + 2 - k).$$

Proof.

Note that

$$\begin{aligned} \sum_{i=0}^{n} q_{k,i} &= \frac{(1-r_2)}{r_1-r_2} \sum_{i=0}^{n} r_1^n + \frac{(r_1-1)}{r_1-r_2} \sum_{i=0}^{n} r_2^n = \frac{(1-r_2)}{r_1-r_2}\left(\frac{1-r_1^{n+1}}{1-r_1}\right) + \frac{(r_1-1)}{r_1-r_2}\left(\frac{1-r_2^{n+1}}{1-r_2}\right) \\ &= \frac{(1-r_2)^2(1-r_1^{n+1})-(r_1-1)^2(1-r_2^{n+1})}{(r_1-r_2)(1-r_1)(1-r_2)} = \frac{1}{(1-r_1)(1-r_2)}\Big(\frac{-(r_1^{n+1})(1-r_2)-r_2^{n+1}(r_1-1)}{(r_1-r_2)} \\ &+ r_1 r_2 \frac{(r_1^n(1-r_2)+r_2^n(r_1-1))}{(r_1-r_2)} + \frac{2(r_1-r_2)-(r_1+r_2)(r_1-r_2)}{r_1-r_2}\Big) \end{aligned}$$

.

By using (2.5), (2.8) and by noting that $(1-r_1)(1-r_2) = 2(1-k)$, we get

$$\sum_{i=0}^{n} q_{k,i} = \frac{1}{2(1-k)}(-q_{k,n+1} + (1-k)q_{k,n} + 2 - k).$$

3. Norms of Hankel Matrices Involving $q_{k,n}$ and $P_{k,n}$

In the literature, some important works have been done about norms of some matrices especially, the norms and bounds for the norms of Hankel matrix involving some integer sequences were studied [11],[12]. In this section, we obtain row and column norms of the Hankel matrix using $q_{k,n}$ and $P_{k,n}$.

Theorem 3.1. Let A be a $n \times n$ matrix with $a_{ij} = P_{k,i+j-1}$. Then, we have

$$\|A\|_1 = \|A\|_\infty = \frac{1}{2(k-1)}(q_{k,2n} - q_{k,n}).$$

Proof.
Using $a_{ij} = P_{k,i+j-1}$, we get

$$\|A\|_1 = \max_{i \leq j \leq 1} \sum_{i=1}^{n} |a_{ij}| = \max_{i \leq j \leq 1} \{|a_{1j}| + |a_{2j}| + ... + |a_{nj}|\} = P_{k,n} + P_{k,n+1} + ... + P_{k,2n-1} = \sum_{i=0}^{2n-1} P_{k,i} - \sum_{i=0}^{n-1} P_{k,i}.$$

Now using (1.6) and Corollary 2.5, we get

$$\|A\|_1 = \frac{1}{2(k-1)}((k-1)P_{k,2n-1} + P_{k,2n-1}) - \frac{1}{2(k-1)}((k-1)P_{k,n-1} + P_{k,n-1}) = \frac{1}{2(k-1)}(q_{k,2n} - q_{k,n}).$$

Theorem 3.2. Let B be a $n \times n$ matrix with $b_{ij} = q_{k,i+j-1}$. Then, we get

$$\|B\|_1 = \|B\|_\infty = \frac{1}{2(1-k)}((k-2)(P_{k,2n+1} - P_{k,n+1}) - k(k-1)(P_{k,2n} - P_{k,n})).$$

Proof.
Using Theorem 2.9, Corollary 2.5 and Corollary 2.6, we obtain

$$\begin{aligned}
\|B\|_1 &= q_{k,n} + q_{k,n+1} + ... + q_{k,2n-1} \\
&= \sum_{i=0}^{2n-1} q_{k,i} - \sum_{i=0}^{n-1} q_{k,i} \\
&= \tfrac{1}{2(1-k)}((1-k)q_{k,2n-1} - q_{k,2n} - (1-k)q_{k,n-1} + q_{k,n}) \\
&= \tfrac{1}{2(1-k)}(-q_{k,2n+1} + (k-1)q_{k,2n} + q_{k,n+1} + (1-k)q_{k,n} \\
&= \tfrac{1}{2(1-k)}((k-2)(-P_{k,2n+1} - (k-1)P_{k,2n} + (k-1)P_{k,2n+1} - (k-1)^2 P_{k,2} \\
&+ P_{k,n+1} + (k-1)P_{k,n} + (1-k)P_{k,n+1} - (k-1)^2 P_{k,n} \\
&= \tfrac{1}{2(1-k)}((k-2)(P_{k,2n+1} - P_{k,n+1}) - k(k-1)(P_{k,2n} - P_{k,n})).
\end{aligned}$$

Author Contributions

The author read and approved the final version of the manuscript.

Conflicts of Interest

The author declares no conflict of interest.

References

[1] A. F. Horadam, *Jacobsthal representation numbers*, Fibonacci Quarterly, 34, (1996), 40–54.

[2] T. Koshy, Fibonacci and Lucas numbers with applications, John Wiley and Sons Inc., New York, 2001.

[3] G. K. Panda, *Sequence balancing and cobalancing numbers*, Fibonacci Quarterly, 45, (2007), 265–271.

[4] A. F. Horadam, *Pell identities*, Fibonacci Quarterly, 9, (1971), 245–252.

[5] S. Halici, *On some inequality and Hankel matrices involving Pell, Pell Lucas numbers*, Mathematical Reports, 15, (2013), 1–10.

[6] G. Bilgici, *New generalizations of Fibonacci and Lucas numbers*, Applied Mathematical Sciences, 8,

(2014) 1429–1437.

[7] S. Falcon, A. Plaza, *On the Fibonacci k-numbers*, Chaos Solitions and Fractals, 32, (2007) 1615–1624.

[8] A. Szynal-Liana, , A. Wloch, I. Wloch, *On generalized Pell numbers generated by Fibonacci and Lucas numbers*, Ars Combinatoria, 115, (2014), 411–423.

[9] D. Tasci , E. Sevgi , *Bi-periodic balancing numbers*, Journal of Science and Arts, 50, (2020), 75–84.

[10] O. M. Yayenie, A. Edson, *New generalization of Fibonacci sequences and extended Binet's formula*, Integers, 9, (2009), 639–654.

[11] L. Trojnar-Spelina, I. Wloch, *On generalized Pell and Pell Lucas numbers*, Iranian Journal of Science and Technology, Transactions A: Science, 43, (2019), 2871–2877.

[12] P. Vasco, P. Catarino, H. Campos,, A. P. Aires, A. Borges, *k-Pell, k-Pell-Lucas and modified k-Pell Numbers: Some identities and norms of Hankel matrices*, International Journal of Mathematical Analysis, 9,(2015), 31-37.

Journal of New Results in Science
https://dergipark.org.tr/en/pub/jnrs
Research Article
Open Access

E-ISSN: 1304-7981 https://doi.org/10.54187/jnrs.1003890

Conditional complements of sets and their application to group theory

Naim Çağman[1]

Keywords
Complement of a set, Conditional complements, Inclusive complement, Exclusive complement, Complement subgroup

Abstract — Among the most important concepts of mathematics are sets, of which one of the critical concepts is the complement of a set. This work defines two conditional complements of sets as a new concept of set theory, i.e., inclusive complement and exclusive complement. By comparing these two, we then explore the relationships between them. We also apply them to the group theory and define complement subgroup of a group. Finally, we conclude the study with two interesting questions about the subject.

Subject Classification (2020): 03E75, 20D05.

1. Introduction

The concept of sets, whose borning dates back to late 1873, was proposed in 1874 by Georg Cantor (1845-1918). Sets are one of the most basic concepts in mathematics. They are now used in all areas of mathematics and form the basis of almost all mathematics. Since set-theoretical language is a very useful tool for describing and structuring mathematical objects, almost all mathematical concepts can be expressed via sets. This is considered one of the greatest achievements in mathematics. This achievement manifests that sets, which have practical mathematical tools, provide a foundation for mathematics.

A universal set, generally represented by U, is a fundamental set that contains all the elements of the considered sets. The complement of a set, which is an essential concept in set theory, consists of the elements of the universal set except for those of the set. In other words, for any subset A of U, the complement of A, denoted by A', is defined as the set of all elements in the universe U that are not in A. It means that

$$A' = U \setminus A$$

In this work, we define two conditional complements of a set as new concepts of set theory, i.e., inclusive complement and exclusive complement. We then investigate the relationships between the two. We finally define complement subgroup of a group and give two questions about it.

[1] naim.cagman@gop.edu.tr (Corresponding Author)
[1] Department of Mathematics, Faculty of Arts and Sciences, Tokat Gaziosmanpasa University, Tokat, Turkey
Article History: Received: 02 Oct 2021 - Accepted: 10 Dec 2021 - Published: 31 Dec 2021

For the basic definitions, theorems and properties of set theory, it can be recommend to look at the references [1, 2].

Throughout this work, U refers to a universe, A' is the complement of A over U, and A'' denotes the complement of A'.

2. Inclusive Complement of Sets

This section defines inclusive complement of a set and investigates its properties.

Definition 2.1. Let A and B be two subsets of U. Then, B-inclusive complement of A is defined by

$$A^{+B} := A' \cup B$$

If $B = \{x\}$, then we will use A^{+x} instead of $A^{+\{x\}}$. Therefore, "x-inclusive complement" is used for "$\{x\}$-inclusive complement".

Example 2.2. Let $U = \{0, 1, 2, ..., 10\}$, $A = \{0, 2, 4, ..., 10\}$, and $B = \{2, 3, 5, 7\}$. Then,

$$A^{+B} = \{1, 2, 3, 5, 7, 9\}$$

Example 2.3. Let us give some examples to show that the inclusive complement is used in daily life. Let $A = \{x \in U : p(x)\}$ and $B = \{x \in U : q(x)\}$ be two subsets of U. Then, B-inclusive complement of A can be defined by

$$A^{+B} = \{x \in U : \neg p(x) \vee q(x)\}$$

where $\neg p$ is the negation of p. Thus,

a) Boss of a business: Call all uncalled customers, including my father.

b) Teacher in a classroom: Except for those who cannot take the exam for this course, those who are not successful in this course will not be able to participate in the weekend trip.

c) A note that is on the door of a shopping center: Those who have a positive Covid-19 test or those who do not have the Covid-19 vaccine cannot enter this building.

Proposition 2.4. Let A and B be any two subsets of U. Then,

i. $A'^{+B} = B'^{+A}$

ii. $A^{+B'} = B^{+A'}$

Proof.
Let us prove (i). The proof of (ii) is done in a similar way.

$$\begin{aligned} A'^{+B} &= A'' \cup B \\ &= A \cup B \\ &= B'' \cup A \\ &= B'^{+A} \end{aligned}$$

Proposition 2.5. Let A be a subset of U. Then,

i. $A^{+\emptyset} = A'$
ii. $\emptyset^{+A} = U$
iii. $U^{+A} = A$
iv. $A^{+U} = U$
v. $A^{+A'} = A'$
vi. $A'^{+A} = A$
vii. $A^{+A} = U$

Proposition 2.6. Let A be a subset of U. Then,

i. $x \notin A \Rightarrow A^{+x} = A'$
ii. $x \in A \Rightarrow \{x\}^{+A} = U$
iii. $x \notin A \Rightarrow \{x\}^{+A} = \{x\}'$

Proposition 2.7. Let A, B and C be three subsets of U. Then, De Morgan's Laws are valid,

i. $(A \cup B)^{+C} = A^{+C} \cap B^{+C}$
ii. $(A \cap B)^{+C} = A^{+C} \cup B^{+C}$

Proof.
Let us prove (i). The proof of (ii) is done in a similar way.

$$\begin{aligned}(A \cup B)^{+C} &= (A \cup B)' \cup C \\ &= (A' \cap B') \cup C \\ &= (A' \cup C) \cap (B' \cup C) \\ &= A^{+C} \cap B^{+C}\end{aligned}$$

Proposition 2.8. Let A, B and C be any three subsets of U. Then,

i. $A^{+(B \cup C)} = A^{+B} \cup A^{+C}$
ii. $A^{+(B \cap C)} = A^{+B} \cap A^{+C}$

Proof.
Let us prove (ii). The proof of (i) can be done in a similar way.

$$\begin{aligned}A^{+(B \cap C)} &= A' \cup (B \cap C) \\ &= (A' \cup B) \cap (A' \cup C) \\ &= A^{+B} \cap A^{+C}\end{aligned}$$

Proposition 2.9. Let A and B be two subsets of U. Then,

i. $(A^{+B})^{+C} = A'^{+C} \cap B^{+C}$
ii. $(A^{+C})^{+B} = A'^{+B} \cap C^{+B}$

Proof.
Let us prove (i). The proof of (ii) can be done in a similar way.

$$\begin{aligned}(A^{+B})^{+C} &= (A^{+B})' \cup C \\ &= (A' \cup B)' \cup C \\ &= (A'' \cap B') \cup C \\ &= (A'' \cup C) \cap (B' \cup C) \\ &= A'^{+C} \cap B^{+C}\end{aligned}$$

Corollary 2.10. Let A and B be any two subsets of U. Then, $(A^{+B})^{+B} = A'^{+B}$.

Remark 2.11. Let A, B and C be three subsets of U. Then, $(A^{+B})^{+C} \neq (A^{+C})^{+B}$.

Proposition 2.12. Let A and B be two subsets of U. Then,

i. $A^{+(B^{+C})} = A^{+C} \cup B^{+C}$

ii. $A^{+(C^{+B})} = A^{+B} \cup C^{+B}$

Proof.
Let us prove (i). The proof of (ii) can be done in a similar way.

$$\begin{aligned} A^{+(B^{+C})} &= A' \cup B^{+C} \\ &= A' \cup (B' \cup C) \\ &= (A' \cup C) \cup (B' \cup C) \\ &= A^{+C} \cup B^{+C} \end{aligned}$$

Remark 2.13. Let A, B and C be any three subsets of U. Then, $A^{+(B^{+C})} \neq A^{+(C^{+B})}$.

3. Exclusive Complement of Sets

This section defines exclusive complement of a set and investigates its properties.

Definition 3.1. Let A and B be two subset of U. Then, B-exclusive complement of A is defined by

$$A^{-B} := A' \setminus B$$

If $B = \{x\}$, then we will use A^{-x} instead of $A^{-\{x\}}$. Therefore, "x-exclusive complement" is used for "$\{x\}$-exclusive complement".

Example 3.2. Let $U = \{0, 1, 2, ..., 20\}$, $A = \{0, 2, 4, ..., 20\}$, and $B = \{2, 3, 5, 7, 11, 13, 17, 19\}$. Then,

$$A^{-B} = \{1, 9, 15\}$$

Example 3.3. Let us give some examples to show that the exclusive complement is used in daily life. Let $A = \{x \in U : p(x)\}$ and $B = \{x \in U : q(x)\}$ be two subsets of U. Since $A' \setminus B = A' \cap B' = (A \cup B)'$, B-exclusive complement of A can be defined by

$$\begin{aligned} A^{-B} &= \{x \in U : \neg p(x) \wedge \neg q(x)\} \\ &= \{x \in U : \neg(p(x) \vee q(x))\} \end{aligned}$$

where $\neg p$ is the negation of p. Thus,

a) Boss of a business: Call all uncalled customers, except my father.

b) Teacher in a classroom: Only those who could not take the exam for this course and those who took the exam for this course but did not fail the exam will participate in the weekend trip.

c) A note that is on the door of a shopping center: Only those who have a positive Covid-19 test or have not been vaccinated for Covid-19 cannot enter this building.

Proposition 3.4. Let A and B be two subsets of U. Then, $A^{-B} = B^{-A}$.

Proof.

$$\begin{aligned} A^{-B} &= A' \setminus B \\ &= A' \cap B' \\ &= B' \cap A' \\ &= B' \setminus A \\ &= B^{-A} \end{aligned}$$

Corollary 3.5. Let A be a subsets of U. Then, $A^{-x} = \{x\}^{-A}$ for all $x \in U$.

Proposition 3.6. Let A be a subset of U. Then,

i. $A^{-\emptyset} = A'$

ii. $A^{-U} = \emptyset$

iii. $A^{-A} = A'$

iv. $A^{-A'} = \emptyset$

v. $\emptyset^{-A} = A'$

vi. $U^{-A} = \emptyset$

Proposition 3.7. Let A, B and C be three subsets of U. Then, De Morgan's Laws are valid,

i. $(A \cup B)^{-C} = A^{-C} \cap B^{-C}$

ii. $(A \cap B)^{-C} = A^{-C} \cup B^{-C}$

Proof.
Let us prove (i). The proof of (ii) is done in a similar way.

$$\begin{aligned} (A \cup B)^{-C} &= (A \cup B)' \setminus C \\ &= (A' \cap B') \cap C' \\ &= (A' \cap C') \cap (B' \cap C') \\ &= (A' \setminus C) \cap (B' \setminus C) \\ &= A^{-C} \cap B^{-C} \end{aligned}$$

Proposition 3.8. Let A, B and C be three subsets of U. Then,

i. $A^{-(B \cup C)} = A^{-B} \cap A^{-C}$

ii. $A^{-(B \cap C)} = A^{-B} \cup A^{-C}$

Proof.
Let us prove (i). The proof of (ii) can be done in a similar way.

$$\begin{aligned} A^{-(B \cup C)} &= A' \setminus (B \cup C) \\ &= A' \cap (B \cup C)' \\ &= A' \cap (B' \cap C') \\ &= (A' \cap B') \cap (A' \cap C') \\ &= (A' \setminus B) \cap (A' \setminus C) \\ &= A^{-B} \cap A^{-C} \end{aligned}$$

Proposition 3.9. Let A and B be two subsets of U. Then,

i. $(A^{-B})^{-C} = A'^{-C} \cup B'^{-C}$

ii. $(A^{-C})^{-B} = A'^{-B} \cap C'^{-B}$

Proof.
Let us prove (i). The proof of (ii) can be done in a similar way.

$$\begin{aligned}
(A^{-B})^{-C} &= (A^{+B})' \setminus C \\
&= (A' \setminus B)' \cap C' \\
&= (A' \cap B')' \cap C' \\
&= (A'' \cup B'') \cap C' \\
&= (A'' \cap C') \cup (B'' \cap C') \\
&= (A'' \setminus C) \cup (B'' \setminus C) \\
&= A'^{-C} \cup B'^{-C}
\end{aligned}$$

Corollary 3.10. Let A and B be any two subsets of U. Then, $(A^{-B})^{-B} = A'^{-B}$.

Remark 3.11. Let A, B and C be any three subsets of U. Then, $(A^{-B})^{-C} \neq (A^{-C})^{-B}$.

Proposition 3.12. Let A and B be two subsets of U. Then, $A^{-(B^{-C})} = A^{-(C^{-B})}$

4. Comparison of Conditional Complements

This section compares the inclusive complement and exclusive complement of a group and investigates the relationships between the two.

Proposition 4.1. Let A and B be any two subsets of U. Then,

i. $A^{+B} = (A'^{-B})'$

ii. $A^{-B} = (A'^{+B})'$

Proof.
Let us prove (i). The proof of (ii) can be done in a similar way.

$$\begin{aligned}
(A'^{-B})' &= (A'' \setminus B)' \\
&= (A'' \cap B')' \\
&= A' \cup B \\
&= A^{+B}
\end{aligned}$$

Corollary 4.2. Let A and B be two subsets of U. Then,

i. $(A^{-B})' = A'^{+B}$

ii. $(A^{+B})' = A'^{-B}$

Proposition 4.3. Let A be a subset of U. Then,

i. $A^{+\emptyset} = A^{-\emptyset}$

ii. $(A^{+U})' = A^{-U}$

iii. $(\emptyset^{+A})' = U^{-A}$

iv. $(A^{+A})' = A^{-A'}$

Proposition 4.4. Let A and B be any two subsets of U. Then,

i. $(A^{+B})^{-B} = A'^{-B}$

ii. $(A^{-B})^{+B} = A'^{+B}$

Proposition 4.5. Let A and B be any two subsets of U. Then,

i. $(A^{+B})^{-C} = A'^{-(B\cup C)}$

ii. $(A^{-B})^{+C} = A'^{+(B\cup C)}$

Proposition 4.6. Let A and B be any two subsets of U. Then,

i. $(A^{-B})^{+C} = (A^{-C})^{+B}$

ii. $(A^{+B})^{-C} = (A^{+C})^{-B}$

Proposition 4.7. Let A and B be any two subsets of U. Then,

i. $A^{+B} \cup A^{-B} = A^{+B}$

ii. $A^{+B} \cap A^{-B} = A^{-B}$

Corollary 4.8. Let A and B be any two subsets of U. Then, $A^{-B} \subseteq A^{+B}$.

5. Complement Subgroup of a Group

This section defines complement subgroup of a group. For the basic definitions, theorems and properties of group theory, please look at the references [3, 4].

Definition 5.1. Let G be a group, H and K be two subgroups of G. If H^{+K} is a subgroup of G, then H^{+K} is called complement subgroup of G. Here, $H^{+K} := (G \setminus H) \cup K$.

Proposition 5.2. Let G be a group with identity e. Then,

i. G^{+e} is a complement subgroup of G.

ii. $\{e\}^{+e}$ is a complement subgroup of G.

Proof.
Let G be a group with identity e. Then,

i. $G^{+e} = G' \cup \{e\} = \emptyset \cup \{e\} = \{e\}$.

ii. $\{e\}^{+e} = \{e\}' \cup \{e\} = G$.

Proposition 5.3. Let G be a group and H be a subgroup of G. Then, H^{+H} is a complement subgroup of G.

Proof.
$H^{+H} = H' \cup H = G$.

Proposition 5.4. Let G be a group, H and K be two subgroups of G. If H is a subgroup of K, then H^{+K} is a complement subgroup of G.

Proof.
$H^{+K} = H' \cup K = G$.

Example 5.5. $2\mathbb{Z}$ and $4\mathbb{Z}$ are two subgroups of $4\mathbb{Z}$. Since $4\mathbb{Z}$ is a subgroups of $2\mathbb{Z}$, then $4\mathbb{Z}^{+2\mathbb{Z}}$ is a complement subgroup of $\mathbb{Z}$.

6. Questions

Questions 1. Let G be a group whose identity is e. Assume that H is a nontrival subgroups of G that is $H \neq G$ and $H \neq \{e\}$. Under these conditions, is there any group G such that H^{+e} is a complement subgroup of G?

Let's generalize this question a little more.

Questions 2. Assume that H and K are two subgroups of a grup G such that $K \nsubseteq H$ and $H \nsubseteq K$. Under these conditions, is there any group G such that K^{+H} is a complement subgroup of G?

7. Conclusion

In this work, we first defined two conditional complements of a set, namely inclusive complement and exclusive complement. By comparing these the two, we then explored the relationships between them. We also applied these complements to the group theory and defined complement subgroup of a group. Finally, we finished the study with two interesting questions about the subject.

Author Contributions

The author read and approved the last version of the manuscript.

Conflicts of Interest

The author declares no conflict of interest.

References

[1] P. R. Halmos, Naive set theory, D. Van Nostrand Company, Inc., New York, 2011.

[2] J. Ferreirós, Labyrinth of thought: A history of set theory and its role in modern mathematics, Birkhäuser, Basel, 2007.

[3] D. S. Dummit, R. M. Foote, Abstract algebra, Wiley, Hoboken, NJ, 2004.

[4] T. Hungerford, Algebra, Springer, New York, 2003.

Journal of New Results in Science 10(3) (2021) 75-88

Journal of New Results in Science
https://dergipark.org.tr/en/pub/jnrs
Review Article
Open Access

E-ISSN:1304-7981 https://doi.org/10.54187/jnrs.1011739

An overview of the activation functions used in deep learning algorithms

Serhat Kılıçarslan[1], Kemal Adem[2], Mete Çelik[3]

Keywords:
Activation function, Neural network, Deep learning

Abstract — In deep learning models, the inputs to the network are processed using activation functions to generate the output corresponding to these inputs. Deep learning models are of particular importance in analyzing big data with numerous parameters and forecasting and are useful for image processing, natural language processing, object recognition, and financial forecasting. Also, in deep learning algorithms, activation functions have been developed by taking into account features such as performing the learning process in a healthy way, preventing excessive learning, increasing the accuracy performance, and reducing the computational cost. In this study, we present an overview of common and current activation functions used in deep learning algorithms. In the study, fixed and trainable activation functions are introduced. As fixed activation functions, sigmoid, hyperbolic tangent, ReLU, softplus and swish, and as trainable activation functions, LReLU, ELU, SELU and RSigELU are introduced.

Subject Classification (2020):

1. Introduction

Deep learning is used to produce solutions to real-world problems, inspired by artificial neural networks and the human brain. Today, deep learning architectures are actively preferred by researchers in many areas such as autonomous vehicles, image processing, signal processing, and prediction [1-3]. Deep learning architectures are consisted of such as the layers convolution, max-pooling, activation, dropout, normalization, flatten, full connection and softmax [4]. Activation functions have a significant contribution to the development of activation functions by scientists due to their positive contribution to learning on deep neural networks [5].

Activation functions are used in deep neural network architectures to decide whether to transfer information to the next neuron. In deep learning algorithms, activation functions have been developed by taking into account features such as performing the learning process in a healthy way, preventing overfitting, increasing the accuracy performance, and reducing the computational cost. Activation functions enable to work and learn better the deep learning models by revealing the hidden features of real-world problems. However, if deep learning models are run without choosing activation functions,

[1]serhat.kilicarslan@gop.edu.tr (Corresponding Author); [2]kemaladem@aksaray.edu.tr; [3]mcelik@erciyes.edu.tr
[1]Department of Informatics, Tokat Gaziosmanpaşa University, Tokat, Turkey
[2]Department of Software Engineering, Engineering Faculty, Aksaray University, Aksaray, Turkey
[3]Department of Computer Engineering, Engineering Faculty, Erciyes University, Kayseri, Turkey
Article History: Received: 18 Oct 2021 — Accepted: 08 Dec 2021 — Published: 31 Dec 2021

the desired success cannot be achieved with limited learning. Therefore, the deep learning architectures used cause it to behave like linear regression. For this reason, non-linear activation functions are preferred in deep neural network architectures. The first is the fixed activation functions, the second is the trainable activation functions [6]. In deep learning algorithms, back propagation algorithm is used to update the parameters. At the end of the update process, the derivative value of the functions is returned. For this reason, the activation functions used in deep learning architectures should have the ability to receive derivative continuously. Deep learning architectures have started to attract the attention of users with the use of activation functions. In the literature, deep neural networks were started to be trained by using ReLU, LReLU, ELU, PReLU, swish and similar activation functions, and success results were achieved [7-11]. Activation functions in deep learning architectures are expected to have features such as being derivative, non-linear, reaching the global optimum without being stuck in the local optimum.

In this study, general research is carried out on the proposed activation functions in the literature. However, non-linear activation functions used on deep learning architectures are examined. In the literature, many fixed and trainable activation functions have been proposed, and the number of studies conducted in this area by years is shown in Figure 1.

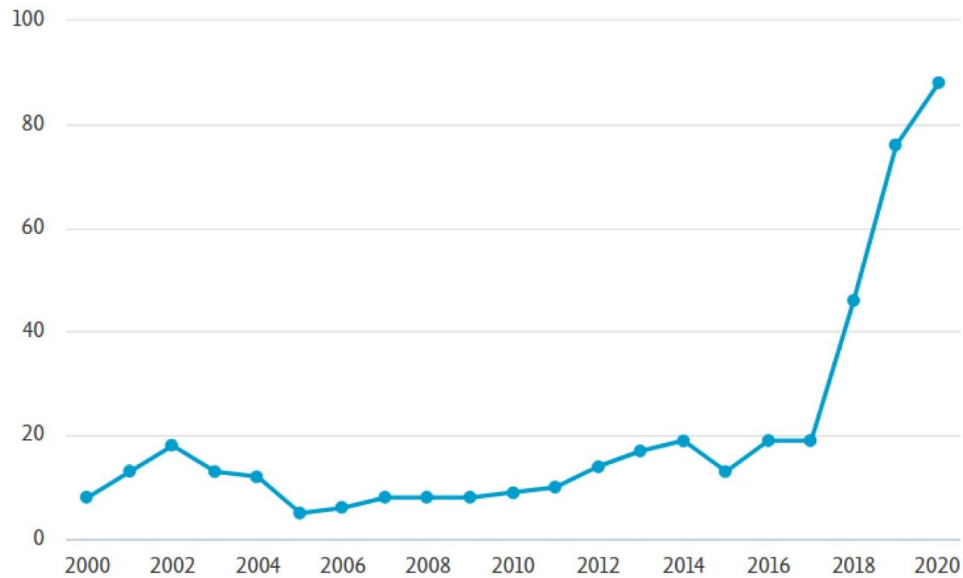

Figure 1. Number of studies conducted in the literature on activation functions [5]

In the literature, with the developing technology is increasing the number of studies on deep learning algorithms. In deep learning algorithms, features such as the ability to perform the learning process properly and increase the accuracy performance are important. Therefore, many studies on the development of the activation function are appear in the literature.

2. Fixed Parameter Activation Functions

Non-linear fixed parameter activation functions has work actively on deep learning architectures without taking any external parameters. Fixed parameter activation functions used in the literature are expressed as sigmoid, hyperbolic tangent, ReLU, softplus, swish [7-11].

2.1. Sigmoid Activation Function

In deep learning architectures, back propagation algorithm has prefer in order to realize the learning process between neurons. The back propagation algorithm are performs the updating process by taking derivatives of the parameters in the architectures. Therefore, it is important that in the activation functions are derivation. In linear activation functions, with the help of back propagation algorithm is returned a fixed value when the derivative is carried out. Therefore, it cannot perform the learning process on deep learning architectures. In order to overcome this problem, a non-linear sigmoid activation function, which can derivative in figure 2, is proposed [12, 13]. In Equations 2.1 and 2.2, the normal and derivatives of the sigmoid activation function are given.

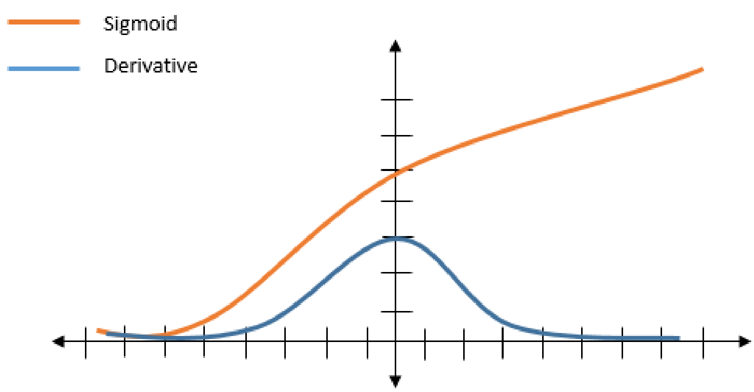

Figure 2. Sigmoid activation function

$$f(x) = \frac{1}{1 + e^{-x}} \tag{2.1}$$

$$\frac{df(x)}{dx} = \frac{e^{x}}{(1 + e^{x})^2} \tag{2.2}$$

In Equation 2.1, parameter x represents the input data in the sigmoid activation function. In figure 2 shows the normal and derivative forms of the sigmoid activation function. Sigmoid is the most commonly preferred activation function among non-linear functions. In Figure 2, the termination of the derivative operation after the interval [-5.5] causes the learning process to stop and reveals the vanishing gradient problem [14 ,15]. In addition, back propagation algorithm is used to be the derivative result small of the sigmoid activation function and to update the parameters in the neural network structure. Therefore, the weights will not be updated at the desired level and the learning process in neural networks will be interrupted. Because of this problem, the sigmoid activation function is not as popularly used as it used to be.

2.2. Hyperbolic Tangent Activation Function

The hyperbolic tangent activation function is a non-linear activation function that and can perform the derivative operation. The hyperbolic tangent activation function is in structure similar to the sigmoid activation function. In Figure 3 and Equation 2.3, 2.4, the hyperbolic tangent activation function is seen its normal and derivative states [16].

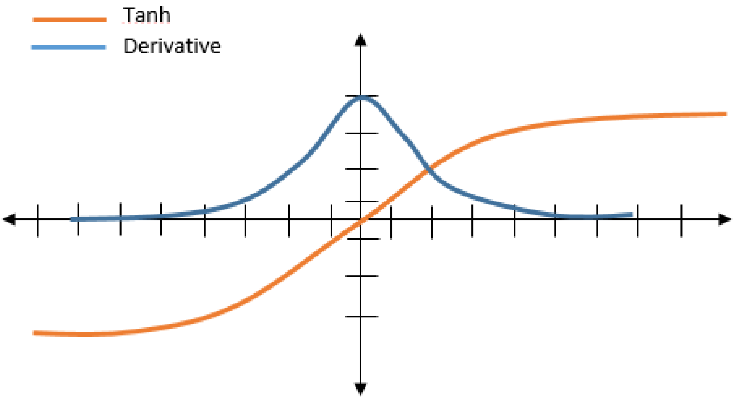

Figure 3. Hyperbolic tangent activation function

$$f(x) = \frac{\sinh(x)}{\cosh(x)} = \frac{e^x - e^{-x}}{e^x + e^{-x}} \tag{2.3}$$

$$\frac{df(x)}{dx} = 1 - f(x)^2 \tag{2.4}$$

When Figure 3 is examined, the hyperbolic tangent activation function are seen in the sigmoidal curve and the S-shaped curve. While the sigmoid activation function can produce output between [0,1], the hyperbolic tangent activation function can produce values between [-1,1]. It is observed that the learning process continues on negative values due to the hyperbolic tangent activation function value range. However, it faces the vanishing gradient problem due to the derivative values approaching zero after [-1,1] values [14].

2.3. ReLU Activation Function

In sigmoid and hyperbolic tangent activation functions, the vanishing gradient problem arises because it cannot be derivative after a certain threshold value. Therefore, the ReLU activation function has been developed in order to find a solution to the vanishing gradient problem. The ReLU activation function is a non-linear activation function that and can perform the derivative operation. Equations 2.5 and 2.6 show the ReLU activation function [7].

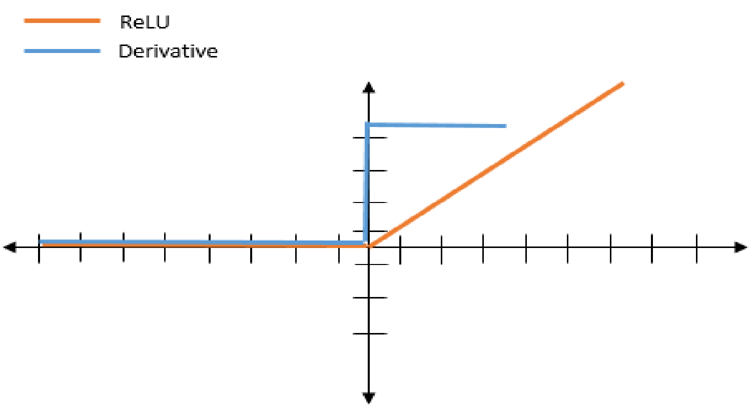

Figure 3. ReLU activation function

$$f(x) = \begin{cases} 0, & x < 0 \\ x, & x \geq 0 \end{cases} \tag{2.5}$$

$$\frac{df(x)}{dx} = \begin{cases} 0, & x < 0 \\ 1, & x \geq 0 \end{cases} \tag{2.6}$$

ReLU is widely used because it overcomes the vanishing gradient problem. However, the ReLU activation function is faces the problem of negative region. Since negative values are set to zero, the derivative of the values cannot be taken and the learning process slows down [4, 18]. One of the biggest advantages of the ReLU activation function is that the computational load is low compared to other functions and it can be widely used in multi-layered architectures. It is one of the most widely used activation functions in deep neural networks.

2.4. Swish Activation Function

The swish activation function was developed by Google researchers, similar to the sigmoid activation function in Equations 2.7 and 2.8 [12]. The Swish activation function does not always have a single and continuous positive or negative derivative throughout the entire architecture. In addition, instead of taking only positive derivatives over all points, like the sigmoid function, it has negative derivatives over certain points. The developers have demonstrated that the swish function outperforms the commonly used ReLU activation function by testing it on challenging datasets. Figure 4 shows the normal and derivatized version of the swish activation function.

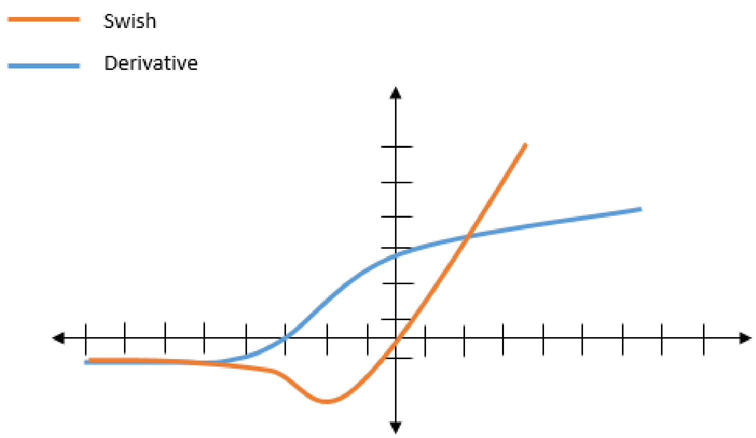

Figure 4. Swish activation function

$$f(x) = x\text{sigmoid}(x) = \frac{x}{1 + e^{-x}} \tag{2.7}$$

$$\frac{df(x)}{dx} = f(x) + \sigma(x)(1 - f(x)) \tag{2.8}$$

In Equation 2.8, the parameter σ represents the sigmoid function. Since the sigmoid function faces the vanishing gradient problem, the learning process is not at the desired level. Due to this problem, the sigmoid function has begun to lose its former popularity. In order to regain its former popularity, it defines the swish function with the help of the multiplication of the current inputs and the sigmoid activation function, as seen in Equation 2.7. In addition, it is seen that the swish function overcomes the negative region problem seen in the ReLU function, as in Figure 4 [12]. It is widely used mainly in image processing studies [19].

3. Parametric Activation Functions

Among the non-linear functions, the parameterized activation function is the functions that allow us to work actively on deep learning architectures thanks to the parameter value. Parametric activation functions used in the literature are expressed as LReLU, ELU, SELU, RSigELU [4, 8- 12].

3.1. LReLU Activation Function

The LReLU activation function was developed to cope with the negative region problem that occurs in the ReLU activation function [8]. The negative zone problem is that negative values are set to zero during processing. As a result of this adjustment, the learning process does not occur as a result of the death of some neurons due to the fact that negative outputs cannot be differentiated. The LReLU activation function, in other words, is an advanced variant of the ReLU activation function. In order to overcome the current problem, LReLU sets the activation function like Equations 3.1 and 3.2 instead of setting zero when the input value x is less than zero as in Equation 2.3. Figure 5 shows the normal and derivatized state of the LReLU activation function.

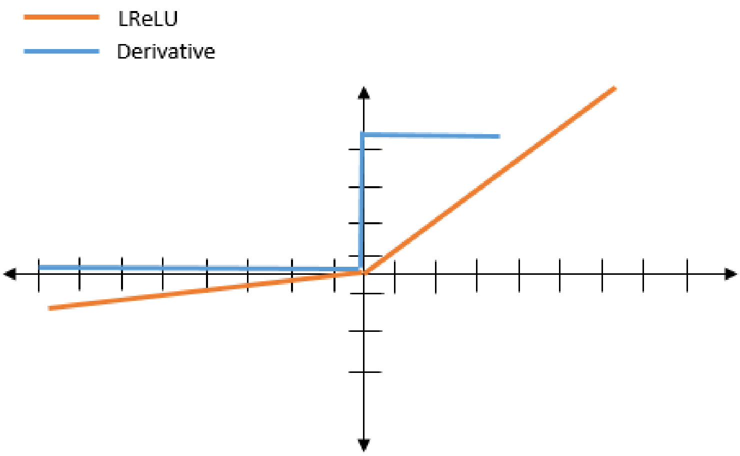

Figure 5. LReLU activation function

$$f(x) = \begin{cases} \alpha x, & x < 0 \text{ and } \alpha = 0.01 \\ x, & x \geq 0 \end{cases} \tag{3.1}$$

$$\frac{df(x)}{dx} = \begin{cases} 0, & x < 0 \\ 1, & x \geq 0 \end{cases} \tag{3.2}$$

By adding a slope parameter α to Equation 3.1 instead of setting negative values to zero as in Equation 2.3, the LReLU activation function that can overcome the negative region problem has emerged. Thus, it is observed in the literature that it is widely used in deep learning studies as an alternative to the ReLU activation function.

3.2. ELU Activation Function

The ELU activation function was developed to cope with the negative region problem arising from the ReLU activation function and inspired by natural gradients [9]. The ELU activation function is adopts the positive region like the ReLU activation function, which effectively avoids the vanishing gradient problem. It is also used like Equations 3.3 and 3.4 as an exponential function in the negative part like the LReLU activation function. Thanks to the ELU activation function, neuron deaths are prevented within the deep learning architecture. Thanks to this feature, it stands out with its faster convergence and continuous learning feature [19]. Figure 6 shows the normal state and the derivatized state of the ELU activation function.

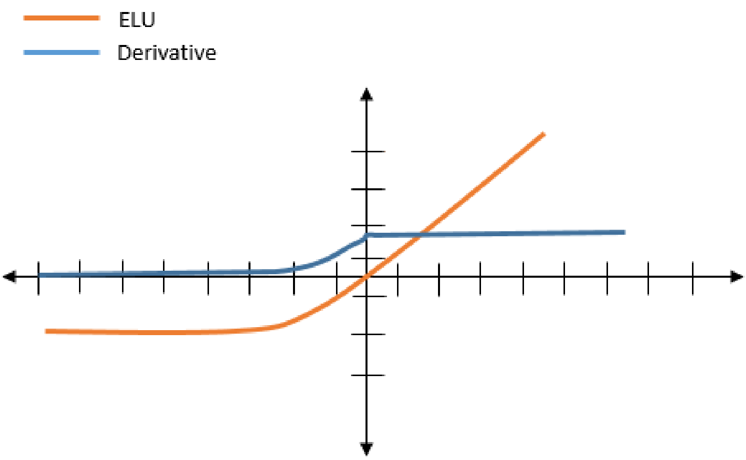

Figure 6. ELU activation function

$$f(x) = \begin{cases} x, & x > 0 \\ \alpha(e^{x} - 1), & x \leq 0 \end{cases} \tag{3.3}$$

$$\frac{df(x)}{dx} = \begin{cases} 1, & x > 0 \\ ae^{x}, & x \leq 0 \end{cases} \tag{3.4}$$

In summary, the ELU activation function works slower than the ReLU activation function due to the exponential expression [9]. Time is an important factor when convolutional neural network architectures are applied on real-time data. Therefore, it is used as an alternative to the ReLU activation function. ELU activation function gives better performance in classification and training speed for α=0.3 [20].

3.3. SELU Activation Function

The SELU activation function developed by Klambauer et al. and was developed as in Equations 3.5 and 3.6 in order to overcome the slow work in the ELU activation function [21]. In addition, the SELU activation function can overcome the negative region problem found in the ReLU activation function, which effectively avoids the vanishing gradient problem. In this way, SELU works actively in both positive and negative regions. Figure 7 shows the normal and derivatized state of the SELU activation function.

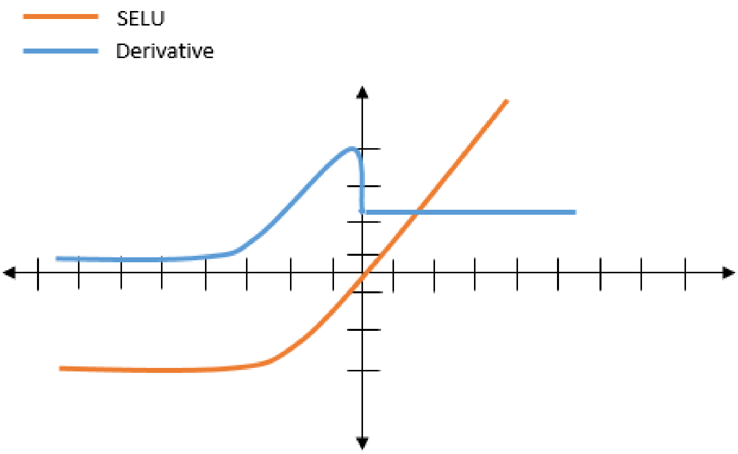

Figure 7. SELU activation function

$$f(x) = \lambda \begin{cases} x, & x > 0 \\ \alpha(e^x - 1), & x \leq 0 \end{cases} \tag{3.5}$$

$$\frac{df(x)}{dx} = \begin{cases} \lambda, & x > 0 \\ f(x) + \lambda\alpha, & x \leq 0 \end{cases} \tag{3.6}$$

Equations 3.5 and 3.6 use two constant parameters α and λ. The best results with SELU are obtained with $\alpha = \sim 1.6732$ and $\lambda = \sim 1.0507$ values. When the equation is examined, when $x > 0$ value, ReLU behaves like an activation function. SELU can perform the learning process robustly due to its self-normalization feature, analytically zero mean and unit variance convergence, and allows it to be trained over many layers [22, 23].

3.4. RSigELU Activation Function

It was developed to deal with the problem of the vanishing gradient problem occurring in the sigmoid and tangent activation functions and the negative region problem occurring in the ReLU activation function [4]. The proposed activation function has proposed single and double parameter RSigELUS and RSigELUD activation functions to overcome the existing problems. It is ensured that the proposed activation function works actively in positive, negative and linear regions. Equations 3.7, 3.8, 3.9 and 3.10 of the activation functions of RSigELUS and RSigELUD are given. Figure 8 shows the behavior of the RSigELU activation function.

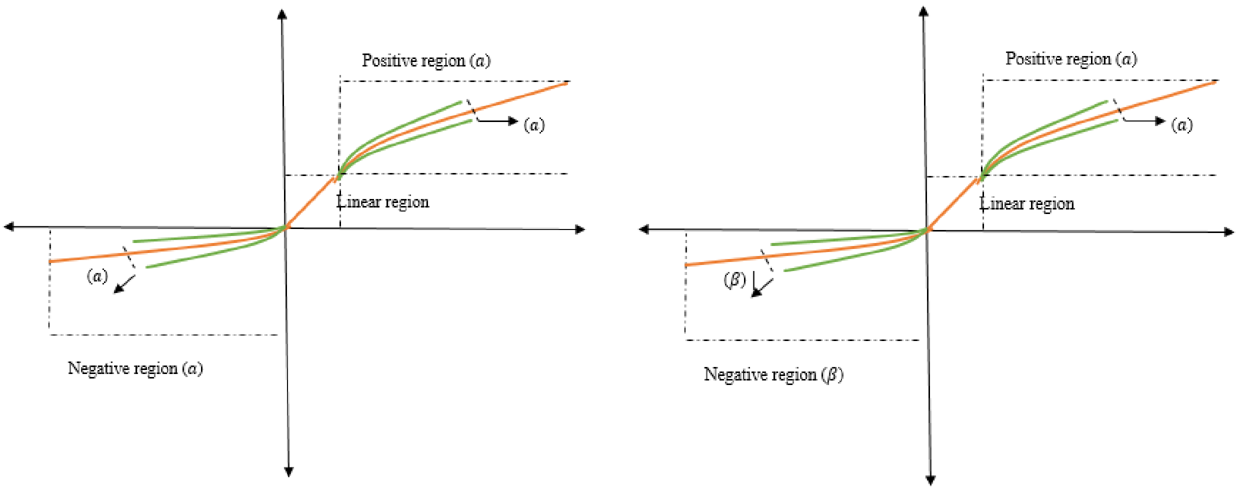

(a) (b)

Figure 8. Behavior of proposed RSigELUS (a) and RSigELUD (b) function

$$f(x) = \begin{cases} x * \left(\dfrac{1}{1+e^{-x}}\right) * \alpha + x, & 1 < x \\ x, & 0 \leq x \leq 1 \\ \alpha(e^{x} - 1), & x < 0 \end{cases} \tag{3.7}$$

$$f(x) = \begin{cases} x \left(\dfrac{1}{1+e^{-x}}\right) \alpha + x, & 1 < x \\ x, & 0 \leq x \leq 1 \\ \beta(e^{x} - 1), & x < 0 \end{cases} \tag{3.8}$$

$$\frac{df(x)}{dx} = \begin{cases} \dfrac{-\alpha x}{(e^{x}+1)^{2}} + \dfrac{\alpha x - \alpha}{(e^{x}+1)} + \alpha + 1, & 1 < x \\ 1, & 0 \leq x \leq 1 \\ \alpha e^{x}, & x < 0 \end{cases} \tag{3.9}$$

$$\frac{df(x)}{dx} = \begin{cases} \dfrac{-\alpha x}{(e^{x}+1)^{2}} + \dfrac{\alpha x - \alpha}{(e^{x}+1)} + \alpha + 1, & 1 < x \\ 1, & 0 \leq x \leq 1 \\ \beta e^{x}, & x < 0 \end{cases} \tag{3.10}$$

In Equations 3.7, 3.8, 3.9 and 3.10, α and β represent the defined slope coefficients. While the slope coefficient of a provides the control of the positive region, the control of the negative region is provided with β. As a result, the activation functions should have features that allow the network to converge easily and quickly. In addition, there should be no vanishing gradient problem in the designed activation functions, the outputs should be symmetrical to zero, it should be applicable after each layer and can be calculated millions of times in deep neural networks. When the equations were examined, they reported that the behaviour of the activation function was like ReLU when the parameter a was 0. Also, when a parameter is 0 and β value is 0.2, RSigELUD activation function behaves like ELU activation function [40-42]. When Equations 3.9 and 3.10 are examined, it is seen that RSigELUS and RSigELUD activation functions work on both negative and positive regions when derivatives are taken. Other activation functions defined in the literature are shown in Table 1.

Table 1. Activation Functions Used in the Literature

Activation Name	Year	State Function	Derivative State Function
Softplus [26]	2001	$f(x) = \ln(1 + e^{x})$	$\frac{df(x)}{dx} = \frac{1}{1 + e^{x}}$
Softsing [24]	2009	$f(x) = \frac{x}{1 + \lvert x \rvert}$	$\frac{df(x)}{dx} = \frac{1}{(1 + \lvert x \rvert)^2}$
PReLU [28]	2015	$f(x) = \begin{cases} ax & x < 0 \\ x & x \geq 0 \end{cases}$	$\frac{df(x)}{dx} = \begin{cases} a & x < 0 \\ 1 & x \geq 0 \end{cases}$
DReLU [30]	2017	$f(x) = \begin{cases} \begin{cases} 0 & a \leq 0 \text{ and } b \leq 0 \\ a & a > 0 \text{ and } b \leq 0 \end{cases} \\ \begin{cases} -b & a \leq 0 \text{ and } b > 0 \\ a - b & a > 0 \text{ and } b > 0 \end{cases} \end{cases}$	$\frac{df(x)}{dx} = \begin{cases} \begin{cases} 0 & a \leq 0 \\ 1 & a > 0 \end{cases} \\ \begin{cases} 0 & b \leq 0 \\ -1 & b > 0 \end{cases} \end{cases}$
PELU [31]	2017	$f(x) = \begin{cases} \frac{a}{b}x & x \geq 0 \\ a\left(\exp\left(\frac{x}{b}\right) - 1\right) & x < 0 \end{cases}$	$\frac{df(x)}{dx} = \begin{cases} \frac{ax}{b^2} & x \geq 0 \\ -\frac{a}{b^2}\exp\left(\frac{x}{b}\right) & x < 0 \end{cases}$
CELU [32]	2017	$f(x) = \begin{cases} a\left(\exp\left(\frac{x}{a}\right) - 1\right) & x < 0 \\ x & x \geq 0 \end{cases}$	$\frac{df(x)}{dx} = \begin{cases} \exp\left(\frac{x}{a}\right) & x < 0 \\ 1 & x \geq 0 \end{cases}$
Hexpo [34]	2017	$(x) = \begin{cases} -a\left(e^{-\frac{x}{b}} - 1\right) & x \geq 0 \\ c\left(e^{\frac{x}{d}} - 1\right) & x < 0 \end{cases}$	$\frac{df(x)}{dx} = \begin{cases} \frac{a}{b}e^{-\frac{x}{b}} & x \geq 0 \\ \frac{c}{d}e^{\frac{x}{d}} & x < 0 \end{cases}$
SignReLu [25]	2018	$f(x) = \begin{cases} \alpha\frac{x}{1 + \lvert x \rvert} & x < 0 \\ x & x \geq 0 \end{cases}$	$\frac{df(x)}{dx} = \begin{cases} a\frac{1}{(1 + \lvert x \rvert)^2} & x < 0 \\ 1 & x \geq 0 \end{cases}$
LISA [27]	2019	$f(x) = \begin{cases} \alpha_1 x - \alpha_1 + 1 & 1 < x < \infty \\ x & 0 \leq x \leq 1 \\ \alpha_2 x & -\infty < x < 0 \end{cases}$	$\frac{df(x)}{dx} = \begin{cases} \alpha_1 & 1 < x < \infty \\ 1 & 0 \leq x \leq 1 \\ \alpha_2 & -\infty < x < 0 \end{cases}$
FELU [29]	2019	$f(x) = \begin{cases} \alpha\left(2^{x/\ln(2)} - 1\right) & x < 0 \\ x & x \geq 0 \end{cases}$	$\frac{df(x)}{dx} = \begin{cases} \alpha 2^{x/\ln 2} & x < 0 \\ 1 & x \geq 0 \end{cases}$
Mish [33]	2019	$f(x) = x\,\text{tangent}(\ln(1 + e^{x}))$	$\frac{df(x)}{dx} = \frac{e^{x}\omega}{\delta^2}$
Logish [43]	2021	$f(x) = x\ln[1 + sigmoid(x)]$	$\frac{df(x)}{dx} = \ln\left(1 + \frac{1}{1 + e^{-x}}\right) + \frac{xe^{-x}}{(1 + e^{-x})(2 + e^{-x})}$
SAAF [44]	2021	$f(x) = \frac{x}{\frac{x}{a} + e^{-\frac{x}{\beta}}} \quad 0 < \frac{\beta}{a} < e$	$\frac{df(x)}{dx} = \frac{\left(1 + \frac{x}{\beta}\right)e^{-\frac{x}{\beta}}}{\left(\frac{x}{a} + e^{-\frac{x}{\beta}}\right)^2}$
Soft-Clipping Swish [45]	2021	$f(x) = \frac{1}{a}\log\left(\frac{1 + e^{ax}}{1 + e^{a(x-1)}}\right) \quad a > 0$	

Activation functions enable to work and learn better the deep learning models by revealing the hidden features of real-world problems. However, if deep learning models are run without choosing activation functions, the desired success cannot be achieved with limited learning. Therefore, the deep learning architectures used cause it to behave like linear regression. For this reason, non-linear activation functions are preferred in deep neural network architectures. The first is the fixed activation functions, the second is the trainable activation functions. Also, activation functions commonly evaluated according to error value, success rate, and confidence interval profile.

4. Conclusion

Since deep learning architectures work on complex problems, linear activation functions lose their competence. Because activation functions are the basis for learning the complex and continuous relationship between the variables and reaching the global optimum. In addition, there should be no vanishing gradient problem in the designed activation functions, and the outputs should be applicable after each layer in deep neural networks [35-42]. In this article, we have discussed, focusing on those that are the most common fixed and trainable activation functions presented in the literature. Non-linear activation functions are except for the sigmoid and hyperbolic tangent activation functions, the vanishing gradient problem is overcome and it is seen that deep neural networks are trained continuously. In the study, we report the best values obtained without paying attention to the different architectures or experimental setup used for different purposes in the literature.

Author Contributions

All authors contributed equally to this work. They all read and approved the final version of the manuscript.

Conflicts of Interest

The authors declare no conflict of interest.

References

[1] K. Adem, S. Kılıçarslan, O. Cömert, *Classification and diagnosis of cervical cancer with stacked autoencoder and softmax classification,* Expert Systems with Applications, 115, (2018) 557– 564.

[2] S. Kılıçarslan, K. Adem, M. Çelik, *Diagnosis and classification of cancer using hybrid model based on ReliefF and convolutional neural network,* medical hypotheses, 137, (2020) 199577.

[3] S. Kılıçarslan, M. Çelik, Ş. Sahin, *Hybrid models based on genetic algorithm and deep learning algorithms for nutritional Anemia disease classification*, *Biomedical Signal Processing and Control*, *63*, (2021) 102231.

[4] S. Kılıçarslan, M. Çelik, RSigELU: A nonlinear activation function for deep neural networks, Expert Systems with Applications, 174, (2021) 114805.

[5] A. Apicella, F. Donnarumma, F. Isgrò, R. Prevete, *A survey on modern trainable activation functions,* Neural Networks, 138 (2021) 14–32.

[6] S. Scardapane, S. Van Vaerenbergh, S. Totaro, A. Uncini, *Kafnets: Kernel-based non-parametric activation functions for neural networks*, Neural Networks, 110, (2019) 19–32.

[7] V. Nair, G. E. Hinton, *Rectified linear units improve restricted Boltzmann machines*, In Proceedings of the 27th international conference on machine learning (ICML-10), 2010, pp. 807–814.

[8] A. L. Maas, A. Y. Hannun, A. Y. Nug, *Rectifier nonlinearities improve neural network acoustic models*, S. Dasgupta, D. McAllester (Eds.), International Conference on Machine Learning Workshop on Deep Learning for Audio, Speech, and Language Processing, Atlanta, USA, 2013, pp. 1–6.

[9] D. A. Clevert, T. Unterthiner, S. Hochreiter, *Fast and accurate deep network learning by exponential linear units (elus)*, arXiv preprint arXiv:1511.07289, (2015).

[10] L. Trottier, P. Gigu, B. Chaib-draa, *Parametric exponential linear unit for deep convolutional neural networks,* in: X. Chen, B. Luo, F. Luo, V. Palade, M. A. Wani (Eds.), 16th IEEE International Conference on Machine Learning and Applications, Cancun, Mexico, 2017, pp. 207–214.

[11] P. Ramachandran, B. Zoph, Q. V. Le, *Searching for activation functions*, arXiv preprint arXiv:1710.05941, (2017).

[12] K. I. Funahashi, *On the approximate realization of continuous mappings by neural networks*, Neural Networks, 2, (1989) 183–192.

[13] G. Cybenko, *Approximation by superpositions of a sigmoidal function*, Mathematics of Control, Signals and Systems, 2, (1989) 303–314.

[14] Y. Bengio, P. Simard, P. Frasconi, *Learning long-term dependencies with gradient descent is difficult,* IEEE Transactions on Neural Networks, 5, (1994) 157–166.

[15] S. Hochreiter, S. Jurgen, *Long Short-Term Memory*, Neural Computation, 9, (1997) 1735–1780.

[16] A. Benjemmaa, I. Klabi, M. S. Masmoudi, J. el Ouni, M. Masmoudi, *Implementations approaches of neural networks lane following system,* O. Faten, B. A. Faouzi (Eds.), in: 16th IEEE Mediterranean Electrotechnical Conference, Yasmine Hammamet, Tunisia, 2012, pp. 515–518.

[17] M. Goyal, R. Goyal, P. Reddy, B. Lall, *Activation Functions*, In Deep Learning: Algorithms and Applications, Springer, Cham, 2020.

[18] N. Jinsakul, C. F. Tsai, C. E. Tsai, P. Wu, *Enhancement of deep learning in image classification performance using exception with the swish activation function for colorectal polyp preliminary screening,* Mathematics, 7, (2019), 1170.

[19] B. Ding, H. Qian, J. Zhou, *Activation functions and their characteristics in deep neural networks*, F. Wang, G. H. Yang (Eds.), in: Chinese Control and Decision Conference, Shenyang, China, 2018, pp. 1836–1841.

[20] D. J. Rumala, E. M. Yuniarno, R. F. Rachmadi, S. M. S. Nugroho, I. K. E. Purnama, *Activation functions evaluation to improve performance of convolutional neural network in brain disease classification based on magnetic resonance images,* S. M. S. Nugroho (Ed.), in: 2020 International Conference on Computer Engineering, Network, and Intelligent Multimedia, Surabaya, Indonesia, 2020, pp. 402–407.

[21] G. Klambauer, T. Unterthiner, A. Mayr, S. Hochreiter, *Self-normalizing neural networks*, U. V. Luxburg, I. Guyon, S. Bengio, H. Wallach, R. Fergus (Eds.), in: Advances in Neural Information Processing Systems, Long Beach, CA, USA, 2017, pp. 971–980.

[22] T. Yang, Y. Wei, Z. Tu, H. Zeng, P. Ren, *Design space exploration of neural network activation function circuits,* IEEE Transactions on Computer-Aided Design of Integrated Circuits and Systems, 38(10), (2018) 1974–1978.

[23] D. Pedamonti, *Comparison of non-linear activation functions for deep neural networks on MNIST classification task*, arXiv preprint arXiv:1804.02763, (2018).

[24] J. Bergstra, G. Desjardins, P. Lamblin, Y. Bengio, Quadratic polynomials learn better image features, Technical Report, (2009), 1337.

[25] G. Lin, W. Shen, *Research on convolutional neural network based on improved Relu piecewise activation function,* Procedia Computer Science, 131, (2018) 977–984.

[26] C. Dugas, Y. Bengio, F. Belisle, C. Nadeau, R. Garcia, *Incorporating second-order functional knowledge for better option pricing,* Advances in Neural Information Processing Systems, 20, (2001) 472–478.

[27] V. S. Bawa, V. Kumar, *Linearized sigmoidal activation: A novel activation function with tractable non-linear characteristics to boost representation capability,* Expert Systems with Applications, 120, (2019), 346–356.

[28] K. He, X. Zhang, S. Ren, J. Sun, *Delving deep into rectifiers: Surpassing human-level performance on imagenet classification*, R. Bajcsy, G. Hager, Y. Ma (Eds.) in: IEEE International Conference on Computer Vision, Santiago, Chile, 2015, pp. 1026–1034.

[29] Z. Qiumei, T. Dan, W. Fenghua, *Improved convolutional neural network based on fast exponentially linear unit activation function*, IEEE Access, 7, (2019) 151359–151367.

[30] F. Godin, J. Degrave, J. Dambre, W. De Neve, *Dual Rectified Linear Units (DReLUs): a replacement for tangent activation functions in quasi-recurrent neural networks*, Pattern Recognition Letters, 116, (2018), 8–14.

[31] L. Trottier, P. Giguere, B. Chaib-Draa, *Parametric exponential linear unit for deep convolutional neural networks,* In 2017 16th IEEE International Conference on Machine Learning and Applications, 2017, pp. 207–214.

[32] J. T. Barron*, Continuously differentiable exponential linear units,* arXiv preprint arXiv:1704.07483, 2017.

[33] D. Misra, *Mish: A self-regularized non-monotonic activation function*. arXiv preprint arXiv:1908.08681, 2019.

[34] S. Kong, M. Takatsuka, *Hexpo: A vanishing-proof activation function,* Y. Choe (Ed.) in: International Joint Conference on Neural Networks, Anchorage, AK, USA, 201, pp. 2562–2567.

[35] A. L. Hodgkin, A. F. Huxley, *A quantitative description of membrane current and its application to conduction and excitation in nerve,* The Journal of Physiology, 117(4), (1952) 500–544.

[36] N. Jinsakul, C. F. Tsai, C. E. Tsai, P. Wu, *Enhancement of deep learning in image classification performance using xception with the swish activation function for colorectal polyp preliminary screening,* Mathematics, 7(12), (2019) 1170.

[37] H. Ma, Y. Liu, Y. Ren, J. Yu, *Detection of collapsed buildings in post-earthquake remote sensing images based on the improved YOLOv3,* Remote Sensing, 12(1), (2020) 44.

[38] M. A. Bülbül, C. Öztürk, *Optimization, modeling and implementation of plant water consumption control using genetic algorithm and artificial neural network in a hybrid structure*, Arabian Journal for Science and Engineering, (2021) 1–15.

[39] I. Pacal, D. Karaboğa, *A Robust Real-Time Deep Learning Based Automatic Polyp Detection System*, Computers in Biology and Medicine, 134, (2021) 104519.

[40] S. Memiş, S. Enginoğlu, U. Erkan, *A classification method in machine learning based on soft decision-making via fuzzy parameterized fuzzy soft matrices,* Soft Computing (2021). https://doi.org/10.1007/s00500-021-06553-z

[41] S. Memiş, S. Enginoğlu, U. Erkan, *Numerical Data Classification via Distance-Based Similarity Measures of Fuzzy Parameterized Fuzzy Soft Matrices*, IEEE Access, 9, (2021) 88583–88601.

[42] U. Erkan, *A precise and stable machine learning algorithm: Eigenvalue classification (EigenClass),* Neural Computing & Applications, 33, (2021), 5381–5392.

[43] H. Zhu, H. Zeng, J. Liu, X. Zhang, Logish: *A new nonlinear nonmonotonic activation function for convolutional neural network,* Neurocomputing, 458, (2021), 490–499.

[44] Y. Zhou, D. Li, S. Huo, S. Y. Kung, *Shape autotuning activation function*, Expert Systems with Applications, 171, (2021) 114534.

[45] M. A. Mercioni, S. Holban, *Soft-Clipping Swish: A Novel Activation Function for Deep Learning*, L. Kovács, R. E. Precup (Eds.), in: IEEE 15th International Symposium on Applied Computational Intelligence and Informatics, Timisoara, Romania, 2021, pp. 225–230.

Journal of New Results in Science 10(3) (2021) 89-97

Journal of New Results in Science
https://dergipark.org.tr/en/pub/jnrs
Research Article
Open Access

E-ISSN:1304-7981 https://doi.org/10.54187/jnrs.1013381

Investigation of the Lorenz number and the carrier concentration of the GaAs semiconductor depending on temperature

Ebru Çopuroğlu[1]

Keywords:
Hall Coefficient,
Fermi integral,
Carrier concentration,
Semiconductors

Abstract — As is known, semiconductors are insulators under normal conditions but can become conductive with external excitation. Considering the effects of acting on these materials, the number of free electrons and the electrical conductivity will increase with increasing temperature. The increase in the concentration of free electrons in the semiconductor can be shown as the increase in electrical conductivity. If a semiconductor is exposed to an electric field with increasing concentration, we can have an idea about how the number of free electrons or the speed of free electrons will be affected. It is well known that it is necessary to calculate two-parameter Fermi functions to solve the properties of kinetic effects and electron transport phenomena in semiconductors. Effective methods have been developed for the calculation of two-parameter Fermi functions in literature. In this study, analytical calculations for the Lorenz number and the carrier concentration of the GaAs semiconductor were made using the two-parameter Fermi function.

Subject Classification (2020):

1. Introduction

Thermoelectric effects observed in various materials, such as metals, semiconductors, and superconductors, occur when a conductor with free temperature carriers is exposed to an electric field under temperature change. The analysis of thermoelectric effects is widely used to study the physical properties of materials [1-12]. Due the fact that developments in determining thermal and electrical properties in solid state materials have a significant role in industrial revolution, there has been an increase in the study of thermoelectric effects in materials. The most known thermoelectric effects are the Joule, Seebeck, Thomson, and Peltier effects in literature. Also, the Lorenz number is the coefficient which determines the thermal conductivity with respect to Wiedemann- Franz Law. It is well known that depending on temperature the Lorenz number deviate significantly from its limit value especially in non-degenerated semiconductors [13-17]. In the 1960s, many studies were carried out to examine the thermoelectric and thermomagnetic properties of semiconductors, to understand the variation of the Lorenz number and carrier concentration with temperature, the type of energy spectrum, the properties of the band structure and their effects on the scattering character. The use of thermoelectric

[1]ebrucopuroglu@gmail.com (Corresponding Author)
[1]Department of Physics, Faculty of Arts and Sciences, Tokat Gaziosmanpaşa University, Tokat, Turkey
Article History: Received: 22 Oct 2021 — Accepted: 07 Dec 2021 — Published: 31 Dec 2021

coefficients to determine the changes in Lorenz number and carrier concentration is essential in this study.

There is a group of semiconductors in which the conduction band has spherical symmetry but cannot be accurately described by known dispersion laws. Therefore, scientists have been interested in deriving formulas for kinetic coefficients under the most general assumptions about the shape of the region and scattering mechanisms. As a result of these studies, the formulas of the fundamental kinetic coefficients are derived with the help of a two-parameter Fermi function by B.M. Askerov [10] for the first time. In this study, an alternative analytical method for evaluating Lorenz number and carrier concentration is suggested by using the two-parameter Fermi function. As an application of the given approach, the calculations have been performed for the GaAs semiconductor.

2. Material Method

2.1. Analytical Investigation of Two-Parameter Fermi Function

Fermi distribution functions with one-, two- and three-parameters can be used to define the kinetic coefficients of the semiconductor [10-13]. However, it is necessary to use two-parameter Fermi integrals for solutions involving both thermal and electric effects.

Accurate analytical formulas of the two-parameter Fermi functions are of great importance in evaluating problems related to solid state physics, especially kinetic effects and the theory of transport phenomena in semiconductors [12]. The physical properties of carriers and the relationships of semiconductors in non-parabolic energy bands are usually reduced to solving the two-parameter Fermi distribution function for any degree of degeneration. Therefore, the correct analysis and interpretation of this function are important issues that need to be studied. Both numerical and analytical solutions are available for solving the Fermi function. The two-parameter Fermi integral can be defined as [12]:

$$I_{n,k}^{m}(\eta,\beta) = \int_0^\infty \left(-\frac{\partial f_0(x,\eta)}{\partial x}\right) \frac{x^m (x+\beta x^2)^n}{(1+2\beta x)^k}\, dx \tag{2.1}$$

Here, $\eta = \frac{\xi}{k_0 T}$ is the reduced chemical potential, $\beta = \frac{k_0 T}{\varepsilon_g}$ is the amount of deviation from the parabolic, ε_g is forbidden energy bandgap, ξ is the chemical potential, k_0 is the Boltzman temperature and $f_0(x,\eta)$ is the Fermi distribution function defined as follows:

$$f_0(x,\eta) = \frac{1}{1+e^{x-\eta}} \tag{2.2}$$

Effective methods have been developed for the calculation of two-parameter Fermi functions. Zawadzki et al. [18] proposed a general procedure for calculating two-parameter Fermi functions for values of integral parameters. Here, $-5 \le \eta \le 20$ and $0 \le \beta \le 1$. Askerov used the numerical method to approximate two-parameter Fermi functions. This proposed approach is correct in the region of $\eta \ge 10$ strongly degenerate and is written as [11, 12]:

$$\begin{aligned} I_{n,k}^{m}(\eta,\beta) \approx \frac{\eta^{n+m}(1+\beta\eta)^n}{(1+2\beta\eta)^k}\Bigg\{1 + \frac{\pi^2}{6}\Bigg[&\frac{(n+m)(n+m-1)}{\eta^2} + \frac{2n(n+m)\beta}{\eta(1+\beta\eta)} - \frac{4k(n+m)\beta}{\eta(1+2\beta\eta)} \\ &+ \frac{n(n-1)\beta^2}{(1+\beta\eta)^2} - \frac{4nk\beta^2}{(1+2\beta\eta)(1+\beta\eta)} + \frac{4k(k+1)\beta^2}{(1+2\beta\eta)^2}\Bigg]\Bigg\} \text{for} \left(\frac{k_0 T}{\zeta}\right) << 1 \end{aligned} \tag{2.3}$$

In the non-degenerate case, the two-parameter Fermi functions can be evaluated by using the following given formula:

$$I_{n,k}^{m}(\eta,\beta) \approx e^{\eta}\,\Gamma\,(n+m+1)\frac{(1+n\beta+m\beta)^{n}}{(1+2n\beta+2m\beta)^{k}} \quad \text{for } \eta \le -5 \text{ and } n \ne 0 \text{ or } m \ne 0 \tag{2.4}$$

Here $\Gamma(\alpha)$ is the well-known Gamma function. Zawadzki examined different methods used in the evaluation of two-parameter Fermi functions [18]:

$$I_{n,k}^{m}(\eta,\beta) = \sum_{p=0}^{\infty} a_p \beta^{p} F_{n+m+p-1}(\eta) \tag{2.5}$$

and

$$I_{n,k}^{m}(\eta,\beta) = \sum_{p=0}^{\infty}\sum_{r=1}^{\infty}(-1)^{r-1} a_p \beta^{p} \frac{e^{r\eta}}{r^{n+m}}\, for \eta < 1 \tag{2.6}$$

Here,

$$a_p = (n+m+p)!\sum_{l=0}^{p}\frac{[n(n-1)\ldots(n-p+l+1)][-k(-k-1)\ldots(-k-p-l+1)]2_l}{(p-l)!\,l!} \tag{2.7}$$

$F_p(\eta)$ is the Fermi function and defined as:

$$F_p(\eta) = \int_{0}^{\infty}\frac{e^{x-\eta_x p}}{e^{x-\eta}+1}dx \tag{2.8}$$

The Fermi functions are well-known and can be studied with standard techniques without numerical difference in its use [19-21]. One of the efficient methods is the using following binomial expansion method for the evaluation of Fermi functions [22]:

$$(x \pm y)^{n} = \begin{cases} \sum_{m=0}^{\infty}(\pm 1)^{m} f_m(n) x^{n-m} y^{m} & \text{for noninteger } n \\ \sum_{m=0}^{n}(\pm 1)^{m} f_m(n) x^{n-m} y^{m} & \text{for integer } n \end{cases} \tag{2.9}$$

Here $f_m(n)$ is the binomial function:

$$f_m(n) = \begin{cases} \dfrac{n(n-1)\ldots(n-m+1)}{m!} & \text{for integer } n \\ \dfrac{(-1)^{m}\Gamma(m-n)}{m!\,\Gamma(-n)} & \text{for noninteger } n \end{cases} \tag{2.10}$$

By considering equation (2.9), the series expansion formulas for two-parameter Fermi functions were obtained following as [21]:

for $n \ne 0, k \ne 0, m \ne 0$

$$I_{nk}^{m}(\eta,\beta) = e^{-\eta}\lim_{N\to\infty}\sum_{i=0}^{N} f_i(-k)\begin{cases}\sum_{j=0}^{n} f_j(n)\left[\beta^{i+j}2^{i}P_{m+n+i+j}\left(\eta,\frac{1}{2\beta}\right)\right. \\ \left.+\beta^{j-k-i}2^{-k-i}Q_{m+n-k-i+j}\left(\eta,\frac{1}{2\beta}\right)\right] & \text{for integer } n \\ \lim_{N\to\infty}\sum_{j=0}^{N} f_j(n)\left[\beta^{i+j}2^{i}P_{m+n+i+j}\left(\eta,\frac{1}{2\beta}\right)\right. \\ \left.+\beta^{n-j-k-i}2^{-k-i}Q_{m+2n-k-i+j}\left(\eta,\frac{1}{2\beta}\right)\right] & for \text{ noninteger } n\end{cases} \tag{2.11}$$

for $n = 0, k = 0$ and $m \neq 0$

$$I_{00}^{m}(\eta,\beta) = e^{-\eta}\begin{cases}\lim_{N\to\infty}\sum_{i=0}^{N}\frac{f_i(-2)}{(1+i)^{m+1}}\left[e^{i\eta}(-1)^{m+1}\gamma(m+1,-(1+i)\eta)\right. \\ \left.+e^{\eta(2+i)}\Gamma(m+1,(1+i)\eta)\right] for \eta > 0 \\ \lim_{N\to\infty}\sum_{i=0}^{N} f_i(-2)\frac{e^{\eta(2+i)}\Gamma(m+1)}{(1+i)^{m+1}} for \eta < 0\end{cases} \tag{2.12}$$

for $n \neq 0, k = 0, m = 0$ and $\eta > 0$

$$I_{n0}^{0}(\eta,\beta) = e^{-\eta}\begin{cases}\sum_{i=0}^{n} f_i(n)\,\beta^{i}L_{n+i}(\eta) & \text{for integer } n \\ \lim_{N\to\infty}\sum_{i=0}^{N} f_i(n)\left(\beta^{i}P_{n+i}\left(\eta,\frac{1}{\beta}\right)+\beta^{n-i}Q_{2n-i}\left(\eta,\frac{1}{\beta}\right)\right) & \text{for noninteger } n\end{cases} \tag{2.13}$$

for $n \neq 0, k = 0, m = 0$ and $\eta < 0$

$$I_{n0}^{0}(\eta,\beta) = e^{-\eta}\begin{cases}\sum_{i=0}^{n} f_i(n)\,\beta^{i}\lim_{N\to\infty}\sum_{j=0}^{N} f_j(-2)\frac{e^{(2+j)\eta}\Gamma(n+i+1)}{(1+j)^{n+i+1}} for n \text{integer} \\ \lim_{N\to\infty}\sum_{i=0}^{N} f_i(n)\sum_{j=0}^{N} f_j(-2)\,e^{(2+j)\eta}\left[\frac{\beta^{i}\gamma(n+i+1,(1+j)/\beta)}{(1+j)^{n+i+1}}\right. \\ \left.+\frac{\beta^{n-i}\Gamma(2n-i+1,(1+j)/\beta)}{(1+j)^{2n-i+1}}\right] for n \text{noninteger}\end{cases} \tag{2.14}$$

for $n = 0, k < 0, m = 0$

$$I_{0k}^{0}(\eta,\beta)=e^{-\eta}\begin{cases}\sum_{i=0}^{k} f_i(k)\,(2\beta)^i \lim_{N\to\infty}\sum_{j=0}^{N} f_j(-2)\left(\frac{e^{-i\eta}(-1)^{i+1}\gamma(i+1,-(1+j)\eta)}{(1+j)^{i+1}}\right.\\ \left.+\frac{e^{(2+j)\eta}\Gamma(i+1,(1+j)\eta))}{(1+j)^{i+1}}\right) & \text{for } \eta>0\\ \sum_{i=0}^{k} f_i(k)\,(2\beta)^i \lim_{N\to\infty}\sum_{j=0}^{N} f_j(-2)\frac{e^{(2+i)\eta}\Gamma(i+1)}{(1+j)^{i+1}} & \text{for } \eta<0\end{cases} \tag{2.15}$$

for $n \neq 0, k < 0, m = 0$

$$I_{nk}^{0}(\eta,\beta)=e^{-\eta}\begin{cases}\sum_{i=0}^{n} f_i(n)\,\beta^i \sum_{j=0}^{k} f_j(k)\,(2\beta)^j \lim_{N\to\infty}\sum_{l=0}^{N} f_l(-2)\left(\frac{e^{-l\eta}(-1)^{n+i+j+1}}{(1+l)^{n+i+j+1}}\right.\\ \left.\times\gamma(n+i+j+1,-(1+l)\eta)+\frac{e^{(2+l)\eta}\Gamma(n+i+j+1,(1+l)\eta))}{(1+l)^{n+i+j+1}}\right) & \text{for } \eta>0\\ \sum_{i=0}^{n} f_i(n)\,\beta^i \sum_{j=0}^{k} f_j(k)\,(2\beta)^j \lim_{N\to\infty}\sum_{l=0}^{N} f_l(-2)\frac{e^{(2+l)\eta}\Gamma(n+i+j+1)}{(1+l)^{n+i+j+1}} & \text{for } \eta<0\end{cases} \tag{2.16}$$

The auxiliary functions $P_n(p,q)$, $Q_n(p,q)$ and $L_n(p)$ occurring in Eqs. (2.11) to (2.16) are expressed through the special functions and can be written as, respectively:

for $p > 0$

$$P_n(p,q)=\lim_{N\to\infty}\sum_{i=0}^{N} f_i(-2)\begin{cases}\left(\frac{(-1)^{n+1}e^{-ip}\gamma(n+1,-(1+i)\,p)}{(1+i)^{n+1}}+e^{(2+i)p}[p^{n+1}E_{-n}((1+i)p)\right.\\ \left.-q^{n+1}E_{-n}((1+i)q)]\right) & \text{for } p\le q\\ \frac{(-1)^{n+1}e^{-ip}\gamma(n+1,-(1+i)\,q)}{(1+i)^{n+1}} & \text{for } p>q\end{cases} \tag{2.17}$$

$$Q_n(p,q)=\lim_{N\to\infty}\sum_{i=0}^{N} f_i(-2)\begin{cases}\left(\frac{e^{(2+i)p}\Gamma(n+1,(1+i)\,p)}{(1+i)^{n+1}}+e^{-ip}[q^{n+1}E_{-n}(-(1+i)q)\right.\\ \left.-p^{n+1}E_{-n}(-(1+i)p)]\right) & \text{for } p>q\\ \frac{e^{(2+i)p}\Gamma(n+1,-(1+i)\,q)}{(1+i)^{n+1}} & \text{for } p\le q\end{cases} \tag{2.18}$$

for $p < 0$

$$P_n(p,q)=\lim_{N\to\infty}\sum_{i=0}^{N} f_i(-2)\frac{e^{(2+i)p}\gamma(n+1,(1+i)\,q)}{(1+i)^{n+1}} \tag{2.19}$$

$$Q_n(p,q)=\lim_{N\to\infty}\sum_{i=0}^{N} f_i(-2)\frac{e^{(2+i)p}\Gamma(n+1,(1+i)\,q)}{(1+i)^{n+1}} \tag{2.20}$$

and

$$L_n(p) = \lim_{N\to\infty} \sum_{i=0}^{N} f_i(-2)\left(\frac{(-1)^{n+1}e^{-ip}\gamma(n+1,-(1+i)\,p)}{(1+i)^{n+1}} + \frac{e^{(2+i)p}\Gamma(n+1,(1+i)\,p)}{(1+i)^{n+1}}\right) \tag{2.21}$$

where $\Gamma(\alpha)$ and $\Gamma(\alpha,x)$ are the incomplete Gamma functions defined by [22]

$$\Gamma(\alpha) = \int_0^\infty t^{\alpha-1}e^{-t}dt \tag{2.22}$$

and

$$\Gamma(\alpha,x) = \int_x^\infty t^{\alpha-1}e^{-t}dt \tag{2.23}$$

$$\gamma(\alpha,x) = \int_0^x t^{\alpha-1}e^{-t}dt \tag{2.24}$$

In this study, the suggested formulas (2.11-2.16) for the two-parameter Fermi function has been used in Lorenz number and carrier concentration calculations.

2.2. The Definition of Lorenz Number and Carrier Concentration of a Semiconductor

As is known, the carrier concentration in the conduction band is shown as follows [10-12]:

$$n = \int_{E_c}^{E_{wp}} f(E)g(E)dE \tag{2.25}$$

$$n = \int_{E_c}^{E_{wp}} \frac{(4\pi 2m_e{}^*/h^2)^{\frac{3}{2}}(E-E_c)^{1/2}}{1+e^{\frac{E-E_F}{kT}}} \tag{2.26}$$

By the use of two-parameter Fermi function $I_{nk}^m(\eta,\beta)$, the carrier concentration can be defined as [23]:

$$n = \frac{(2m_n k_B T)^{\frac{3}{2}}}{3\pi^2\hbar^3} I_{\frac{3}{2},0}^{0}(\eta,\beta). \tag{2.27}$$

As we know, the Wiedeman-Franz law and its relation with the Lorenz number in the general form are as follows:

$$\frac{\kappa}{\sigma} = A(r,\eta,\beta)\left(\frac{k_B}{e}\right)^2 T = L(r,\eta,\beta)T \tag{2.28}$$

where $L(r,\eta,\beta)$ is Lorenz number, κ is thermal conductivity, σ is electric conductivity, k_B is Boltzmann constant, e is the electron charge, T is temperature. Also, $A(r,\eta,\beta)$ function is defined as:

$$A(r,\eta,\beta) = \frac{I_{r+1,2}^2(\eta,\beta)}{I_{r+1,2}^0(\eta,\beta)} + \left(\frac{I_{r+1,2}^1(\eta,\beta)}{I_{r+1,2}^0(\eta,\beta)}\right)^2. \tag{2.29}$$

It is clear that the Lorenz number can be written as [23]:

$$L(r,\eta,\beta) = A(r,\eta,\beta)\left(\frac{k_B}{e}\right)^2. \tag{2.30}$$

Thus, the Lorenz number turns into the following form by using $I_{nk}^{m}(\eta,\beta)$ two-parameter Fermi functions:

$$L(r,\eta,\beta) = \left(\frac{I_{r+1,2}^{2}(\eta,\beta)}{I_{r+1,2}^{0}(\eta,\beta)} + \left(\frac{I_{r+1,2}^{1}(\eta,\beta)}{I_{r+1,2}^{0}(\eta,\beta)}\right)^2\right)\left(\frac{k_B}{e}\right)^2. \tag{2.31}$$

As can be seen from formulas (2.27) and (2.31), the carrier concentration and the Lorenz number of a semiconductor can be defined using two-parameter Fermi functions. To show the efficiency of given algorithms, the Lorenz number and carrier concentration calculations of GaAs semiconductors have been done for wide temperature ranges (Figure 1 and 2). In addition, the comparative results of the carrier concentration with the available semi-empirical study [24] are presented in Table 1.

Table 1. Temperature dependence of carrier concentration of GaAs semiconductor (in semi-empirical methods [24] carrier concentration is taken as $n = 1.83 \times 10^{21} T^{3/2}$) ($N = 150$)

T	Ref. [24]	This study
150	3.361 E+24	2.981 E+24
100	1.84 E+24	1.162 E+24
80	1.309 E+24	0.958 E+24
50	6.47 E+23	5.651 E+23
40	4.629 E+23	3.487 E+23

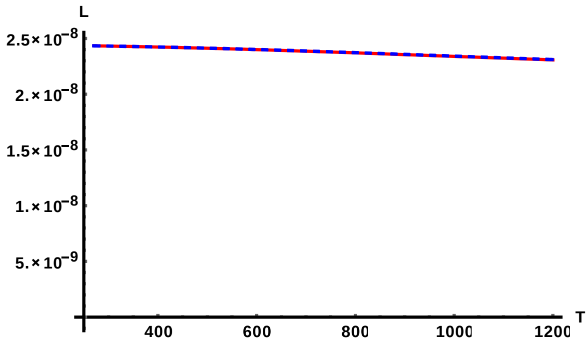

Figure 1. Temperature dependence of Lorenz number of GaAs semiconductor ($N = 150$) (red line-analytical results from suggested formula in this study, blue line-Mathematica numerical results)

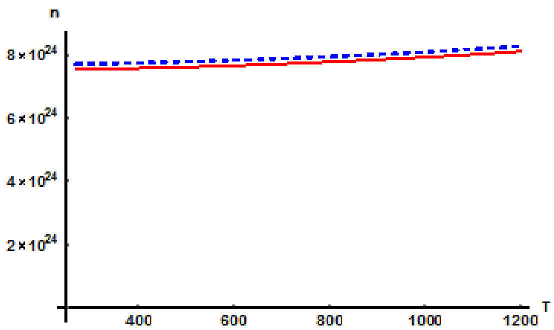

Figure 2. Temperature dependence of carrier concentration of GaAs semiconductor ($N = 150$) (red line-analytical results from suggested formula in this study, blue line-Mathematica numerical results)

3. Conclusion

The thermoelectric effect is based on examining the thermal effect acting on the semiconductor. For this purpose, in this study, the effects of the thermal effect on basic parameters of a semiconductor are numerically discussed. The carrier concentration variation, which is the main variable of the thermal conductivity relation that can be solved by the two-parameter Fermi function, has been investigated for GaAs semiconductors with increasing temperature. In order to demonstrate the effectiveness of our study, the calculation results obtained from available semi-empirical methods for the carrier concentration of GaAs semiconductors have been presented in Table 1. In Fig.1 and 2, the comparisons of the Lorenz number and carrier concentration calculation results of the GaAs semiconductor with the Mathematica numerical method have been demonstrated concerning temperature. Our calculation results are in good agreement with those obtained from numerical and semi-empirical methods. In all calculations the upper limits of summation (N) have been taken as 150. Also, in our previous paper [21] one can see the convergence of derived expression for $I_{nk}^{m}(\eta,\beta)$ as a function of summation limits N. It is well known that the little discrepancy of comparisons in Table 1 is due to the fact that the semi-empirical method neglects some parameters in calculations. Our analytical method has no restriction in its use and can apply to other semiconductors.

Author Contributions

All authors contributed equally to this work. The author read and approved the last version of the manuscript.

Conflicts of Interest

The author declares no conflict of interest.

References

[1] C. Kittel, Introduction to solid state physics, John Wiley & Sons. Inc., Sixth Edition, New York, 1986.

[2] N. W. Ashcroft, N.D. Mermin, Solid state physics, Philadelphia Pa., New York, 1976.

[3] H. P. Myers, Introductory solid state physics. CRC Press, London, 1997.

[4] E. O. Kane, *Band structure of indium antimonide*, Journal of Physics and Chemistry of Solids, 1(4), (1957) 249–261.

[5] B. Šantić, B., U. V. Desnica, *Thermoelectric effect spectroscopy of deep levels—application to semi-insulating GaAs,* Applied Physics Letters, 56(26), (1990) 2636–2638.

[6] L. Zhu, R. Ma, L. Sheng, M. Liu, D. N. Sheng, *Universal thermoelectric effect of Dirac fermions in graphene*, Physical Review Letters, 104(7), (2010) 076804.

[7] D. Segal, *Thermoelectric effect in molecular junctions: A tool for revealing transport mechanisms*, Physical Review B, 72(16), (2005) 165426.

[8] P. E. Nielsen, P. L. Taylor, *Theory of thermoelectric effects in metals and alloys*, Physical Review B, 10(10), (1974) 4061.

[9] G. Sansone, A. Ferretti, L. Maschio, *Ab initio electronic transport and thermoelectric properties of solids from full and range-separated hybrid functionals*, The Journal of Chemical Physics, 147(11), (2017) 114101.

[10] B. M. Askerov, F. M. Gashimzade, *Determination of parameters of degenerate semiconductors,* Physica Status Solidi (b), 21(2), (1967) 155–158.

[11] B. M. Askerov, Kinetic effects in semiconductors, Science, Leningrad, 1970.

[12] B. M. Askerov, Electron transport phenomena in semiconductors. World Scientific, London, 1994.

[13] H. S. Kim, Z. M. Gibbs, Y. Tang, H. Wang, G. J. Snyder, *Characterization of Lorenz number with Seebeck coefficient measurement*, APL materials, 3(4), (2015) 041506.

[14] M. Thesberg, H. Kosina, N. Neophytou, *On the Lorenz number of multiband materials*, Physical Review B, 95(12), (2017) 125206.

[15] P. J. Price, *Theory of transport effects in semiconductors: Thermoelectricity*, Physical Review, 104(5), (1956) 1223.

[16] A. Putatunda, D. J. Singh, *Lorenz number in relation to estimates based on the Seebeck coefficient*, Materials Today Physics, 8, (2009) 49–55.

[17] O. S. Gryazanov, Tables for the calculation of kinetic coefficients in semiconductor, Nauka, Leningrad, 1971.

[18] W. Zawadzki, R. Kowalczyk, J. Kolodziejczak, *The Generalized Fermi-Dirac integrals,* Physica Status Solidi (b), 10(2), (1965) 513–518.

[19] G. Rzadkowski, S. Łepkowski, *A generalization of the Euler-Maclaurin summation formula: an application to numerical computation of the Fermi-Dirac integrals*, Journal of Scientific Computing, 35(1), (2008) 63–74.

[20] I. I. Guseinov, B. A. Mamedov, B. A. *Unified treatment for accurate and fast evaluation of the Fermi–Dirac functions,* Chinese Physics B, 19(5), (2010) 050501.

[21] B. A. Mamedov, E. Copuroglu, *Unified analytical treatments of the two-parameter Fermi functions using binomial expansion theorem and incomplete gamma functions*, Solid State Communications, 245, (2016) 42–49.

[22] I. M. Ryzhik, I. S. Gradshteyn, Tables of integrals and sums, series, and products, Academic Press, New York, 1980.

[23] E. Çopuroğlu, I. M. Askerov, A. Aslan, *Analytical calculation of temperature dependence of the Lorenz number in semiconductors*, Journal of Science and Arts, 20(1), (2020)197–202.

[24] M. Shur, Physics of semiconductor devices, Englewood Cliffs, Prentice-Hall, 1990.

Journal of New Results in Science 10(3) (2021) 98-113

Journal of New Results in Science
https://dergipark.org.tr/en/pub/jnrs
Research Article
Open Access

E-ISSN:1304-7981 https://doi.org/10.54187/jnrs.851917

Magnetohydrodynamic peristaltic transport of Casson fluid embedded with chemical reaction in an asymmetrical permeable conduit

Asha Kotnurkar[1], Chandrashekhar Hadapad[2]

Keywords:
Magnetohydrodynamic, Peristaltic transport, Casson fluid, Chemical reaction, Porous medium.

Abstract — The present study investigates the magnetohydrodynamic non-Newtonian peristaltic flow of the Casson fluid model embedded with a chemical reaction. The assumption of small Reynolds number and approximations of long-wavelength are considered. The constituent equations are analytically solved by the method of decomposition by Adomian. Distributions of the velocity field, pressure gradient and concentration field are obtained. The simulations of influencing parameters on the behaviour of the fluid model have been elaborated with the help of graphs, and detailed analysis has been done. It can be observed that both the reaction parameter and Schmidt Number show similar behaviour for concentration profile. The graphs clearly show that the fluid parameter drastically reduces the pressure rise and pressure gradient. The pressure gradient will be increased by the increase in Hartmann number, but it reduces the pressure rise.

Subject Classification (2020):

1. Introduction

Peristalsis refers to a spontaneous wave mechanism like muscular contractions of the digestive tract or other tube-like structures. It is characterised by alternating contraction and relaxation, which helps push indigested food through the digestive duct towards its release at the anus. The pioneering work in this regard was initiated by starling and Bayliss [1], who described it as an ability of fluid to move or get around. Some of the peristaltically governing bodily flows are organs of the digestive system, oesophagus and intestine. Latham [2] study on peristaltic transport is influenced many researchers to develop many experimental and theoretical studies to understand the mechanical behaviour of fluids in different conditions. These works have been done by incorporating blood and other bodily fluids as Newtonian fluids. But it is much more significant to study the peristaltic transport of Bio-fluids by considering them as non-Newtonian fluids as human blood in arterioles, intestine etc., behave like a non-Newtonian fluid.

A key point in considering the non-Newtonian fluid model ahead of the Newtonian model is its viscosity, which is dependent on the forces being applied to it. Some of the applications include syrup drugs, toothpaste, colloids. A Casson fluid model with a distinct feature and its rheological behaviour

[1]as.kotnur2008@gmail.com (Corresponding Author); [2]chandruh.h4@gmail.com
[1]Department of Mathematics, Karnatak University, Dharwad, India.
[2]Department of Mathematics, Karnatak University, Dharwad, India.
Article History: Received: 01 Jan 2021 — Accepted: 31 Dec 2021 — Published: 31 Dec 2021

was pioneered by Casson [3]. Some more research work related to the peristaltic transport of the Casson model is seen in refs. [4-10].

However, studies related to a complex interaction of peristaltic motion of conducting fluid with extremely imposed magnetic field will enhance a better understanding of the performance of conductive physiological fluids like blood flow in small vessels (Casson fluid model), blood pump machines etc., Magnetohydrodynamics (MHD) or Magento fluid dynamics deal with magnetic properties and nature of fluids which easily have electrons pass through them, for instance, blood plasmas, saline. The motive behind using MHD is that applied magnetic fields can trigger currents in a flowing conductive fluid, which polarizes the fluid and that inertly changes the magnetic field itself. Some applications include sensors, casting by electromagnetic radiation, power generation with MHD, drug targeting by the applied magnetic field. Magneto hydrodynamic equations analyse the correlation between the external magnetic field and magnetic fluid particles in the bloodstream [11-23].

In many industrial and technological fields, problems that deal with differences in temperature and concentration difference have importance on chemical reaction processes. This phenomenon has its role in the conduction of heat and mass in a fluid motion. Chemical reactions are essential to chemical engineering, fluid dynamics, where they can be utilised to produce new compounds from naturally occurring raw materials like ores and petroleum. Related work can be seen in [24-32].

A semi-analytical method has been adopted to solve subsequent governing non-linear partial differential equations. This method allows a non-linear portion of the differential equation for solution convergence. Motivated by this, we attempted to analyse Casson fluid's peristaltic transport by the Adomian Decomposition Method (ADM). MHD and chemical reaction effects are considered. We have discussed the present study results through graphs, and the impact of pertinent parameters like rate of chemical reaction, Hartmann number and fluid parameter on pressure gradient, flow rate and, concentration profile are analysed in detail.

2. Problem formulation

The peristaltic motion of a steady condensed MHD Casson fluid model is considered with chemical reaction in a 2D channel with asymmetry at the walls. Where $\left(\overline{X}', \overline{Y}'\right)$ is the coordinate with $\overline{X}'$ along the direction of wave and $\overline{Y}'$ perpendicular to $\overline{X}'$ axis. The motion of the fluid model is driven by the sine wave having a constant speed c along the channel walls. The description of the walls is given by $\overline{Y} = \overline{h_1}'$ and $\overline{Y} = \overline{h_2}'$ representing the boundaries of the channel (Figure 1).

$$\overline{h_1}'(\overline{X}',\bar{t}) = d_1 + a_1 \mathrm{Cos}[\frac{2\pi}{\lambda}(\overline{X}' - c\bar{t})], \text{ upper wall} \tag{2.1}$$

$$\overline{h_2}'(\overline{X}',\bar{t}) = d_2 - a_2 \mathrm{Cos}[\frac{2\pi}{\lambda}(\bar{\varphi} + \overline{X}' - c\bar{t})]. \text{ lower wall} \tag{2.2}$$

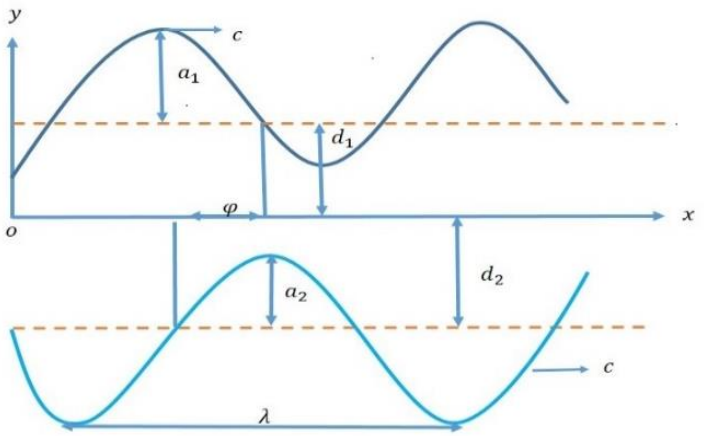

Figure1. A physical model of asymmetric channel.

where a_2, a_1 the amplitude of the lower wall waves is λ the wavelength, time $\bar{t}$, phase- difference φ. It is noted that for the symmetric channel, $\varphi = 0$ that means waves out of phase and $\varphi = \pi$ waves are in phase. and d_2, d_1 satisfies a criterion: $a_1^2 + 2b_1a_1 \cos\varphi + b_1^2 \le d_2^2 + d_1^2$.

Vector form of velocity V is $V = (\overline{U}, \overline{V}, 0)$ where $\overline{U}, \overline{V}$ are the velocity coordinates of the velocity field in the laboratory frame of reference.

The Rheological model of a Casson fluid is

$$\tau_{ij} = (\mu_0 + \frac{\rho_y}{\sqrt{2\pi_c}})2e_{ij}, \quad \text{when } \pi < \pi_c \tag{2.3}$$

$$\tau_{ij} = (\mu_0 + \frac{\rho_y}{\sqrt{2\pi_c}})2e_{ij}, \quad \text{when } \pi > \pi_c \tag{2.4}$$

Where ρ_y is the fluid yield stress, expressed as:

$$\rho_y = \frac{\mu_0\sqrt{2\pi}}{\beta}, \tag{2.5}$$

μ_0 is the fluid's plastic dynamic viscosity.

π is given by $\pi = e_{ij}.e_{ij}$.

e_{ij} - $(i, j)^{th}$ is the constituent of deformation rate and

π_c is the critical value relying on the non-Newtonian behaviour.

Denoting the velocity components $\overline{U}$ and $\overline{V}$ respectively along with X, Y directions in a fixed frame.

The governing equations of the flow are defined as:

$$\rho\left(\overline{U}\frac{\partial\overline{U}}{\partial\overline{X}}+\overline{V}\frac{\partial\overline{U}}{\partial\overline{Y}}+\frac{\partial\overline{U}}{\partial\overline{t}}\right)=\mu_B\left(1+\frac{1}{\gamma}\right)\left(\frac{\partial^2\overline{U}}{\partial x^2}+\frac{\partial^2\overline{U}}{\partial y^2}\right)-\sigma\overline{B_0}^2\overline{U}-\frac{\mu_B\overline{U}}{K_1}+\rho g\beta(\overline{C}-\overline{C_0})-\frac{\partial\overline{P}}{\partial\overline{X}}, \tag{2.6}$$

$$\rho\left(\frac{\partial\overline{V}}{\partial\overline{t}}+\overline{U}\frac{\partial\overline{V}}{\partial\overline{X}}+\overline{V}\frac{\partial\overline{V}}{\partial\overline{Y}}\right)=-\frac{\partial\overline{P}}{\partial\overline{Y}}+\mu_B\left(1+\frac{1}{\gamma}\right)\left(\frac{\partial^2\overline{V}}{\partial x^2}+\frac{\partial^2\overline{V}}{\partial y^2}\right)-\sigma\overline{B_0}^2\overline{V}-\frac{\mu_B\overline{V}}{K_1}, \tag{2.7}$$

$$\left(\overline{U}\frac{\partial\overline{C}}{\partial\overline{X}}+\overline{V}\frac{\partial\overline{C}}{\partial\overline{Y}}+\frac{\partial\overline{C}}{\partial\overline{t}}\right)=D_B\left(\frac{\partial^2\overline{C}}{\partial\overline{Y}^2}+\frac{\partial^2\overline{C}}{\partial\overline{X}^2}\right)-k_1(\overline{C}-\overline{C_0}), \tag{2.8}$$

where $\overline{V}$ and $\overline{U}$ are the velocity components along with the Y, X directions, respectively, ρ denotes the fluid's density, μ_B - viscosity of the fluid, γ the Casson parameter, $\overline{P}$ - pressure, σ - fluid's electrical conductivity, B_0 the applied magnetic field, β volumetric expansion coefficient, C the concentration, D_B the Brownian diffusion coefficient, g is the acceleration due to gravity, K_1 the thermal conductivity of the fluid as seen in Equations 2.6-2.8 respectively.

The flow can be considered unsteady if seen in the laboratory frame; however, in a coordinate plane moving at speed c in the wave frame (x, y), it can be treated as steady.

In two frames, velocities, coordinates, pressure, and concentration are

$x=\overline{X}+(-c)\overline{t},\ u=\overline{U}+(-c),\ y=\overline{Y},\ v=\overline{V},\ c=\overline{C},\ p=\overline{P},$

Here $\overline{U},\overline{V}$ and u,v are the components of velocity for the corresponding Cartesian systems.

The dimensional boundary conditions are

$$\overline{U}=-c\,,\quad \overline{C}=\overline{C_0}\qquad \text{at}\quad y=\overline{h_1}', \tag{2.9}$$

$$\overline{U}=-c\,,\quad \overline{C}=\overline{C_1}\qquad \text{at}\quad y=\overline{h_2}', \tag{2.10}$$

The following non-dimensional parameters are

$$\begin{aligned}&u=\frac{\overline{U}}{c},\ v=\frac{\overline{V}}{c},\ t=\frac{c\overline{t}}{\lambda},\ p=\frac{\overline{P}d_1^2}{c\lambda\mu_B},\ x=\frac{\overline{X}}{\lambda},\ y=\frac{\overline{Y}}{d_1},\ Sc=\frac{\mu_B}{D},\ R'=\frac{k_1d_1^2}{\mu_B},\\&C=\frac{\overline{C}-\overline{C_0}}{\overline{C_1}-\overline{C_0}},\ \delta=\frac{d_1}{\lambda},\ M=\sqrt{\frac{\sigma}{\mu_B}}B_0d_1,\ Da=\frac{k}{d_1^2},\ G_m=\frac{\rho gB_cd_1^2(\overline{C_1}-\overline{C_0})}{c\mu_B}.\end{aligned} \tag{2.11}$$

In view of Equation 2.11, Equations 2.6 - 2.8, reduce to

$$\frac{\partial p}{\partial x}=\left(1+\frac{1}{\gamma}\right)\frac{\partial^2u}{\partial y^2}-\left(M^2+\frac{1}{k}\right)u+G_mC, \tag{2.12}$$

$$\frac{\partial^2C}{\partial y^2}=ScR'C, \tag{2.13}$$

The dimensionless boundary conditions are

$$C = 0, u = 1, \quad \text{at } y = h_1, \tag{2.14}$$

$$C = 1, u = -1 \text{ at } y = h_2. \tag{2.15}$$

3. Method of solution

Using Adomian decomposition method, Equation 2.12 can be written as

$$L_{yy}u - N^2 u = \left\{ \frac{\gamma \frac{dp}{dx}}{1+\gamma} - \frac{G_m \gamma C}{1+\gamma} \right\}, \tag{3.1}$$

Where $N^2 = \frac{\left(M^2 + 1/k\right)\gamma}{1+\gamma}$, $L_{yy} = \frac{d^2}{dy^2}$,

Since L_{yy} is a second order differential operator, L_{yy}^{-1} is an inverse integration operator of order 2 defined by

$$L_{yy}^{-1}(.) = \int_0^y \int_0^y (.)dydy. \tag{3.2}$$

Employing L_{yy}^{-1}, Equation 3.1 becomes

$$u = C_1 + C_2 y + L_{yy}^{-1}\left(\frac{\gamma \frac{dp}{dx}}{1+\gamma} - \frac{G_m \gamma C}{1+\gamma} \right) + L_{yy}^{-1}\left(N^2 u\right). \tag{3.3}$$

By the semi-analytical Adomian Decomposition method we get

$$u = \sum_{n=0}^{\infty} u_n. \tag{3.4}$$

Equation 3.3 gives,

$$u_0 = C_1 + C_2 y + \left(\left(\frac{\gamma \frac{dp}{dx}}{1+\gamma}\right)\right)\frac{y^2}{2!} - \left(\frac{G_m \gamma}{1+\gamma}\right)\frac{Sinhk(y-h_1)}{k^2 Sinhk(h_2 - h_1)},$$

$$u_{n+1} = N^2 L_{yy}^{-1}(u_n), \; n \geq 0. \tag{3.5}$$

Using boundary conditions in Equation 2.14 and 2.15 to Equations 3.3-3.5, we obtain

$$u_1 = C_1 \frac{(Ny)^2}{2!} + \frac{C_2}{N}\frac{(Ny)^3}{3!} + \left(\left(\frac{\gamma}{N^2(1+\gamma)}\right)\frac{dp}{dx}\right)\frac{(Ny)^4}{4!} - \left(\frac{G_m \gamma}{1+\gamma}\right)\frac{N^2 Sinhk(y-h_1)}{k^4 Sinhk(h_2 - h_1)},$$

$$u_2 = C_1 \frac{(Ny)^4}{4!} + \frac{C_2}{N}\frac{(Ny)^5}{5!} + \left(\left(\frac{\gamma}{N^2(1+\gamma)}\right)\frac{dp}{dx}\right)\frac{(Ny)^6}{6!} - \left(\frac{G_m\gamma}{1+\gamma}\right)\frac{N^4 Sinhk(y-h_1)}{k^6 Sinhk(h_2-h_1)},$$

$$u_3 = C_1 \frac{(Ny)^6}{6!} + \frac{C_2}{N}\frac{(Ny)^7}{7!} + \left(\left(\frac{\gamma}{N^2(1+\gamma)}\right)\frac{dp}{dx}\right)\frac{(Ny)^8}{8!} - \left(\frac{G_m\gamma}{1+\gamma}\right)\frac{N^6 Sinhk(y-h_1)}{k^8 Sinhk(h_2-h_1)},$$

$$u_n = C_1 \frac{(Ny)^{2n}}{2n!} + \frac{C_2}{N}\frac{(Ny)^{2n+1}}{(2n+1)!} + \left(\left(\frac{\gamma}{N^2(1+\gamma)}\right)\frac{dp}{dx}\right)\frac{(Ny)^{2n}}{2n!} - \left(\frac{G_m\gamma}{1+\gamma}\right)\sum_{n=0}^{\infty}\frac{N^{2n}}{k^{2n+2}}\left(\frac{Sinhk(y-h_1)}{Sinhk(h_2-h_1)}\right),$$

$$u = C_1 CoshNy + \frac{C_2}{N} SinhNy + \left(\left(\frac{\gamma}{N^2(1+\gamma)}\right)\frac{dp}{dx}\right)\left(CoshNy - 1\right) - \left(\frac{G_m\gamma}{1+\gamma}\right)\left(\frac{1}{k^2-N^2}\right)\frac{Sinhk(y-h_1)}{Sinhk(h_2-h_1)}. \tag{3.6}$$

where

$$C_1 = \frac{1}{CoshNh_1} - \frac{SinhNh_1}{CoshNh_1}\left\{\begin{matrix}\dfrac{2CoshNh_1}{SinhN(h_1-h_2)} - \dfrac{CoshNh_1 - CoshNh_2}{SinhN(h_1-h_2)} + \left(\dfrac{\gamma}{N^2(1+\gamma)}\right)\dfrac{dp}{dx} \\ \left(\dfrac{CoshNh_2 - CoshNh_1}{SinhN(h_1-h_2)}\right) - \dfrac{G_m\gamma CoshNh_1}{(1+\gamma)(k^2-N^2)SinhN(h_1-h_2)}\end{matrix}\right\}$$
$$- \frac{\gamma \,{}^{dp}\!/_{dx}}{N^2(1+\gamma)}\left(\frac{CoshNh_1 - 1}{CoshNh_1}\right)$$

$$\frac{C_2}{N} = \frac{2CoshNh_1}{SinhN(h_1-h_2)} - \frac{(CoshNh_1 - CoshNh_2)}{SinhN(h_1-h_2)} + \left(\frac{\gamma}{N^2(1+\gamma)}\right)\frac{dp}{dx}\left(\frac{CoshNh_2 - CoshNh_1}{SinhN(h_1-h_2)}\right)$$
$$- \frac{G_m\gamma CoshNh_1}{(1+\gamma)(k^2-N^2)SinhN(h_1-h_2)}$$

$k = \sqrt{scR'}$.

The flow rate in the (x,y) is given as

$$q = \int_{h_1}^{h_2} u\,dy. \tag{3.7}$$

$$q = \frac{\left(SinhNh_2 - SinhNh_1\right)}{N\,CoshNh_1} - \frac{Sinh2Nh_1\left(SinhNh_2 - SinhNh_1\right)}{N\,CoshNh_1\,SinhN(h_1-h_2)} +$$
$$\frac{SinhNh_1\left(CoshNh_1 - CoshNh_2\right)\left(SinhNh_2 - SinhNh_1\right)}{N\,CoshNh_1\,SinhN(h_1-h_2)} -$$
$$\frac{\gamma\dfrac{dp}{dx}\left(\begin{matrix}\left(CoshNh_1 - 1\right)SinhN(h_1-h_2) + \\ \left(CoshNh_2 - CoshNh_1\right)SinhNh_1\end{matrix}\right)\left(SinhNh_2 - SinhNh_1\right)}{N^3(1+\gamma)CoshNh_1\,SinhN(h_1-h_2)} + \frac{2\left(CoshNh_2 - CoshNh_1\right)CoshNh_1}{N\,SinhN(h_1-h_2)}$$

$$+\frac{\left(CoshNh_2-CoshNh_1\right)^2}{N\,SinhN(h_1-h_2)}+\frac{\gamma\frac{dp}{dx}}{N^3(1+\gamma)}\left(\frac{\left(CoshNh_2-CoshNh_1\right)^2}{SinhN(h_1-h_2)}+\left(\left(SinhNh_2-SinhNh_1\right)-N(h_2-h_1)\right)\right)$$

$$-\frac{G_m\gamma}{(k^2-N^2)(1+\gamma)}\left(\frac{2\left(CoshNh_2-CoshNh_1\right)CoshNh_1}{N\,SinhN(h_1-h_2)}+\frac{\left(Coshk(h_2-h_1)-1\right)}{k\,Sinhk(h_2-h_1)}\right)$$

From Equation 3.7,

$$\frac{dp}{dx}=\left(\frac{N^3(1+\gamma)\,CoshNh_1\,SinhN(h_1-h_2)}{\begin{array}{l}\gamma\left(SinhN(h_1-h_2)CoshNh_1\left(\left(SinhNh_2-SinhNh_1\right)-N(h_2-h_1)\right)\right)+\\ CoshNh_1\left(CoshNh_2-CoshNh_1\right)^2-\left(SinhNh_2-SinhNh_1\right)\left(\begin{array}{l}\left(CoshNh_1-1\right)SinhN(h_1-h_2)+\\ SinhNh_1\left(CoshNh_2-CoshNh_1\right)\end{array}\right)\end{array}}\right)$$

$$\left(\begin{array}{l}q-\frac{\left(SinhNh_2-SinhNh_1\right)}{N\,CoshNh_1}+\frac{Sinh2Nh_1\left(SinhNh_2-SinhNh_1\right)}{N\,CoshNh_1\,SinhN(h_1-h_2)}+\\ \frac{SinhNh_1\left(SinhNh_2-SinhNh_1\right)\left(CoshNh_2-CoshNh_1\right)}{N\,CoshNh_1\,SinhN(h_1-h_2)}-\frac{2\left(CoshNh_2-CoshNh_1\right)CoshNh_1}{N\,SinhN(h_1-h_2)}-\\ \frac{\left(CoshNh_2-CoshNh_1\right)^2}{NSinhN(h_1-h_2)}+\frac{G_m\,\gamma}{(1+\gamma)\left(k^2-N^2\right)}\left(\frac{\begin{array}{l}k\,Sinhk(h_2-h_1)CoshNh_1\left(CoshNh_2-CoshNh_1\right)\\ +\left(Coshk(h_2-h_1)-1\right)N\,SinhN(h_1-h_2)\end{array}}{N\,k\,SinhN(h_1-h_2)Sinhk(h_2-h_1)}\right)\end{array}\right)$$

The dimensionless equation of the pressure rise is given by

$$\Delta p=\int_0^1\frac{dp}{dx}dx. \tag{3.8}$$

The volumetric flow rate at a given instant of the fixed frame is provided by,

$$\overline{Q}(x,t)=\int_{h_1'}^{h_2'}U'\left(X',Y',t'\right)dy', \tag{3.9}$$

where h_2' and h_1' are mappings of X' and Y' respectively.

In wave frame the rate of flow is given by,

$$q = \int_{h_2'}^{h_1'} u'\left(x', y'\right) dy'. \tag{3.10}$$

Utilising the transformations into the Equations 3.9 and 3.10, the entity among Q and q can be written as

$$Q = c(h_2' - h_1') + q. \tag{3.11}$$

The mean time flow for a period T at a constant position X' is given by

$$\overline{Q} = \frac{1}{T}\int_0^T Q\, dt. \tag{3.12}$$

Using Equation 3.12 in Equation3.11 the flow rate $\overline{Q}$ is,

$$\overline{Q} = \frac{1}{T}\int_0^T q dt + c(h_1' - h_2') = q + cd_2 + cd_1. \tag{3.13}$$

The dimensionless form of Equation 3.13 is given by

$$\theta = F + d + 1, \tag{3.14}$$

where $\theta = Q' / d_1 c$ and $F = q / d_1 c,$ such that

$$F = \int_{h_2}^{h_1} u\, dy = u(h_1 - h_2). \tag{3.15}$$

Solving Equation 2.13, with the boundary conditions in Equation2.14 and 2.15, we can obtain

$$C = ACoshky + \frac{B}{k} Sinhky,$$

where

$$A = \frac{-Sinhkh_1}{Sinhk(h_2 - h_1)}$$

$$B = \frac{k\, Coshkh_1}{Sinhk(h_2 - h_1)}$$

$$k = \sqrt{ScR'}$$

This may be simplified as

$$C = \frac{Sinhk(y - h_1)}{Sinhk(h_2 - h_1)}. \tag{3.16}$$

The expression determining velocity profile from stream function is given by,

$$u = \frac{\partial \psi}{\partial y}, v = -\frac{\partial \psi}{\partial x}. \tag{3.17}$$

We know that $\psi = u_x \hat{i} + v_x \hat{j}$, and $v_X = 0$ for the flow problem, so we get the desired equation of the streamlines of the flow as

$$\psi = u_x = \frac{\partial u}{\partial x} = C_1 N\, SinhNy + C_2 CoshNy + \left(\left(\frac{\gamma}{N(1+\gamma)}\right)\frac{dp}{dx}\right)\left(SinhNy\right) - \left(\frac{G_m \gamma}{1+\gamma}\right)\left(\frac{1}{k^2 - N^2}\right)\frac{kCoshk(y-h_1)}{Sinhk(h_2-h_1)}. \tag{3.18}$$

4. Interpretation of Results

This section gives numerical simulations with the aid of graphs. The numerical simulations are performed using the computational software Mathematica.

4.1 Pressure Distribution

Figure 2 illustrates the behaviour of numerous embedding parameters on pressure gradient for a given wavelength versus x. The channel walls dp/dx are relatively small, thus helps the fluid in this region flow easily. The middle of the channel dp/dx is large, so relatively much pressure needed for the fluid to pass inside the region. Figure 2a depicts the variation in pressure gradient due to a change in Hartmann number M. Magnetic field parameter M raises the value of pressure gradient; fluid flow requires more pressure gradient to pass through the region. The effect of a fluid parameter γ can be seen in Figure 2b. A rise in fluid parameter γ decreases the pressure gradient.

Similarly, the impact of the phase difference can be seen in Figure 2c. In the narrow part of the channel, there is a decrease in pressure gradient when there is a rise in phase difference and a rise in pressure in the broader part of the channel when we decrease phase difference. Figure 2d and 2e Depict the magnitude of pressure gradient decreases by increasing the Schmidt number Sc and chemical reaction parameter R'.

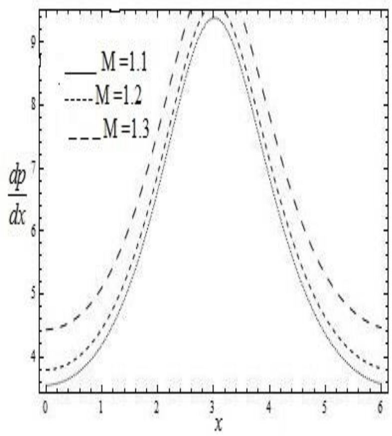

(a)

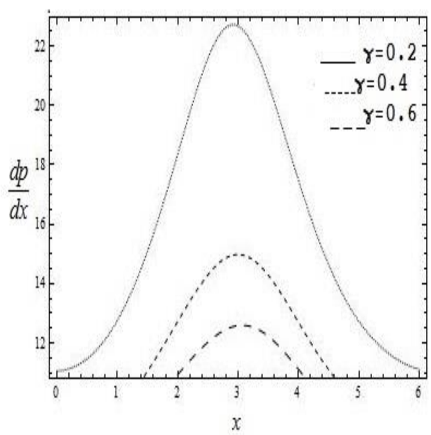

(b)

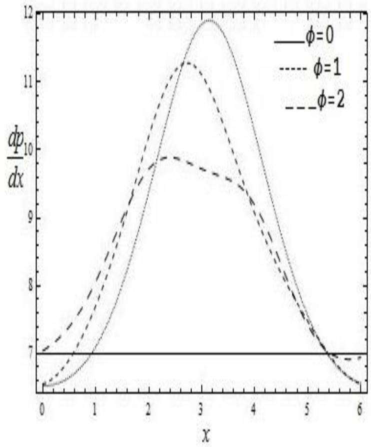

(c)

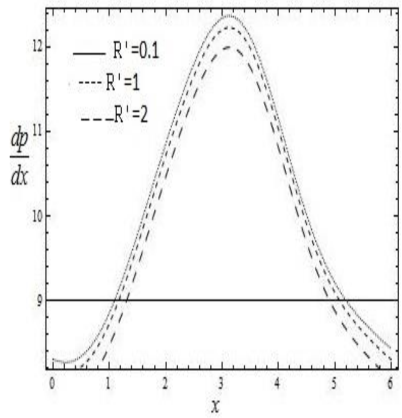

(d)

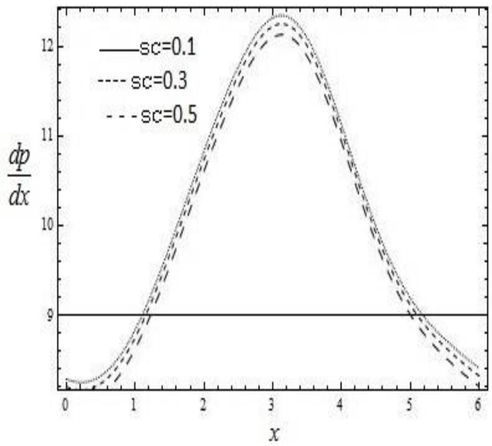

(e)

Figure 2. The figure represents variations of dp/dx versus x for M, γ, ϕ, R' respectively.

In Figure 2a, when $a = 0.1, b = 0.5, \phi = 0.6, d = 1, Sc = 0.7, M, \gamma, \phi, R' = 2, \gamma = 3$.

In Figure 2b when $a = 0.1, b = 0.5, \phi = 0.6, d = 1, Sc = 0.7, R' = 2, M = 3$.

In Figure 2c when $a = 0.1, b = 0.5, d = 1, Sc = 0.7, R' = 2, M = 3$.

In Figure 2d when $a = 0.1, b = 0.5, d = 1, Sc = 0.7, \phi = 0.6, \gamma = 3, M = 3$.

In Figure 2e when $b = 0.5, a = 0.1, d = 1,$.

4.2 Flow Rate Distribution

Figure 3 depicts the change in pressure rise ΔP versus flow rate Q for various parameters $\gamma, M, d, \phi, R', Sc$. Figure 3a Illustrates a non-linear relation between the pressure rise ΔP and flow rate Q . It is observed that higher the value of γ there is a drastic decrease in pressure rise, leading to a decline in the peristaltic pumping rate. Similar behaviour can be seen for the magnetic field M in Figure 3b below. Figure 3c Illustrates that pressure rise ΔP slowly decreases with an increase in d . But in Figure 3d, we can observe that rise in values of ϕ suddenly enhances the pressure rise. In Figure 3e and 3f, it is noted that higher the numbers of there is a linearly increase in pressure rise, leading to rise in the peristaltic pumping rate.

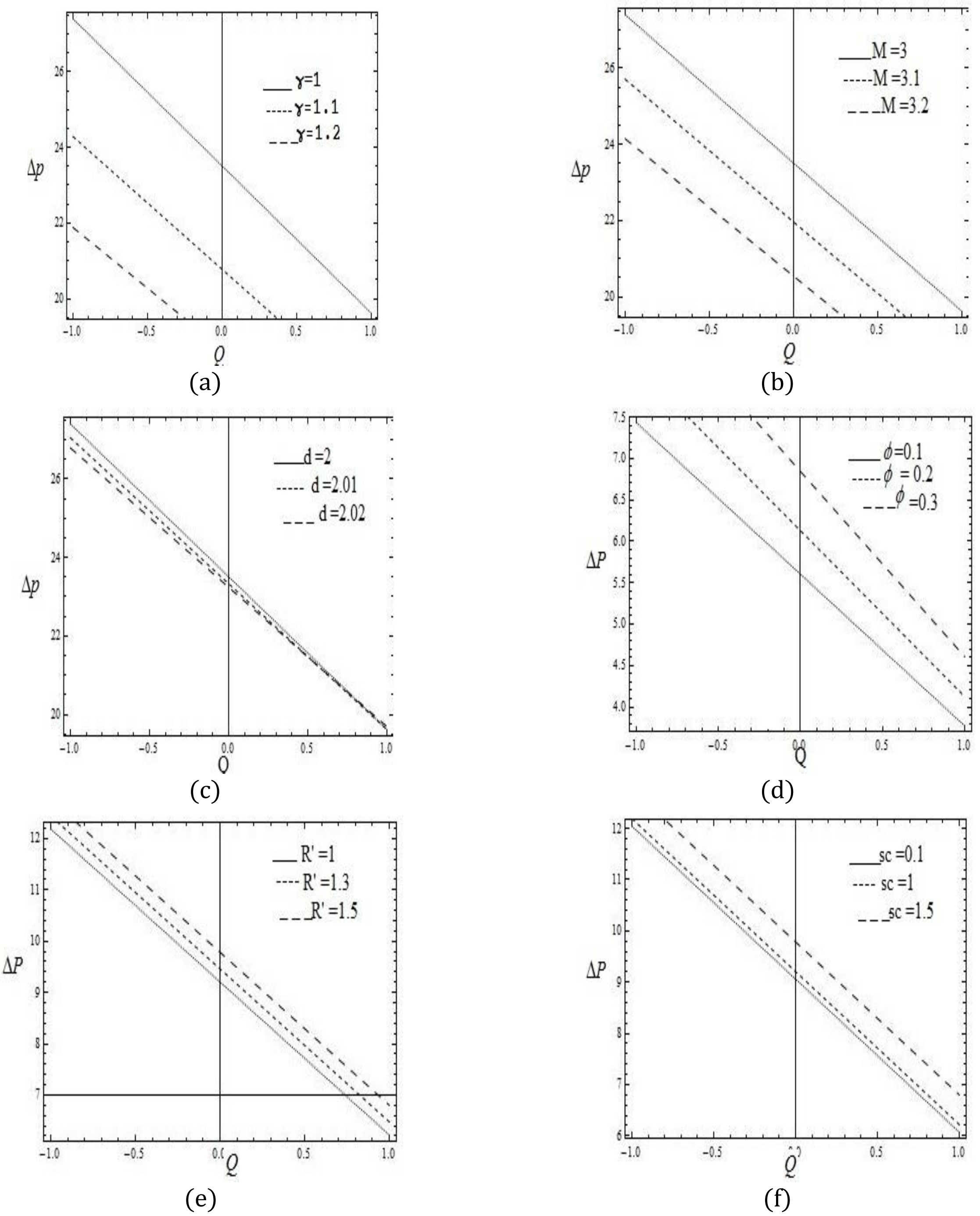

Figure 3. The figure represents variations in pressure rise ΔP versus Q for different values of $\gamma, M, d, \phi, R^{'}, Sc$ of respectively.

In Figure 3a when $a = 0.1, b = 0.5, d = 2, \phi = 0.5, Sc = 1.5, M = 3, R^{'} = 2$.

In Figure 3b when $a = 0.1, b = 0.5, d = 2, \phi = 0.5, \gamma = 1, Sc = 1.5, R^{'} = 2$.

In Figure 3c when $a = 0.1, b = 0.5, \phi = 0.5, \gamma = 1, Sc = 1.5, R^{'} = 2, M = 3$.

In Figure 3d when $a = 0.1, b = 0.5, d = 2, \gamma = 2, Sc = 0.3, R^{'} = 1, M = 2$.

In Figure 3e when $a = 0.1, b = 0.5, d = 2, \phi = 0.7, \gamma = 2, Sc = 1.5, M = 3$

In Figure 3f when $a = 0.1, b = 0.5, d = 2, \phi = 0.7, \gamma = 2, R^{'} = 1.5, M = 3$

4.3 Concentration Profile

Figure 4 illustrates the concentration profile for numerous parameters $a, b, d, \phi, R^{'}, Sc$, respectively. In Figure 4a, we can observe that enhance in Schmidt number Sc gradually minimizes the concentration profile. Figure 4b Shows the same behaviour as the reaction parameter slowly declines the concentration profile. In Figure 4c, we observed that the amplitude value a diminishes the concentration field. Similarly, in Figure 4d, we notice that the parameter b suddenly decreases the concentration field. Figure 4e Illustrates those higher parameter values d reduces the concentration profile. But in Figure 4f, we can see that higher phase difference values drastically enhance the concentration profile.

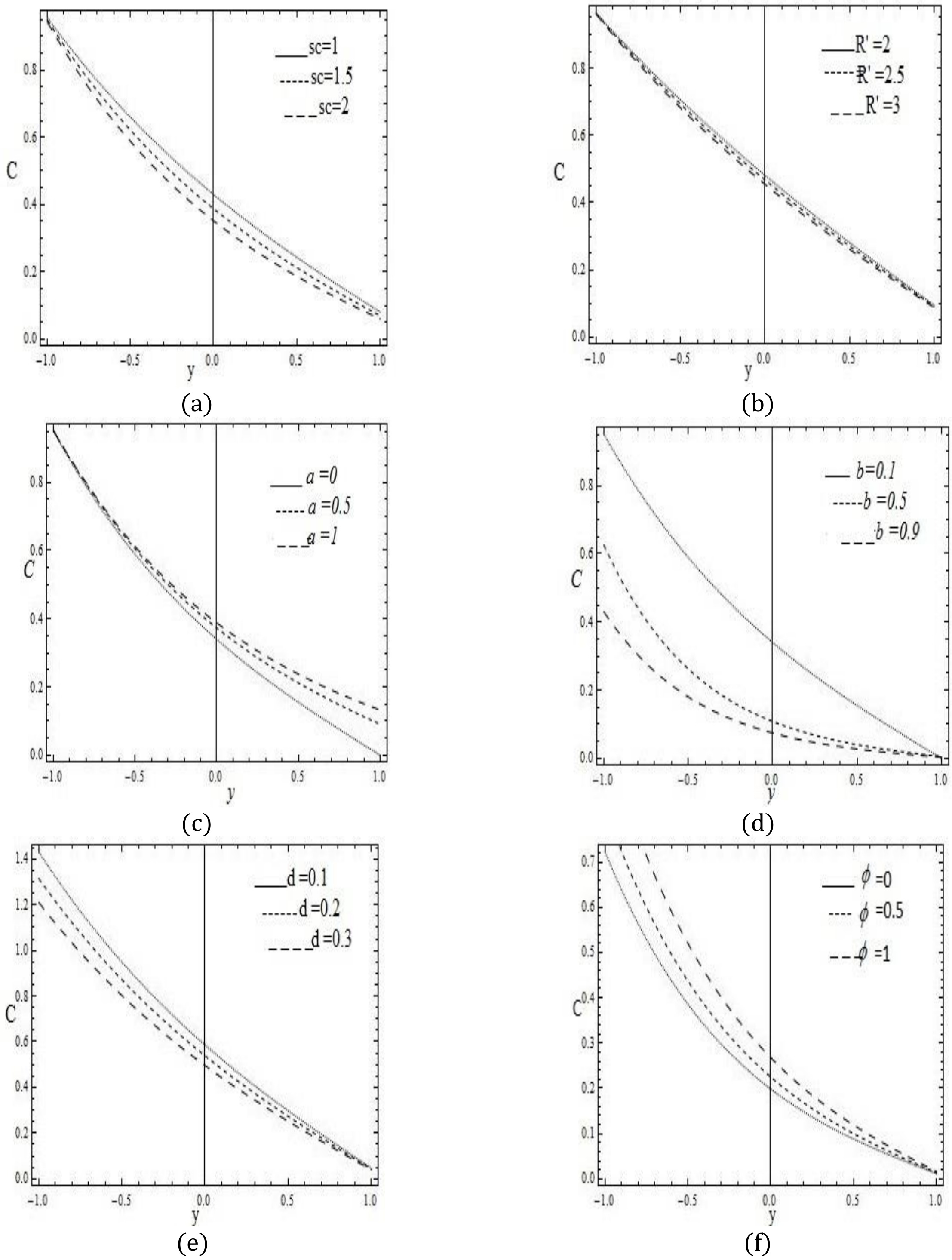

Figure 4. The figure represents variations of C versus y for $Sc, R^{'}, a, b, d, \phi$ respectively.

In Figure 4a when $a = 0.3,\ b = 0.1,\ d = 1,\ \phi = 0.4,\ R' = 0.4$.

In Figure 4b when $a = 0.3,\ b = 0.1,\ d = 1,\ \phi = 0.4,\ Sc = 0.1$.

In Figure 4c when $b = 0.1,\ d = 1,\ \phi = 0.5,\ Sc = 1.5,\ R' = 0.5$.

In Figure 4d when $a = 0.1,\ d = 1,\ \phi = 0.5,\ Sc = 1.5,\ R' = 2$.

In Figure 4e when $a = 0.1,\ b = 0.5,\ \phi = 0.3,\ Sc = 0.5,\ R' = 1,\ \mathrm{x} = 0.1$

In Figure 4f when $a = 0.1,\ b = 0.3,\ \mathrm{d} = 1,\ Sc = 1.5,\ R' = 1$

4.4 Trapping Phenomena

The streamlines are the imaginary lines in a fluid flow such that tangent at any position on a streamline will provide us with the velocity at that point. These lines will exhibit the direction in which a zero-rest mass fluid element will travel at any instant of time. The accumulation of bolus of the fluid in the closed streamlines inside a wave frame is called trapping. The nature of the streamlines against fluid parameter $\beta = 0.1, 0.5, 1.0, 5.0$, respectively, as shown in Figures 5. The fluid's viscosity relies on the parameter β, and it comes out to be highly viscous and turns thicker as we enhance the value of the Casson fluid parameter. Moreover, with the raising the values of the fluid parameter, the bolus will drastically shift to the middle of the channel, and the coupling streamlines sight below the wall.

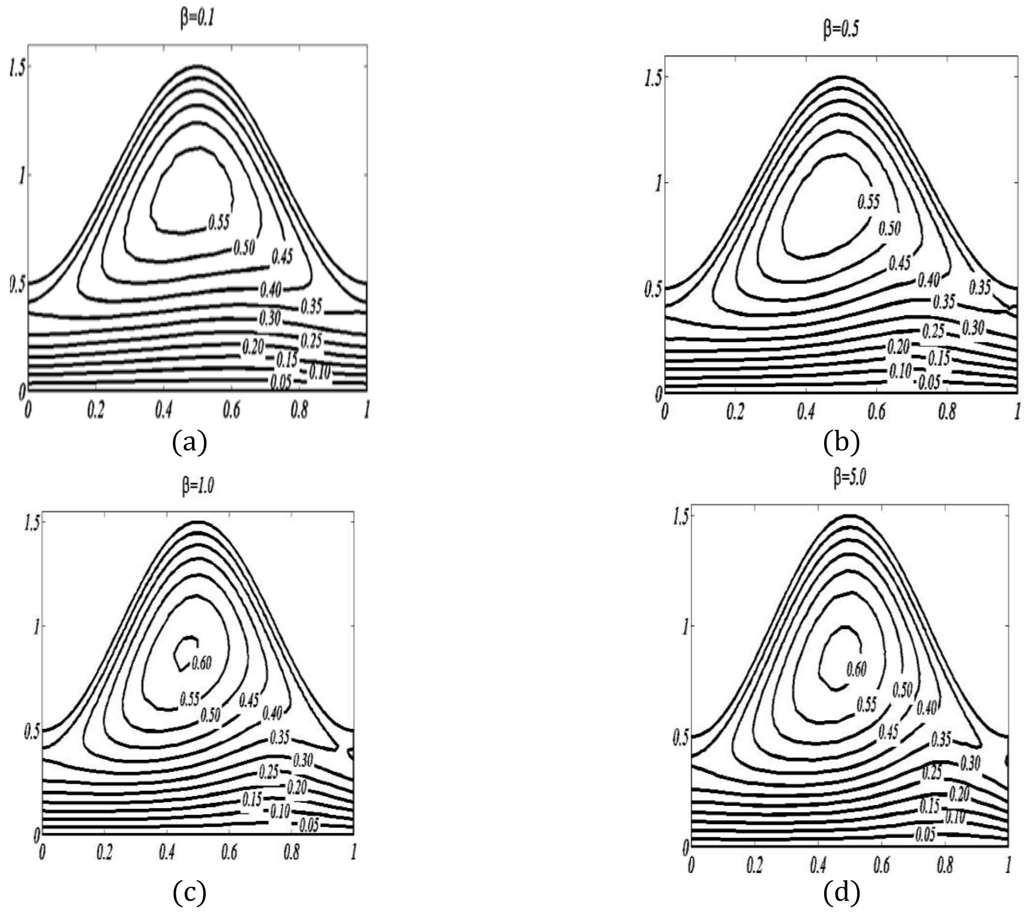

Figure 5. The figure represents streamlines against various values of β in wave frame with $Q = 1.3, a = 0.2, M = 2, \phi = 0.5.$

5. Conclusion

The mass transfer and MHD analysis on peristaltic motion of Casson fluid model embedded with porous medium and asymmetric geometry were considered. The influence of various pertinent governing flow parameters on the fluid model has been analysed with graphs. The concluding points of the present study are stated below.

1. At the centre of the channel, the amount of pressure gradient enhances when there is a magnetic field. But pressure gradient diminishes with an ascendance in parameters like $a = 0.1, b = 0.3, \mathrm{d} = 1, Sc = 1.5, R' = 1.$

2. It is noted that pressure rise decreases with the increase in γ, M, R', Sc and d. However, it increases with an increase in phase difference.

3. The concentration profile reduces when there is a rise in parameters like a, b, d, R' and Sc. However, it increases when we increase the value ϕ.

4. It is equal in value to observe that increase in the Schmidt parameter Sc and chemical reaction term R' decreases the concentration profile.

5. We observe a reduction in both pressure rise and pressure gradient when we enhance values of Schmidt number Sc and reaction parameter R'.

Author Contributions

All authors contributed equally to this work. They all read and approved the final version of the manuscript.

Conflicts of Interest

The authors declare no conflict of interest.

6. References

[1] W. M. Bayliss, E. H. Starling, *Physiology of Peristalsis*, Journal of Physiology (London), 24, (1899) 99–143.

[2] T. W. Latham, *Fluid motion in a peristaltic pump*, Master's Thesis, Massachusetts Institute of Technology (1986), Cambridge, USA.

[3] K. K. Raju, R. Devanathan, *Peristaltic motion of a non-Newtonian fluid*", *Rheologica Acta*, 11, (1972) 170–179.

[4] N. S. Akbar, *Influence of magnetic field on peristaltic flow of a Casson fluid in an asymmetric channel*, application in crude oil refinement. Journal of Magnetism and Magnetic Materials, 378, (2015) 463–468.

[5] K. Ramesh, M. Devakar, *Some analytical solutions for flows of Casson fluid with slip boundary conditions*, Ain Shams Engineering Journal, 6(3), (2015) 967–975.

[6] M. Rashidi, M.Yang, Z. Bhatti, M. M Bhatti, M. A. Abbas, *Heat and mass transfer analysis on MHD blood flow of Casson fluid model due to peristaltic wave*, Thermal Science, 22(6 (A)), (2018) 2439–2448.

[7] V. P. Rathod, L. Devindrappa, *Peristaltic transport in an inclined asymmetric channel with heat and mass transfer by Adomian decomposition method*, Advances in Applied Science Research, 7, (2016) 83–100.

[8] N. Iftikhar, A. Rehman, H. Sadaf, M. N. Khan, *Impact of wall properties on the peristaltic flow of Cu-water nanofluid in a non-uniform inclined tube*, International Journal of Heat and Mass Transfer, 125, (2018) 772–779.

[9] B. B. Divya, G. Manjunatha,C. Rajashekhar, H. Vaidya, K. V. Prasad, *The hemodynamics of variable liquid properties on the MHD peristaltic mechanism of Jeffrey fluid with heat and mass transfer*, Alexandria Engineering Journal, 59(2), (2020) 693–706.

[10] K. Ahmed, R. Nazar, *Magnetohydrodynamic three-dimensional flow and heat transfer over a stretching surface in a visco-elastic fluid*, Journal of Science and Technology, 3(1), (2011) 33–46.

[11] S. Nadeem, R. U. Haq, C. Lee, *MHD flow of a Casson fluid over an exponentially shrinking sheet*, Scientia Iranica, 19, (2012) 1550–1553.

[12] Z. Asghar, N. Ali, R. Ahmed, M. Waqas, W. A. Khan, *A mathematical framework for peristaltic flow analysis of non-Newtonian Sisko fluid in an undulating porous curved channel with heat and mass transfer effects*, Computer Methods and Programs in Biomedicine, 182, (2019) 105040.

[13] S. Nadeem and S. Akram, *Slip effects on the peristaltic flow of Jeffrey fluid in an asymmetric channel under the effect of induced magnetic field*, International Journal for Numerical Methods in fluids, 63, (2010) 374–394.

[14] [14] S. Hina, *MHD peristaltic transport of Eyring-Powell fluid with heat/mass transfer, wall properties and slip conditions*, Journal of Magnetism and Magnetic Materials, 404, (2016) 148–158.

[15] M. Gnaneswara Reddy, *Heat and Mass transfer on Magnetohydrodynamic peristaltic flow in a porous medium with partial slip*, Alexandria Engineering Journal, 55, (2016) 1225–1234.

[16] S. Akram, S. Nadeem, *Influence of induced magnetic field and heat transfer on the peristaltic motion of a Jeffrey fluid in an asymmetric channel: closed-form solution*, Journal of Magnetism and Magnetic Materials, 328, (2013) 11–20.

[17] M. Gnaneswara Reddy, K. Venugopal Reddy, D. O. Makinde, *Heat transfer on MHD peristaltic rotating flow of a Jeffrey fluid in an asymmetric channel*, International Journal of Applied and Computational Mathematics, 3, (2016) 3201–3227.

[18] T. Sarpakaya, *Flow of non-Newtonian fluids in a magnetic field,* American Institute of Chemical Engineers Journal, 7, (1961) 324–328.

[19] T. Hayat, A. Saleem, A. Tanveer, F. Alsaadi, *Numerical study for MHD peristaltic flow of Williamson nanofluid in an endoscope with partial slip and wall properties*, International Journal of Heat and Mass Transfer, 114, (2017) 1181–1187.

[20] C. Vasudev, U. Rajeswara Rao, M. V. Subba Reddy, G. Prabhakar Rao, *Influence of Magnetic field and Heat transfer on Peristaltic flow of Jeffrey fluid through a porous medium in an asymmetric channel*, ARPN Journal of Engineering and Applied Sciences, 5, (2010) 87–103.

[21] V. P. Rathod, Laxmi Devindrappa, *Effects of heat transfer on the peristaltic MHD flow of a Bingham fluid through a porous medium in a channel*, International Journal of biomathematics, 7, (2014) 1450060–1450080.

[22] V. P. Rathod, M. M. Channakote, *Slip effects and heat transfer on MHD peristaltic flow of Jeffrey fluid in an inclined channel*, Journal of Chemical, Biological and Physical Sciences, 2, (2012) 1987–1997.

[23] A. Zeeshan, M. M. Bhatti, T. Muhammad, L. Zhang, *Magnetized peristaltic particle-fluid propulsion with Hall and ion slip effects through a permeable channel,* Physica A: Statistical Mechanics and its Applications, 550, (2019) 123999.

[24] R. Muthuraj, K. Nirmala, S. Srinivas, *Influence of chemical reaction and wall properties on MHD peristaltic transport of a dusty fluid with heat and mass transfer*, Alexandria Engineering Journal, 55, (2016) 597–611.

[25] T. Hayat, S. Hina, A. A. Hendi, S. Asghar, *Influence of compliant walls on peristaltic motion with heat/mass transfer and chemical reaction*, International Journal of Heat and Mass Transfer, 55, (2012) 3386–3394.

[26] T. Hayat, H.Yasmin, M. Al-Yami, *Soret and Dufour effects in peristaltic transport of physiological fluids with chemical reaction: A mathematical Analysis*, Computers and Fluids, 70, (2014) 242–253.

[27] T. Hayat, H. Zahir, A. Tanveer, A. Alsaedi, *Influence of Hall current and chemical reaction in mixed convective peristaltic flow of Prandlt fluid*, Journal of Magnetism and Magnetic materials,407, (2016) 321–327.

[28] M. G. Reddy, K. V. Reddy, *Influence of Joule heating on MHD peristaltic flow of a nanofluid with compliant walls*, Procedia Engineering, 127, (2015) 1002–1009.

[29] K. V. Reddy, O. D. Makinde, M. G. Reddy, *Thermal analysis of MHD electro-osmotic peristaltic pumping of Casson fluid through a rotating asymmetric micro-channel*, Indian Journal of Physics, 92(11), (2018) 1439–1448.

[30] M. G. Reddy, B. C. Prasannakumara, O. D. Makinde, *Cross diffusion impacts on hydromagnetic radiative peristaltic Carreau-Casson nanofluids flow in an irregular channel*, Defect and Diffusion Forum, 377, (2017) 62–83.

[31] O. D. Makinde, M. Gnaneswara Reddy, K. Venugopal Reddy, *Effects of Thermal Radiation on MHD Peristaltic Motion of Walters-B Fluid with Heat Source and Slip Conditions*, Journal of Applied Fluid Mechanics, 10(4), (2017) 1105–1112.

[32] M. Gnaneswara Reddy, K. Venugopal Reddy, O. D. Makinde, *Hydromagnetic peristaltic motion of a reacting and radiating couple stress fluid in an inclined asymmetric channel filled with a porous medium,* Alexandria Engineering Journal, 55(2), (2016) 1841–1853.